Aus dem Institut für Klinische Neuroimmunologie

Klinikum der Ludwig-Maximilians-Universität München

Direktor: Prof. Dr. Martin Kerschensteiner

Krüppel-Like Factor 2: A Key Transcription Factor Mediates CD4$^+$ T Cells Migration in Experimental Autoimmune Encephalomyelitis

Dissertation

zum Erwerb des Doktorgrades der Naturwissenschaften

an der Medizinischen Fakultät der

Ludwig-Maximilians-Universität zu München

vorgelegt von

La Zhuo

aus

Innere Mongolei, China

Jahr

2025

Mit Genehmigung der Medizinischen Fakultät

der Ludwig-Maximilians-Universität München

Betreuer:	**PD Dr. Naoto Kawakami**
Zweitgutachter:	Prof. Dr. Ludger Klein
Dekan:	**Prof. Dr. med. Thomas Gudermann**
Tag der mündlichen Prüfung:	13. Januar 2026

TABLE OF CONTENTS

ABSTRACT

Autoreactive $CD4^+$ T cells migrating into the central nervous system (CNS) has been established as a key driver for the multiple sclerosis (MS) disease onset. Once inside the CNS, these cells are activated by CNS-specific antigens, triggering neuroinflammation, and further neurodegeneration. In recent times, the inhibition of the autoreactive $CD4^+$ T cell migration became a promising therapeutic strategy. However, like other treatments, it cannot fully prevent the MS disease progression and comes with the risk of severe infections.

To develop better therapies, a deeper understanding of the molecular mechanisms guiding $CD4^+$ T cell migration is essential. Our study aims to reveal how autoreactive $CD4^+$ T cells migrate through key stages—from the bloodstream to secondary lymphoid organs (SLOs), back into circulation, and ultimately into the CNS. Our observations are based on the experimental autoimmune encephalomyelitis (EAE) model, a well-established model for MS.

We focused on the two transcription factors, krüpple-like factor 2 (Klf2) and forkhead box protein O1 (Foxo1), identified from our previously published genome-wide CRISPR/Cas9 screening data for their role in regulating autoreactive $CD4^+$ T cell migration. Using CRISPR/Cas9 single-gene knockout technology, we examined the individual functions of Klf2 and Foxo1 in T cell migration in an adoptive transfer EAE model, along with the distinct functions of their downstream effector molecules.

Our study highlights Klf2 as a key transcription factor controlling T cell migration in EAE. Knocking out Klf2 caused T cells to accumulate in the parathymic lymph nodes (ptLNs) and spleen. Based on our findings, this is due to an increase in C-C chemokine receptor 7 (Ccr7) expression and the absence of sphingosine-1-phosphate receptor 1 (S1pr1). Additionally, Klf2 deficiency reduced Itga4 and Itgb1 expression, disrupting very late antigen 4 (VLA4) and preventing T cells from adhering to CNS blood vessels. As a result, Klf2-KO cells cannot infiltrate the CNS to induce EAE. Interestingly, knocking out Foxo1, an upstream regulator of Klf2, led T cells to a higher accumulation in ptLNs but did not affect their migration to the CNS. This is likely because Foxo1 promotes Ccr7 expression, but its absence does not impact Itga4.

Beyond migration, our findings reveal Klf2 as a crucial switch between the activated and migratory states of T cells. Without Klf2, autoreactive T cells remain in an activated state, showing increased CD25 expression and elevated pro-inflammatory cytokines (TNF-α, IFN-γ, and IL-17A). This abnormal activation, combined with their failure to infiltrate the CNS, suggests that Klf2 is essential for shifting T cells into a migratory phenotype in SLOs.

By uncovering these molecular pathways, our study offers new insights into potential therapeutic targets that could block autoreactive T cell migration into the CNS without broadly suppressing the immune system.

ZUSAMMENFASSUNG

Die Migration autoreaktiver $CD4^+$ T-Zellen in das zentrale Nervensystem (ZNS) wurde als ein entscheidender treibender Faktor für den Ausbruch der Multiplen Sklerose (MS) etabliert. Sobald diese Zellen in das ZNS gelangen, werden sie durch ZNS-spezifische Antigene aktiviert, was eine Neuroinflammation auslöst und zu fortschreitender Neurodegeneration führt. Die Hemmung der Migration autoreaktiver $CD4^+$ T-Zellen wird heutzutage als eine vielversprechende therapeutische Strategie angesehen. Allerdings kann dieser Ansatz, wie andere bestehende Behandlungen, das Fortschreiten von MS nicht vollständig verhindern und birgt zudem das Risiko schwerwiegender Infektionen.

Um bessere Therapien zu entwickeln, ist ein tieferes Verständnis von den molekularen Mechanismen, die die $CD4^+$ T-Zellen Migration steuern, erforderlich. In dieser Studie wird untersucht, wie autoreaktive $CD4^+$ T-Zellen verschiedene Migrationsschritte durchlaufen – vom Blutstrom in sekundäre lymphatische Organe (SLOs), zurück in die Zirkulation und schließlich in das ZNS. Die Observationen basieren auf dem experimentellen autoimmunen Enzephalomyelitis-(EAE)-Modell, einem etablierten Tiermodell für MS.

Diese Studie konzentriert sich auf die beiden Transkriptionsfaktoren krüpple-like factor 2 (Klf2) und forkhead box protein O1 (Foxo1), die in unserer zuvor veröffentlichten genomweiten CRISPR/Cas9-Screening-Analyse als Regulatoren der Migration autoreaktiver $CD4^+$ T-Zellen identifiziert wurden. Durch gezielte CRISPR/Cas9-Knockout-Experimente analysierten diese Studie die individuellen Rollen von Klf2 und Foxo1 bei der T-Zell-Migration im adoptiven Transfer-EAE-Modell, sowie die spezifischen Funktionen ihrer nachgeschalteten Effektormoleküle.

Diese Studie hebt Klf2 als einen zentralen Transkriptionsfaktor für die Steuerung der T-Zell-Migration im EAE-Modell hervor. Der Knockout von Klf2 führte dazu, dass sich die T-Zellen in den parathymischen Lymphknoten (ptLNs) und der Milz anreicherten. Die Ergebnisse zeigen, dass dies auf eine erhöhte C-C chemokine receptor 7 (Ccr7) -Expression und das Fehlen von sphingosine-1-phosphate receptor 1 (S1pr1) zurückzuführen ist. Zudem reduzierte das Fehlen von Klf2 die Expression von Itga4 und Itgb1, wodurch very late antigen 4 (VLA4) nicht mehr gebildet wurde. Infolgedessen konnten Klf2-defiziente T-Zellen nicht an die Blutgefäße des ZNS binden, nicht ins ZNS einwandern und dadurch keine EAE-Erkrankung auslösen. Interessanterweise führte der Knockout von Foxo1, einem upstream-Regulator von Klf2, zu einer erhöhten Anreicherung von T-Zellen in den ptLNs, beeinträchtigte jedoch nicht deren Migration ins ZNS. Dies könnte daran liegen, dass Foxo1 ebenfalls die Ccr7-Expression fördert, während Itga4 von Foxo1‘s Abwesenheit nicht beeinflusst wird.

Über die Migration hinaus zeigt die durchgeführte Studie, dass Klf2 eine entscheidende Rolle beim Übergang von $CD4^+$ T-Zellen vom aktivierten in den migrierenden Zustand spielt. Ohne Klf2 bleiben autoreaktive T-Zellen in einem hyperaktivierten Zustand, mit erhöhter CD25-Expression und verstärkter Produktion proinflammatorischer Zytokine (TNF-α, IFN-γ und IL-17A). Diese abnormale Aktivierung, kombiniert mit ihrem Versagen, in das zentrale Nervensystem (ZNS) einzudringen, deutet darauf hin, dass Klf2 entscheidend dafür ist, dass T-Zellen in den SLOs in einen migratorischen Phänotyp transformiert werden.

Durch die Identifizierung dieser molekularen Pfade liefert die Studie neue Erkeenntnisse über potenzielle therapeutische Ansätze, die die Migration autoreaktiver T-Zellen ins ZNS gezielt blockieren, ohne dabei das gesamte Immunsystem zu unterdrücken.

LIST OF FIGURES

LIST OF ABBREVIATIONS

APCs	antigen-presenting cells
BBB	blood-brain barrier
BFP	blue fluorescent protein
Cas9	CRISPR-associated protein 9
Ccl	C-C chemokine ligand
Ccr	C-C chemokine receptor
CD	cluster of differentiation
CFA	complete Freund's adjuvant
CIS	clinically isolated syndrome
CNS	central nervous system
CRISPR	clustered regularly interspaced short palindromic repeats
CSF	cerebrospinal fluid
dcLNs	deep cervical lymph nodes
DCs	dendritic cells
DNA	deoxyribonucleic acid
EAE	experimental autoimmune encephalomyelitis
EBV	Epstein-Barr virus
EGFP	enhanced green fluorescent protein
FACS	fluorescence-activated cell sorting
FBS	fetal bovine serum
Foxo	forkhead box protein O
GPCR	G protein coupled receptor
HEV	high endothelial venule
HLA	human leukocyte antigen
IIH	idiopathic intracranial hypertension
IFN	interferon
IL	interleukin
ISF	interstitial fluid
Itga	integrin α
Itgb	integrin β
Klf2	krüpple-like factor 2
KO	knockout
LFA1	lymphocyte function-associated antigen 1
MBP	myelin basic protein
MFI	mean fluorescent intensity
MHC	major histocompatibility complex
MOG	myelin oligodendrocyte glycoprotein
MS	multiple sclerosis

NF-κB	nuclear transcription factor-kappa B
NT	non-targeted
OE	overexpressed
OVA	Ovalbumin
PB	intracellular staining perm wash buffer
PFA	paraformaldehyde
PLP	proteolipid protein
PMA	phorbol 12-myristat 13-acetat
PPMS	primary-progressive multiple sclerosis
PSGL-1	P-selectin glycoprotein ligand 1
ptLNs	parathymic lymph nodes
PTX	pertussis toxin
RM	restimulation medium
RNA	ribonucleic acid
RNP	ribonucleoprotein
RRMS	relapsing-remitting multiple sclerosis
S1p	sphingosine-1-phosphate
S1pr1	sphingosine-1-phosphate receptor 1
sgRNA	single guide RNA
SLO	secondary lymphoid organ
SNP	single nucleotide polymorphism
SPMS	secondary-progressive multiple sclerosis
TCGF	T cell growth factor medium
TCM	T cell medium
TCR	T cell receptor
TGF	transforming growth factor
T_{MBP} cell	MBP-specific T cell
TNF	tumor necrosis factor
Treg	regulatory T cell
VCAM1	vascular cell adhesion molecule 1
VLA4	very late antigen 4

1. INTRODUCTION

1.1. Characteristic of MS

Multiple sclerosis (MS) is widely recognized as a long-term autoimmune disease that leads to massive myelin sheath breakdown and axonal degeneration in the central nervous system (CNS). The chronic immune reaction in MS lesions induces both structural and functional damage to myelin and axons, resulting in impaired or failed neural signaling, which in turn contributes to the corresponding clinical symptoms. As the MS lesion could be anywhere in the CNS parenchyma, the symptoms varied broadly. In the early 18th century, these completely unrelated symptoms were not recognized as being connected and instead were considered separate diseases. Finally, in 1868, the French neurologist Jean-Martin Charcot identified the link between consistent postmortem pathological findings and varied clinical symptoms. He summarized these observations and recognized them as a specific disease (Charcot, 1868). He described the special pathological change “sclerotic plaques” within the white matter of the brain and spinal cord. He also found this pathological change was strongly linked to the relapse and remitting neurological dysfunction. He named this disease “sclérose en plaques”. At a later time, Elvin Kabat discovered the presence of oligoclonal immunoglobulin bands in the cerebrospinal fluid (CSF) of MS patients, confirming localized immune response contributes to the disease pathology (Kabat et al., 1942). Around a similar time, the first animal model of MS was established by Thomas Rivers (Rivers et al., 1933). Rivers and his team discovered that immunizing monkeys with rabbit brain extracts could induce encephalomyelitis, closely mimicking the neuroinflammatory response that occurs in MS patients (Rivers et al., 1933).

Since then, based on the discoveries of these pioneering scientists, more researchers have continued to explore the disease, conducting meaningful studies and looking deeper into both its characterization and treatment. Still many fundamental issues remain unclear, particularly the precise mechanisms underlying disease onset and progression. Understanding the complexity of MS, including its interplay between genetic, environmental, and immunological factors, continues to challenge researchers. These persistent unknowns highlight the need for ongoing research and breakthrough discoveries to fully understand and effectively fight against the MS.

1.1.1. Epidemiology of MS

The MS epidemiology shows that genetic susceptibility, environmental factors, and geographic influences interact with each other and together contribute to the disease onset. Young adults exhibited higher risk of developing MS, with the highest incidence occurs around the age of 30 (Harbo et al., 2013). In terms of gender, females have a 2-3 times higher incidence than male (Harbo et al., 2013). Multiple studies have confirmed that this gender difference is due to the effects of sex hormones on immune system regulation (de Andres et al., 2004, Sanchez-Ramon et al., 2005). The relapse rate of MS in female patients visibly drops during pregnancy but increases significantly after delivery, which is due to the hormonal changes that temporarily enhances immune tolerance (Whitaker, 1998, Salemi et al., 2004).

In general, the incidence of MS is rising worldwide, understanding causes and developing new treatments for MS is urgently needed. MS is most common in Europe, the United States, Canada, New Zealand, and parts of Australia, where incidence rates still continuously increase over the years (Wingerchuk, 2011). Other regions which were previously considered to have lower MS incidence, such as Asia and Africa, have also seen an upward trend in recent years (Wingerchuk, 2011). In Germany, a 2019 statistical study estimated that approximately 250,000 people out of 83.7 million people are suffering from MS (Wallin et al., 2019). The geographical distribution of MS incidence is mainly caused by two key factors: environment and genetics. Environmental factors linked to high MS incidence regions, include vitamin D and sunlight exposure. Multiple studies have proven that low sunlight exposure and reduced serum vitamin D levels are strongly correlate with an increased risk of MS onset (van der Mei et al., 2003, Munger et al., 2004, Munger et al., 2006, Ueda et al., 2014). The widely accepted explanation of this is that vitamin D plays important role in immune regulation. Its regulatory function influences both innate and adaptive immune responses (Hewison, 2011). Vitamin D has also been shown to promote immune tolerance by modulating dendritic cell activity, inhibiting their differentiation, and reducing pro-inflammatory cytokine production such as IL-12 (Banchereau and Steinman, 1998, Penna and Adorini, 2000, Rosen et al., 2016, Ao et al., 2021). Besides region related environmental factors, early-life lifestyles and viral infections have also been found to affect MS risk. For instance, smoking, obesity, and dietary habits all involved in modulating immune function and systemic inflammation, contributing to MS susceptibility and progression (Olsson et al., 2017). Virus infection is one of the most frequently discussed environmental risk in recent years, particularly the Epstein-Barr virus (EBV). Evidence of individuals with infectious mononucleosis history, a clinical symptom of EBV infection, showed over twice the risk of developing MS (Handel et al., 2010, Robinson and Steinman, 2022).

Genetic factors are another key influence on MS susceptibility. MS shows clear familial clustering and an obviously higher incidence in certain populations (Sawcer et al., 2014). Genetic epidemiology studies showed that people with a closer relative that has MS are more likely to develop the disease, with recurrence risks varying based on genetic relatedness. Monozygotic twins and individuals with both parents affected by MS showed 25-35% of recurrence risks, while dizygotic twins showed around a 5% of recurrence risks (Dyment et al., 2004). These rates are significantly higher than those of the general population or adopted children within the same family (Dyment et al., 2004). However, no single gene can fully explain its genetic susceptibility. Among these genes associated with MS genetic susceptibility, the human leukocyte antigen (HLA) stands out as a key factor, particularly HLA-DRB1*15:01, with an odds ratio of 3.08 (Hollenbach and Oksenberg, 2015). The epidemiological profile of MS reveals that its impact on MS risk is primarily through immune dysfunction. Both genetic and environmental factors have been found to disrupt the balance between immune activation and tolerance.

1.1.2. Clinical Diagnose and Subtypes of MS

The diagnosis of MS relies on a thorough clinical evaluation. This includes a detailed review of the neurological history, comprehensive physical examination and the evidence support from magnetic resonance imaging (MRI) and laboratory analysis of the CSF. The neurological symptoms in MS patients can affect any functional system of the CNS, including motor, sensory, visual, autonomic, and other neurological systems dysfunction (Tejera-Alhambra et al., 2016). According to the McDonald criteria, an MS diagnosis is confirmed by identifying damages within the CNS, either through clinical findings or MRI. The lesions must demonstrate dissemination in space and/or time (Tejera-Alhambra et al., 2016, Thompson et al., 2018b). During the MS diagnosis, neurologists also need to identify the subtype that the MS patient has. According to the 2017 revisions of the McDonald criteria, MS is divided into four clinical subtypes, including clinically isolated syndrome (CIS), relapsing-remitting MS (RRMS), primary progressive MS (PPMS), and secondary progressive MS (SPMS) (Thompson et al., 2018a). Due to the complexity and variability of the MS disease progression, the MS subtype of a patient is not fixed and can change according to the progression of the disease.

CIS is a single clinical attack of the CNS, with MRI scanning showing one or more lesions of neuroinflammation and demyelination (Efendi, 2015). Although, if strictly base on the diagnostic criteria, CIS should not be classified as a subtype of MS, statistics show that around 85% of MS patients experience CIS as their first clinical symptom (Scalfari et al., 2010). It is important to classify

CIS as MS, since evidence shows that early detection and treatment of CIS can effectively delay disease progression and reduce the frequency of relapses (Kappos et al., 2006, Fisniku et al., 2008).

Most MS patients present with the RRMS phenotype (Katz Sand, 2015). In RRMS patients, MS symptoms come in waves, with periods of complete or partial symptom relief followed by a new attack reappearing. In between those phases, there are also period of relative clinical stability (Katz Sand, 2015). In MS, an attack is referred to as a "relapse", defined as "patient-reported symptoms or objectively observed signs typical of an acute inflammatory demyelinating event in the CNS, current or historical, with duration of at least 24 h, in the absence of fever or infection" (Katz Sand, 2015). The neurological symptoms in MS patients gradually become irreversible and progressive over time. When patients experience continuous disease progression without further remitting phases, the condition is classified as SPMS. Around 65% of RRMS cases progress to the SPMS in 10-15 years (Scalfari et al., 2010). Also, not all MS patients initially present with RRMS or CIS. About 20% of patients experience progressive symptoms from the early onset of the disease, rather than relapsing and remitting. Those cases are clinically classified as PPMS (Compston and Coles, 2008).

Different subtypes of MS are driven by distinct pathological changes. The relapsing and remitting feature of RRMS is primarily caused by neuroinflammatory changes in lesions. Over time, repeated waves of immune reactions at these sites lead to structural damage, such as demyelination and axonal loss. In SPMS, the pathology shifts more toward neurodegeneration and axonal damage, with milder inflammatory infiltration. This also explains why immune therapies are less effective in SPMS patients. PPMS shares similarities with SPMS, showing more neurodegenerative lesions along with mild to moderate inflammatory activity (Klineova and Lublin, 2018).

The different pathological changes in MS patients at various stages need different therapeutic strategies. In RRMS the immune reaction is the primary pathological factor, which makes immunomodulatory therapy effective. Treatment for RRMS includes interferon β, glatiramer acetate, and siponimod, as well as newly introduced monoclonal antibodies and immunosuppressive drugs. Using one or a combination of these therapies, depending on the patient's individual condition, can effectively reduce the frequency of relapses. However, these treatments are still unable to prevent disease progression (Saleem et al., 2019).

In the progressive stage, where neurodegeneration becomes dominant, immunotherapy is no longer the main approach. Instead, neuroprotective treatments are used to fight against myelin and nerve degeneration. As mentioned earlier, current MS treatments cannot fully prevent disease progression, therefore further research is needed to better understand the disease underlying mechanisms and develop new treatment strategies.

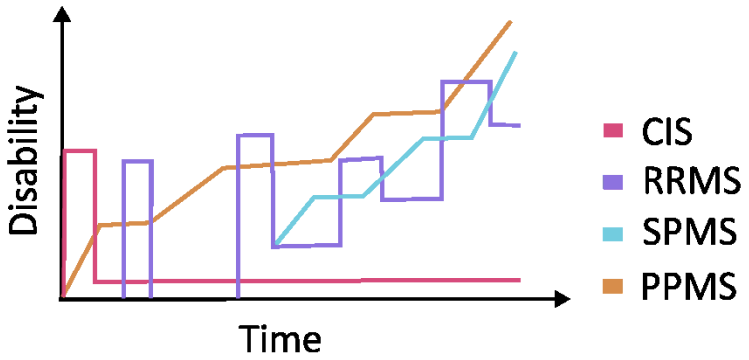

Figure 1 Clinical subtype of MS

MS disease onset can start with CIS or RRMS or PPMS. The differentiation of MS subtypes is based on the clinical disease course, including the frequency of relapses and the presence or absence of remission phases. CIS (pink) can be reclassified as RRMS (purple) if a subsequent relapse happens. PPMS (orange) is characterized by continuous disease progression from the onset without periods of remission. In RRMS, after repeated relapses and remissions, symptoms often become less reversible. Eventually, the RRMS transition into a phase of continuous progression without further relapses, known as SPMS (blue).

1.2. Pathology of MS

Corresponding to the clinical phenotype of MS, its key pathological features include neuroinflammation and demyelinating lesions that are distributed across both in space and time. In the early days the understanding of the MS pathology came from postmortem autopsies. First reports of a summarization of the MS pathological features were published by Charcot (Charcot, 1868) and Bourneville (Bourneville and Guérard, 1869). Both researchers observed MS plaques throughout the brain and spinal cord, that are showing spatial and temporal dissemination. Spatial dissemination means the presence of plaques were in multiple regions within the same patient, affecting both the brain and spinal cord. Their distribution is unrelated to any specific vascular supply regions or other anatomical divisions (Lumsden, 1970). The temporal dissemination shows that lesions found within the same patients were at different stages of disease progression. Some lesions exhibited acute features, such as tissue edema, poorly defined edges, obvious myelin swelling and lymphocytes and macrophages infiltration under the microscope (Hickey, 1999). Older lesions displayed more chronic changes, including well-defined boundaries, reduced edema. Under the microscope neurologist could observe gliosis and fewer inflammatory cells infiltration, which were mainly found at the lesion edges in contrast to the characteristics of acute lesions (Hickey, 1999). Axonal loss was also commonly observed in older lesions (Hickey, 1999).

The development of MRI technology has greatly improved our understanding of the pathological changes in MS. Unlike postmortem samples, MRI imaging allows for real-time observation of

changes that are happening in the CNS of living patients. In MRI scans, T1-weighted imaging provides a view of the CNS anatomy reveals variations in tissue composition. The inflammatory and demyelinating lesions contain more water, which makes them appear as lower-signal areas compared to surrounding unaffected tissue on T1-weighted images (Hemond and Bakshi, 2018). Gadolinium-enhanced T1 imaging further helps assess blood-brain barrier (BBB) integrity. Gadolinium shows high-signal in T1 sequences. When gadolinium is injected intravenously in patients, it leaks into CNS parenchyma if the BBB is impaired. The leakage creates high-signal areas, often surrounded by low-signal edemas (Hemond and Bakshi, 2018). Research has also shown that gadolinium leakage happens at the same time as the massive infiltration of peripheral lymphocytes into the CNS (Hemond and Bakshi, 2018).

T2-weighted imaging and fluid-attenuated inversion recovery (FLAIR) imaging are even more sensitive to MS lesions, showing them as oval-shaped high-signal areas, often with a central vein visible in the middle of the lesion (Hemond and Bakshi, 2018). High signals on T2 sequences indicate pathological changes such as inflammation, demyelination, edema, axonal damage, or Wallerian degeneration (Hemond and Bakshi, 2018). These MRI-detected lesions are able to point out significant histological changes.

Different subtypes of MS also exhibit varied pathology changes. In RRMS, white matter is mostly affected by lesions, which are primarily characterized by inflammatory demyelination. Massive inflammatory cells are found within these lesions, including T cells, B cells, macrophages, and activated microglia (Kutzelnigg et al., 2005, Pender and Greer, 2007). Myelin changes in RRMS are mainly presenting as a myelin loss, while axons remain mostly intact (Kutzelnigg et al., 2005, Pender and Greer, 2007). In contrast to the presentation of RRMS, pathological changes found in SPMS and PPMS patients are mainly identified as cortical demyelination, marked by significant loss of myelin and axons. The distribution of inflammatory cells is more diffused and milder than RRMS, with mononuclear cell infiltration observed in the meninges (Kutzelnigg et al., 2005, Pender and Greer, 2007).

As summary of all pathological changes in MS, it is clear that immune cell infiltration plays a critical role in disease pathology. In the early stages, massive infiltration of T cells and activated microglia (Ulvestad et al., 1994) are particularly crucial for disease onset and progression. These activated immune cells contribute to BBB disruptions and demyelination. Histological research has also detected myelin degradation products within infiltrating immune cells in MS lesions (Babinski, 1885). In later stages, such as in SPMS, although the immune response is no longer the primary pathological change, ectopic B-cell lymphoid-like follicles have been found in the meninges (Serafini et al., 2004).

These follicles contain B cells, plasma cells, T cells, and dendritic cells (DCs), indicating that chronic inflammatory stimulation might contribute to continued disease progression.

1.3. Immunology of MS

The CNS has been wrongly believed to be an immune-privileged site for a long time. Early studies reported that tissue grafts within the CNS were less likely to be rejected (Shirai, 1921, Medawar, 1948) and that bacterial or viral antigens introduced into the CNS could escape from the systemic immune recognition (Galea et al., 2007). Another factor supporting this concept was the historical lack of identified conventional lymphatic vessels within the CNS (Wood, 2015). However, development in imaging technology has revealed that T cells can cross the BBB even under normal conditions, though in limited numbers (Nishihara et al., 2020). And more directly evidence, immune cells are found in the immune-privileged CNS of MS patients (Lock et al., 2002).The exchange of soluble substances between CSF and interstitial fluid (ISF), followed by drainage to deep cervical lymph nodes (dcLNs), also indicates the existence of a lymphatic system function in the CNS (Aspelund et al., 2015).

In MS patients the disruption of the BBB allows large numbers of peripheral immune cells, primarily lymphocytes, to infiltrate the CNS. This is an early pathological feature of the disease. MRI scans show that newly formed or active lesions often exhibit inflammatory changes as a primary characteristic (Rocca et al., 2024). Lesions in gray matter, particularly those near the meninges, frequently display inflammatory infiltration into the adjacent meninges during early stages (Howell et al., 2011). This implies that soluble mediators released by the immune cells that infiltrated into the meninges might lead to the formation of those gray matter lesions (Howell et al., 2011).

The effectiveness of immunosuppressive therapy further highlights the central role of the immune system in MS. Early immune intervention can help reduce long-term disability in patients (Attfield et al., 2022). Oligoclonal bands (OCBs) are widely present in the CSF of MS patients and are produced by B cells in the CSF (Obermeier et al., 2008). These OCBs mainly consist of antibodies targeting intracellular proteins, suggesting that B cells likely become more active after the initial immune response in the CNS (Sospedra and Martin, 2005, Kaskow and Baecher-Allan, 2018). They further amplify the immune cascade and contribute to widespread damage to CNS tissues. However, to date, no common specific autoantigens have been identified in MS patients.

The relationship between CNS inflammation and MS pathology raises an important question: Is immune infiltration a cause or a consequence of the disease? As described above, genetic and environmental factors showed a significant impact on MS susceptibility, with genetic factors

accounting for approximately 30% of the risk (Genet, 2013). GWAS analysis has identified more than 100 single nucleotide polymorphisms (SNPs) associated with MS, many of which are linked to T cell differentiation and function (Consortium et al., 2013). Among them, HLA class II alleles, such as DRB1*1501, DRB1*0301, and DRB1*1303, are the most highly correlated. These alleles increase MS susceptibility by regulating antigen presentation and T cell activation. On the other hand, environmental factors such as gut microbiota composition, EBV infection, smoking, and vitamin D deficiency contribute to disease susceptibility by promoting abnormal T cell activation and impairing regulatory T cells (Tregs) function (Ascherio et al., 2010, Levin et al., 2010, Berer et al., 2011). The most commonly used animal model of MS, experimental autoimmune encephalomyelitis (EAE), further confirms the role of T cells in MS. It confirmed that peripheral activated autoreactive T cells are able to migrate into the CNS, further disrupt the BBB, trigger immune responses, and cause neurological deficits (Fletcher et al., 2010).

In summary, the immune system plays a crucial role in MS pathogenesis, with T cells being central to disease initiation and progression. Understanding how these immune cells contribute step-by-step to disease onset and how other immune components participate in this complex process remains the key to advancing MS research and treatment.

1.4. Animal Model of MS

To further uncover mechanisms of MS and develop potential therapeutic approaches, finding an appropriate animal model to replicate the disease onset and pathological changes is essential. Due to the complex pathology and unclear causes of MS, no single animal model can fully replicate all aspects of the disease. The application of a specific animal model depends on the specific topic or stage of MS being studied. For example, in the research focused on demyelination and remyelination in MS, chemically induced demyelination models are commonly used. Typical agents include ethidium bromide, lysolecithin, lipopolysaccharide, and cuprizone (Dedoni et al., 2023). Although chemically induced demyelination models offer a reliable and standardized method for studying demyelination, it still differs fundamentally from the demyelination process occurs in MS. While peripheral immune cell infiltration also occurs in these models, the immune response is secondary to the tissue damage, leading them unsuitable for exploring the early immune-mediated processes of MS pathogenesis.

The EAE model is currently the most widely used animal model for investigating autoimmune attack in MS. Its main mechanism involves artificially inducing CNS-specific immune reactivity, particularly immune activation against specific myelin proteins. Activated autoreactive peripheral immune cells migrate to the CNS and attack myelin proteins, triggering an inflammatory immune response.

Nowadays mice are the most commonly used animal for EAE establishment. Different to spatial dissemination in MS, in EAE the spinal cord is typically the most affected CNS region. Clinical symptoms in an experimental animal include ascending paralysis, beginning with tail weakness and progressing to the hind and forelimbs (McRae et al., 1992, Batoulis et al., 2011, Rangachari and Kuchroo, 2013). Overall, the EAE model effectively mimics an autoimmune mediated spinal cord inflammation, with the key process involving the migration of peripherally activated autoreactive T cells into the CNS.

EAE can be classified into three types based on the method of induction: active EAE, passive EAE, and spontaneous EAE. In 1925, the first active EAE model was introduced. At the time, researchers used human spinal cord homogenates to immunize rabbits, leading to spinal cord inflammation and neurological deficits (Koritschoner and Schweinburg, 1925). Later, a similar method was used to induce EAE in monkeys through multiple times of immunization with normal rabbit brain tissue (Stromnes and Goverman, 2006). Since then, active EAE models have been mainly induced by subcutaneous injection of CNS-derived peptides such as myelin oligodendrocyte glycoprotein (MOG), myelin basic protein (MBP), or proteolipid protein (PLP). They are emulsified in complete Freund's adjuvant (CFA) containing heat-killed Mycobacterium tuberculosis and then injected into mice. Myeloid immune cells then phagocytose the mixture and present the antigen to lymphocytes, initiating the immune response (Lazarević et al., 2024). In active EAE models, the clinical features exhibited, including acute, chronic, and relapsing-remitting forms, depends on several factors, such as the animal strain, the specific antigen used, and any additional adjuvants administered (Levine et al., 1966, Tsunoda et al., 2000). For example, PLP immunization induces a relapsing-remitting disease course in mice (Tuohy et al., 1989), while MOG immunization typically leads to a chronic disease phenotype (Tompkins et al., 2002). The distinct characteristics of these active EAE models allow researchers to investigate more specific aspects of MS pathogenesis and treatment.

As research progressed, $CD4^+$ T cells were identified as the key mediator of MS pathogenesis. To directly examine their role, passive EAE models were introduced. These models are induced by the intravenous or intraperitoneal transfer of pre-activated myelin-reactive $CD4^+$ T cells into recipient animals, which then develop EAE symptoms (Robinson et al., 2014). When studying $CD4^+$ T cells, passive EAE offers significant advantages over the active models. First, the disease is induced by $CD4^+$ T cells which is in contrast to active EAE which immunization induce activation of different immune cell types. In addition, it allows researchers to modify T cells in vitro and use well-matched control T cells. This enables precise research of gene expression, migration, and cellular function of $CD4^+$ T cells during EAE. Additionally, passive EAE in rats is highly reproducible and stable, making it a valuable tool for investigating the specific role of $CD4^+$ T cells in autoimmune neuroinflammation.

Spontaneous EAE is a type of disease model that naturally occurs by genetically modifying the T cell receptor (TCR) in mice to specifically recognize CNS-related antigens, such as the MOG, MBP, or PLP. The underlying theory of spontaneous EAE is based on the abnormal recognition and attack of CNS self-antigens by T cells, mimicking the initiation and progression of autoimmune attacks in MS. Commonly used spontaneous EAE models include the MBP $_{Ac1-10}$-specific TCR transgenic mice (Goverman et al., 1993), the MOG_{35-55}-specific 2D2 mice (Bettelli et al., 2003), and the $PLP_{139-151}$-specific TCR transgenic mice (Waldner et al., 2000, Croxford et al., 2011). These models particularly help us gain a deeper understand of factors that contribute to the onset of CNS autoimmunity. However, spontaneous EAE models also show obvious limitations, such as inconsistent disease onset, significant variability in incidence, and a strong dependence on specific genetic backgrounds and environmental conditions (Croxford et al., 2011).

In conclusion, although the EAE model, despite being widely used in MS related animal research, has its limitations. Many EAE models cannot fully replicate the complexity of MS. In addition, MS is induced by artificial stimulation such as immunization, T cell transfer or transgenic mice which have high proportion of autoreactive T cells while trigger of MS is still largely unknown. Therefore, it is crucial to carefully select the most suitable EAE model for each research objective, acknowledging the inherent limitations of each approach.

1.5. Role of Immune Cells in MS

1.5.1 $CD4^+$ T Cells in MS/EAE

As mentioned above, $CD4^+$ T cells have been widely recognized as the key initiators of MS and EAE. Numerous clinical, histological, and experimental studies have shown that these cells play a critical role in both the initiation and progression of the disease (Kunkl et al., 2020, Schafflick et al., 2020).

Among $CD4^+$ T cells, the T helper 1 (Th1) and T helper 17 (Th17) subsets are pointed out in the MS/EAE (Voskuhl et al., 1993, McKenzie et al., 2006). Although Th1 and Th17 cells have distinct functions, both can independently induce the passive EAE model through adoptive transfer activated Th1/Th17 cells (Domingues et al., 2010), which confirmed their pathogenic role in the disease. The differentiation of naive T cells into Th1 cells is primarily driven by IL-12 and interferon-γ (IFN-γ) (Romagnani et al., 2009). Under IL-12 stimulation, STAT4 in T cells is activated, promoting Th1 differentiation (Murphy et al., 1999). IFN-γ further enhances Th1 differentiation by activating STAT1 (Murphy et al., 1999).

The main function of Th1 cells is to activate macrophages and cytotoxic T lymphocytes, enhancing the immune response by secreting cytokines such as IFN-γ, tumor necrosis factor-β (TNF-β), and IL-2

(Kunkl et al., 2020). In MS and EAE, Th1 cells contribute to CNS inflammation by releasing IFN-γ and TNF-β at lesion sites, leading to BBB disruptions, myelin damage, and axonal degeneration. Additionally, Th1 cells recruit other immune cells, such as monocytes and macrophages, into the CNS, further intensifying inflammation and tissue destruction (Kunkl et al., 2020). In the early stages of active MS lesions, levels of Th1-related cytokines, such as IFN-γ, increase at the lesion site (Lock et al., 2002). Although the pathogenic role of IFN-γ in the MS/EAE is clear, the effectiveness of anti-IFN-γ treatment is still controversial. Mice lacking IFN-γ or STAT1 did not develop resistance to EAE; instead, they experienced more severe EAE symptoms (Gran et al., 2004, Ferber et al., 1996). While a lack of T-bet in mice, the key transcription factor guiding T cell differentiation into the Th1 phenotype, creates resistance to developing EAE (Nath et al., 2006).

Th17 cells are another important subset of $CD4^+$ T cells and play crucial role in the pathogenesis of MS/EAE. Several cytokines, including IL-1β (Sato et al., 2023), IL-6 (Kimura and Kishimoto, 2010), IL-23 (Stritesky et al., 2008), and TGF-β (Choi et al., 2021), have been reported to induce Th17 differentiation. These cells are named for their hallmark expression of IL-17 but also produce IL-21 and IL-22 (Nalbant, 2019). Notably, IL-23 knockout mice exhibit an impaired Th17 response and resistance to EAE (Awasthi et al., 2009). IL-17, a highly proinflammatory cytokine, is particularly destructive to the BBB (Huppert et al., 2010). Within the CNS, IL-17 stimulates microglia (Sasaki et al., 2020), astrocytes (You et al., 2017), and oligodendrocytes (Wang et al., 2017), amplifying their inflammatory gene expression. This cascade of immune activation exacerbates neuroinflammation, intensifies immune responses within CNS lesions, and ultimately contributes to tissue damages.

1.5.2 $CD8^+$ T Cells in MS/EAE

As the understanding of MS/EAE deepens, the role of $CD8^+$ T cells is gaining increasing attention. While $CD4^+$ T cells have been firmly proven as the main drivers of MS/EAE, growing evidence points that $CD8^+$ T cells also play an important role in disease onset and progression. In fact, the number of $CD8^+$ T cells in MS lesions has been confirmed to be far greater than the number of $CD4^+$ T cells (Battistini et al., 2003). They are often found near oligodendrocytes and demyelinated axons, and their activity shows a clear association with the axonal damage (Liblau et al., 2002, Neumann et al., 2002, Frischer et al., 2009), which suggests that $CD8^+$ T cells may contribute to CNS damage through direct mechanisms.

From numerous immunology studies, the cellular function of $CD8^+$ T cells is being widely accepted as eliminating target cells via cytotoxic effects by releasing cytotoxic molecules such as granzyme B and perforin, as well as through Fas/FasL-mediated cytotoxic pathways (Medana et al., 2000, Giuliani et al., 2003). Additionally, $CD8^+$ T cells secrete pro-inflammatory cytokines like IFN-γ and IL-17, further

amplifying the inflammatory response. These cytokines not only cause direct damage to CNS tissues but also enhance inflammation by recruiting other immune cells, such as $CD4^+$ T cells and monocytes (Biddison et al., 1998). In MS lesions, $CD8^+$ T cells have been proven by studies to contribute to CNS damage through above mentioned mechanisms. First, they induce cytotoxic effects, leading to demyelination and axonal injury. For example, in vitro study has shown that $CD8^+$ T cells can rapidly trigger axonal transection upon contact with neurons expressing MHC class I (Medana et al., 2001). $CD8^+$ T cells also activate microglia and astrocytes by secreting pro-inflammatory cytokines like IFN-γ and IL-17, worsening inflammation and tissue damage (Salou et al., 2015). In RRMS patients, $CD8^+$ T cells were found to be significantly reactive to CNS peptides than those from healthy controls, whereas $CD4^+$ T cells did not show this difference (Crawford et al., 2004). Animal models provide additional evidence of $CD8^+$ T cell involvement in MS/EAE. For example, transferring MOG_{35-55}-specific $CD8^+$ T cells into C57BL/6 mice induces a more severe disease than the traditional EAE model (Sun et al., 2001).

In summary, $CD8^+$ T cells contribute to CNS damage in MS and EAE through cytotoxicity and secretion of pro-inflammatory cytokines. Their high numbers in lesions, strong migration ability, and antigen-specific responses further support their important role in disease pathology. However, the exact mechanisms of $CD8^+$ T cell activity in MS require further study.

1.5.3 B Cells in MS/EAE

In the MS patients B cells, plasmablasts, and plasma cells are found in the CSF, meninges, and parenchyma (Michel et al., 2015). Over 90% of MS patients exhibit OCBs, which represent intrathecally produced antibodies, in the CSF (Link and Huang, 2006). These intrathecal antibodies are produced by clonally expanded B cells and are likely the result of secondary immune responses during CNS damage (Brandle et al., 2016). Post-mortem studies have demonstrated the presence of B cells and plasma cells in perivascular demyelinating lesions (Lassmann et al., 2007, Barnett et al., 2009) and, notably, they are also found within ectopic follicle-like aggregates in the leptomeninges (Serafini et al., 2004). These aggregates are composed of B cells, plasma cells, T cells, and follicular DCs. They are frequently observed in SPMS patients and are associated with greater disease severity (Howell et al., 2011). The aggregates secrete cytotoxic factors that diffuse into the gray matter, creating a gradient of neuronal damage, demyelination and microglia activation from the meninges to deeper CNS tissues (Magliozzi et al., 2010).

The functional contributions of B cells extend beyond their antibody-secreting capabilities. They could serve as APCs and secrete pro-inflammatory cytokines such as IL-6, which amplify immune responses (Getahun and Cambier, 2019). In EAE models, MOG-specific B cells have been shown to

promote disease by activating pathogenic T cells and accelerating disease onset through IL-6-driven myeloid expansion, rather than directly via antibody production (Thomann et al., 2023). B cell-depleting therapies, such as rituximab and ocrelizumab, have demonstrated significant efficacy in reducing relapse rates and inflammatory lesions in RRMS (Cross et al., 2006, Hauser et al., 2008, del Pilar Martin et al., 2009). These therapies target CD20-expressing B cells, efficiently deplete memory and naive B cells but cannot target plasmablasts or plasma cells, as these lack CD20 expression. Consequently, the clinical benefits of these therapies are attributed to reduced antigen presentation and cytokine production rather than decreases in antibody levels (Hauser et al., 2008, Hauser et al., 2017).

1.5.4 Myeloid Cells in MS/EAE

As mentioned above, the CNS is a unique system that lacks a typical lymphatic structure. Its fragile parenchyma, which has a rich blood supply, is mechanically protected by the meninges and a dense BBB, keeping it relatively isolated from the peripheral immune system. Under normal conditions, peripheral immune cells rarely migrate to the CNS for patrolling. Instead, special groups of myeloid cells residing in the CNS, such as microglia and CNS-associated macrophages (CAMs), are responsible for maintaining immune homeostasis within the CNS (Herz et al., 2017).

Microglia are the resident macrophages of the CNS, continuously monitoring for pathogens and damage through their highly dynamic processes and extensive expression of immune receptors (Galatro et al., 2017, Prinz et al., 2019). During CNS inflammation, their roles become more complex and diverse, ranging from promoting neuroinflammation and tissue damage to facilitating repair and regeneration. The specific function of microglia depends on the local environment and activation state.

Microglial activation is an early and persistent feature of MS/EAE lesions. Even before the onset of clinical symptoms, microglia become activated by serum proteins such as fibrinogen (Davalos et al., 2012). Fibrinogen crosses the BBB, guides and activates microglia aggregate around blood vessels in the perivascular area. Activated microglia then release reactive free radicals, pro-inflammatory cytokines, and chemoattractants, initiating a mild neuroinflammation and recruiting peripheral immune cells into the CNS (Maggi et al., 2014). Studies have shown that depletion of microglia can attenuate disease severity and demyelination in EAE (Heppner et al., 2005). This highlights the potential role of microglia in driving disease onset and promoting T cell infiltration. However, microglia are not only active during the disease onset, but continuously play a role throughout the entire course of MS. In MS patients, the microglial activation has been observed to correlate with disability progression (Politis et al., 2012).

In demyelinating MS lesions, activated microglia contribute to oligodendrocyte and axonal damage. They were found to exacerbate neuronal injury by producing pro-inflammatory cytokines such as TNF and release reactive oxygen species and nitric oxide (Takeuchi et al., 2006). Additionally, microglia can interact directly with infiltrating T cells, enhancing their reactivation (Strachan-Whaley et al., 2014). For instance, in vitro studies have demonstrated that microglia preactivated with IFN-γ can effectively induce the proliferation of naive T cells and activate pro-inflammatory Th1 cells (Aloisi et al., 1999). This interaction creates a self-reinforcing loop of inflammation, as activated T cells further stimulate microglia to produce additional inflammatory mediators. Microglia can also show anti-inflammatory and reparative functions under certain conditions. Within MS and EAE lesions, microglia can adopt diverse activation states, ranging from pro-inflammatory (M1-like) to anti-inflammatory and reparative (M2-like) phenotypes (Lloyd and Miron, 2019). Pro-inflammatory microglia dominate early lesion formation, but during the resolution phase or remission in EAE, anti-inflammatory alternatively activated microglia emerge that are thought to promote tissue repair (Lloyd and Miron, 2019).

CNS-associated macrophages (CAMs), located at CNS interface regions such as the perivascular space, leptomeninges, and choroid plexus, serve as critical mediators at the border of peripheral circulation and CNS systems (Dermitzakis et al., 2023). Notably, perivascular CAMs reside between the endothelial and parenchymal basement membranes of post-capillary venules, where they encounter infiltrating leukocytes (Mishra and Yong, 2016). These macrophages present self-antigens to infiltrating T cells, reactivating them and driving their effector functions. Reactivated effector T cells, such as Th1 and Th17 cells, release cytokines and proinflammatory molecules that induce a proinflammatory phenotype in CAMs. This self-amplifying inflammatory loop disrupts the BBB, increasing the infiltration of activated T cells and other immune cells into the CNS. In summary, CAMs contribute significantly to the initiation and maintenance of neuroinflammation.

Another major group of myeloid cells, called monocytes, infiltrate CNS lesions from the bloodstream and differentiate into macrophages. This makes them play a direct role in demyelination. These cells accumulate at lesion sites, phagocytose myelin debris. Inhibiting monocyte migration markedly reduces EAE severity (Agrawal et al., 2011). In MS patients, monocyte profiles differ from control group, showing higher levels of pro-inflammatory profiles in circulation during active disease states (Chuluundorj et al., 2014, Waschbisch et al., 2016). To disrupt the BBB and access the CNS, monocytes need to express matrix metalloproteinases (MMPs), which degrade extracellular matrix components (Wells et al., 2015). Multiple studies have proven that monocytes produce significant amounts of MMPs during EAE (Yong et al., 2001, Nuttall et al., 2007). Once infiltrated into the CNS, the monocytes contribute to the local immune responses by secreting cytokines and chemokines

that recruit additional immune cells and further amplify inflammation (Benveniste, 1997, King et al., 2009). The monocytes differentiate into macrophages, which exhibit remarkable functional plasticity depending on the local environment. Traditionally classified into pro-inflammatory (M1) and anti-inflammatory (M2) phenotypes. M1 macrophages, mediated by IFN-γ and lipopolysaccharides, generate oxidative stress and release inflammatory mediators that exacerbate tissue injury (Nikic et al., 2011, van Horssen et al., 2011, Mossakowski et al., 2015). Conversely, M2 macrophages, which are mediated by IL-4, IL-10, and IL-13, display enhanced phagocytic activity, secrete regulatory cytokines like IL-10, and support tissue repair, including remyelination (Murray et al., 2014).

DCs, another myeloid cell subtype, play a pivotal role in antigen presentation and T cell activation, bridging innate and adaptive immunity (Eisenbarth, 2019). DCs have been found within the CNS during EAE, where they function as key APCs (Mundt et al., 2019). Moreover, in MS, DCs in circulation and in the CSF exhibit increased expression of costimulatory molecules and increased pro-inflammatory cytokines, such as IFN-γ, TNF, and IL-6 (Mishra and Yong, 2016). The enhanced pro-inflammatory profile of DCs correlates with disease activity, as evidenced by increased numbers of DCs in the CSF during relapse. Although once thought to exist primarily in peripheral compartments, accumulating evidence indicates that dendritic cells migrate to the CNS during MS and EAE, contributing directly to the local immune response (Clarkson et al., 2014).

In summary the immune system's balance is disrupted in MS/EAE, with various immune cells contributing to inflammation and neurodegeneration. Among these, $CD4^+$ T cells are identified as the initiators of disease, making them central to understanding MS pathogenesis. These CNS autoreactive T cells escape tolerance, become activated in the periphery, migrate to the CNS, and trigger local inflammation by interacting with resident immune cells like microglia, macrophages, and DCs. This inflammatory cascade recruits additional immune cells, including $CD8^+$ T cells and B cells, amplifying CNS damage.

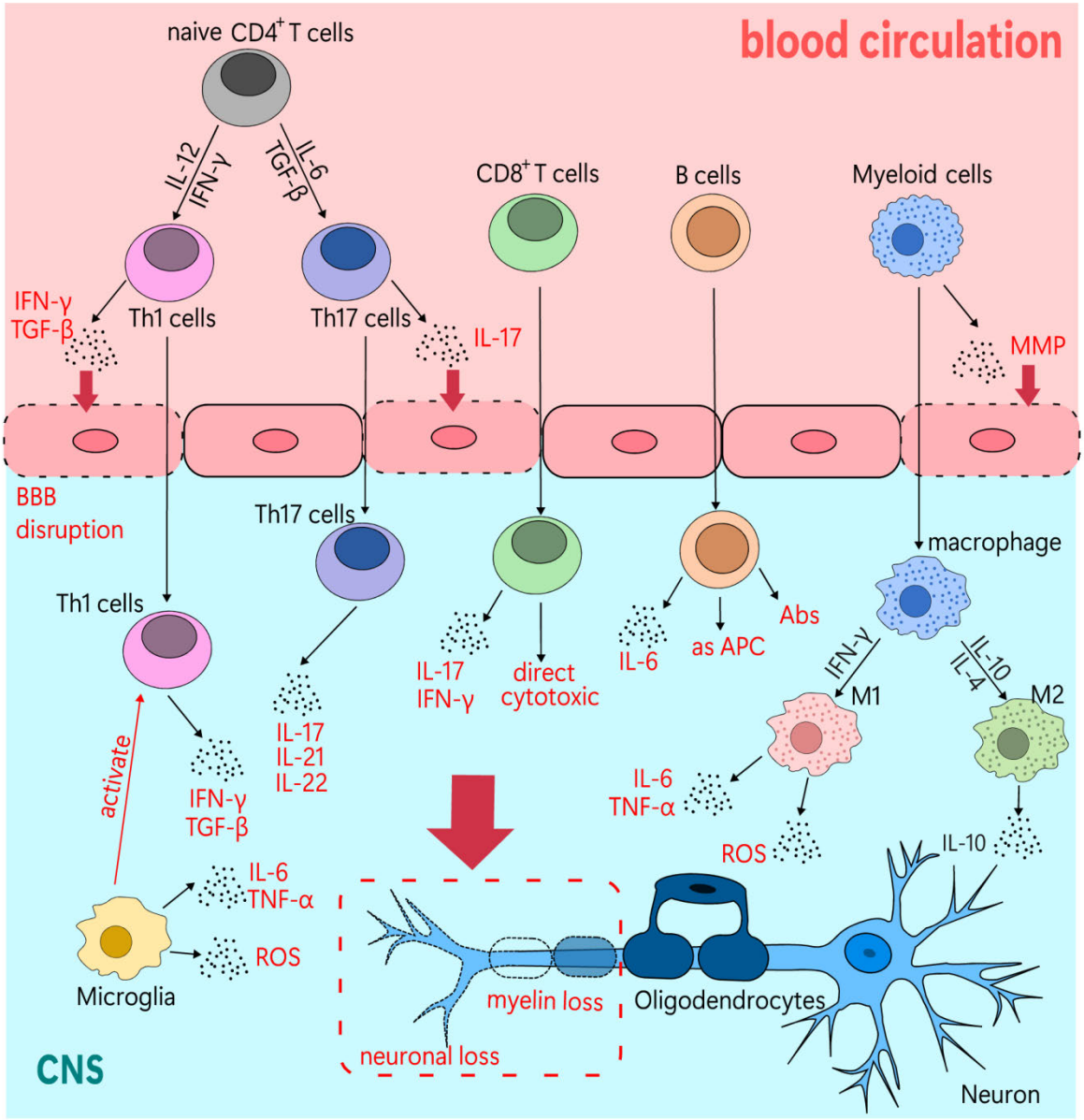

Figure 2 Role of Immune Cells in MS

Multiple immune cells, including Th1, Th17, and CD8⁺ T cells, along with B cells, monocytes, macrophages, and microglia, work together to drive inflammation in CNS lesions during MS. Peripherally activated CD4⁺ T cells differentiate into Th1 and Th17 subsets in response to specific cytokine signals. When they reach the CNS vasculature, Th1 cells secrete IFN-γ and TGF-β, while Th17 cells produce IL-17, both of which contribute to BBB disruption. Once inside the CNS, these cells further amplify inflammation and trigger myelin and neuronal loss by releasing distinct proinflammatory cytokines. As MS progresses, CD8⁺ T cells infiltrate CNS lesions as well, causing additional myelin damage and tissue destruction through direct cytotoxicity and the secretion of proinflammatory cytokines, including IL-17 and IFN-γ. Meanwhile, B cells secrete antibodies, produce proinflammatory cytokines such as IL-6, and act as APCs to activate infiltrating T cells. Moreover, monocytes from the peripheral migrate to CNS blood vessels, where they release MMPs, further weakening the BBB. Upon entering the CNS parenchyma, they differentiate into macrophages, which adopt either an M1 or M2 phenotype depending on the surrounding cytokine environment. M1 macrophages produce large amounts of reactive oxygen species (ROS) and proinflammatory cytokines like IL-6 and TNF-α, driving tissue damage. In contrast, M2 macrophages secrete anti-inflammatory cytokines such as IL-10, playing a role in controlling inflammation and promoting tissue repair. Activated microglia in MS function in a similar manner to

macrophages, releasing ROS and inflammatory cytokines (IL-6, TNF-α) that worsen tissue damage. In addition, they interact with infiltrating $CD4^+$ T cells to enhance Th1 activation, further intensifying neuroinflammation. The red labels in the figure highlight the key factors responsible for myelin and neuronal loss.

1.6. $CD4^+$ T Cell Pathogenicity

1.6.1. Autoreactive T Cells Appear in the Circulation

CNS autoreactive $CD4^+$ T cells are widely regarded as the primary initiators of MS/EAE. While a small population of autoreactive T cells exists commonly in healthy individuals (Danke et al., 2004), these cells typically remain quiescent and do not provoke autoimmune diseases. The reason of their existence in the periphery, particularly in MS remains unclear, thymic education disruptions and degeneracy of T cell recognition might be the factors leading it.

1.6.1.1 Thymic Education Disruption

T cells originate in the bone marrow and mature in the thymus. During their development, immature T cells randomly express unique TCRs generated through random recombination of gene segments to generate a highly diverse repertoire capable of recognizing various antigens presented by MHC molecules. Positive selection ensures that T cells can recognize self-MHC molecules, while negative selection eliminates T cells that strongly bind to self-MHC molecules. Cells that successfully pass these processes mature into functional $CD4^+$ or $CD8^+$ single-positive T cells, joining the circulating pool of naive T cells prepared to recognize foreign antigens (Kaskow and Baecher-Allan, 2018). However, some autoreactive T cells with low-affinity TCRs can escape negative selection and enter the peripheral immune system as naive $CD4^+$ T cells. Tregs, a special subset of autoreactive T cells that arise during thymic selection under physiological conditions, are critical for maintaining immune tolerance (Sakaguchi et al., 2007). Beyond Tregs, a small population of autoreactive $CD4^+$ T cells persists in healthy individuals as well as MS patients, typically remaining quiescent (Danke et al., 2004).

Normally APCs in thymus, including medullary thymic epithelial cells (mTECs) and DCs, express the autoimmune regulator (AIRE), enabling the presentation of tissue-specific antigens (TSAs) to immature T cells (Yu et al., 2015, Perry et al., 2014). Autoreactive T cells are then either inactivated or eliminated in a process known as negative selection. Deficiencies in AIRE expression or genetic factors, such as certain HLA alleles, can impair negative selection, resulting in the escape of autoreactive T cells into the circulation and increasing the risk of autoimmune diseases. For example,

it has been reported that AIRE knockout mice can develop spontaneous autoimmune disease with lymphocytes infiltration into multiple organs and tissues (Nalawade et al., 2018).

The gut microbiota also plays a critical role in thymic education. The microbiome itself and its metabolites contribute to immune homeostasis and have been implicated in the regulation of immune tolerance. Dysbiosis of the gut microbiota has been linked to a range of autoimmune diseases, including MS (Yurkovetskiy et al., 2015). Germ-free (GF) mice exhibit thymic growth deficits, pointing out the importance of gut microbes in thymic development (Bealmear and Wilson, 1966, Wilson et al., 1965). The microbiota influences thymic function through two primary mechanisms (Kawakami and Wekerle, 2024). One is the soluble compounds, like bacterial metabolites and other molecules for example short-chain fatty acids (SCFAs). They enter the bloodstream, reach the thymus, and influence T cell maturation. Another mechanism are signals carried by macrophages and DCs, who are directly transmitted to the thymus. These signals can reach the thymus via leaky medullary blood vessels, bypassing the cortex, and influencing T cell maturation and the antigen-specific repertoire within the medulla. Bacterial components can activate pattern recognition receptors on thymic epithelial cells, inducing the AIRE and TSAs expression, leading to the elimination of autoreactive T cells. However, reduced AIRE expression in GF mice impairs this process, leading to the survival of autoreactive T cells (Nakajima et al., 2014). Additionally, SCFAs metabolites produced by dietary fiber digestion, enhance AIRE expression and promote Treg differentiation by binding to G-protein-coupled receptors (GPCRs) on thymic epithelial cells (Ni et al., 2023). Together, these pathways highlight the essential role of gut microbiota in shaping the T cell repertoire and maintaining immune tolerance.

Therefore, dysfunction of the gut microbiota may disrupt thymic education, allowing autoreactive T cells to escape into circulation and contribute to autoimmune disease development in distant organs. While experimental evidence supports the role of the microbiota in regulating thymic education, direct evidence linking specific microbial populations to the leakage of CNS autoreactive T cells remains incomplete.

1.6.1.2 Degeneracy of T Cell Recognition

The pathogenesis of MS is complex, with no single self-antigen identified as solely responsible for driving the autoimmune response. Among the proposed mechanisms, degeneracy of T cell recognition and molecular mimicry have emerged as a theory with high likelihood, thus offering insights into how autoreactive T cells emerge and contribute to the disease.

Degeneracy of T cell recognition refers to the capacity of T cells to recognize and respond to a wide variety of antigens due to the structural flexibility of degenerated TCRs (Joshi et al., 2001). This degeneracy of T cell recognition is not limited to recognizing specific peptides but can also interact with multiple structurally similar antigens, including both microbial peptides and self-antigens. They may even bind directly to MHC molecules without requiring specific peptide presentation (Markovic-Plese, 2009). While this flexibility enhances adaptive immunity by enabling a broad response to diverse pathogens, it also increases the likelihood of autoreactivity, as degenerated TCRs can mistakenly recognize self-antigens. Research has estimated that a single TCR can potentially interact with up to 106 ligands under physiological conditions (Mason, 1998), providing a broad spectrum of antigen recognition but simultaneously predisposing the immune system to errors that can lead to autoimmune diseases.

In MS, degeneracy of T cell recognition appears to be important in the activation of CNS autoreactive $CD4^+$ T cells. While the frequency of these autoreactive $CD4^+$ T cells in the circulation is similar between MS patients and healthy controls (Ngono et al., 2012), these cells in MS patients exhibit enhanced proinflammatory properties, as demonstrated by their higher production of proinflammatory cytokines (Cao et al., 2015, Paroni et al., 2017). This suggests that functional, rather than numerical, differences in T cells drive disease pathogenesis. Importantly, studies have found a greater proportion of autoreactive T cells showed highly degenerated T cell recognition in MS patients compared to healthy individuals (Bielekova et al., 2000). These autoreactive T cell with degenerated T cell recognition are thought to be repeatedly activated and proliferate in vivo, leading to an expansion of their precursor populations in MS. Therefore, degeneracy of T cell recognition could be the reason for the existence of autoreactive $CD4^+$ T cells. Originally these $CD4^+$ T cells should be reactive to pathogen peptides, however degeneracy of T cell recognition leads them to also react to self-antigen.

1.6.2. Autoreactive T Cells Activated in the Peripheral

Under physiological conditions, antigens targeted by autoreactive T cells are restricted within the CNS and remain isolated from the peripheral circulation and lymphatic system due to the dense BBB protection and lack of a CNS draining lymphatic system. While the presence of CNS autoreactive $CD4^+$ T cells is a necessary condition for the development of EAE, their activation is the critical initiating step that determines whether the disease will occur. In EAE models, particularly adoptive transfer EAE models, disease induction requires the transfer of activated autoreactive T cells into recipient animals. These T cells are typically activated ex vivo using specific myelin-derived antigens

(Holda et al., 1980, Panitch, 1980) or nonspecific mitogenic agents (Panitch, 1980, Takenaka et al., 1986), such as lectins, to mimic their activation in vivo. Importantly, inactivated or naive T cells fail to induce EAE (Peters and Hinrichs, 1982, Panitch, 1980), highlighting the necessity of their prior activation. In addition, autoreactive T cells are activated by immunized antigen in active EAE models. Therefore, these transfer and active EAE models are not suitable to study natural stimulation of autoreactive T cells in the periphery. Nevertheless, the investigation to identify the natural stimulation were carried out.

1.6.2.1 Gut Microbiota Activate CNS Autoreactive $CD4^+$ T cells

Gut microbiota studies have made people realize the close connection between microbes and the immune system. The gut microbiota was found not only indispensable in immune system maturation, but also helps to maintain immune balance by educating immune cells, promoting tolerance to commensal microbes, and regulating inflammatory responses. The balanced gut microbiota ensures the immune system proper reaction to external antigens while preventing attacks on self-antigens. On the contrary, the absence/ unbalanced gut microbiota led to immune dysregulation and an increased risk of autoimmune diseases. Indeed, microbiota can stimulate autoreactive T cells in the periphery.

For example, it was shown that in relapsing-remitting (RR) mice, transgenic modified TCR specific to MOG peptide 92-106 on the $CD4^+$ T cells led to spontaneous development of EAE in most of the mice (Berer et al., 2011). However, when mice were kept in GF condition, they rarely develop EAE (Berer et al., 2011). The result suggests that without gut microbiota, MOG-reactive $CD4^+$ T cells fail to activate. When GF mice were immunized with MOG or received pre-activated MOG reactive T cells, they started to develop EAE symptoms. This finding is a firm evidence that gut microbiota is the indispensable factor to activated autoreactive $CD4^+$ T cells (Berer et al., 2011).

By combining intravital imaging with calcium-sensing protein Twitch-2B, the activation of autoreactive $CD4^+$ T cells in the small intestinal lamina propria has been successfully visualized. When the same experimental setup was applied to GF 2D2 mice or after administering an anti-MHC class II antibody, the activation signals were obviously weakened (Bauer et al., 2023). Additionally, specific bacterial strains within the human gut microbiota have been linked to MS. For example, Lactobacillus reuteri mimics the MOG epitope, directly triggering T cell activation, while members of the Erysipelothrix family act as adjuvants, enhancing Th17 polarization and function, ultimately leading to more severe EAE symptoms (Miyauchi et al., 2020).

1.6.2.2 Lungs as an Alternative Site of T Cell Activation

Beyond the gut, the lung is another main site for peripheral T cell activation, especially under extra environmental triggers, such as smoking, air pollution, and viral respiratory infections (e.g. influenza). These factors induce local inflammation and irritation in the lungs, creating a microenvironment that supports T cell activation. In smoking-related lung inflammation, T cells were found displaying high proliferative and activated phenotype. Also, these environmental factors triggered lung inflammation has been proved to exacerbate MS development and increase the risk of disease onset (Wu et al., 2023, Marrodan et al., 2019, Hedström et al., 2023).

Studies combining additional lung inflammation, caused by smoking or infection, with the EAE model have shown that lung inflammation indeed can activate autoreactive T cells. Once activated in the lung, these T cells can migrate directly to the CNS and initiate autoimmunity (Odoardi et al., 2012).

1.6.2.3 T Cell Activated via Molecular Mimicry

As previous described, the gut and lung are two sites that induce autoreactive T cells activation which further contributes to MS/EAE. However, CNS-related antigens are not naturally present in these organs. This raises an important question: how are these cells activated in the periphery? Indeed, molecular mimicry can explain how microbiota activate peripheral CNS self-reactive T cells. Molecular mimicry means microbial peptides share a similar structure as self-antigens, allowing T cells to cross-react with both of them. In MS, molecular mimicry is a research hotspot, particularly in relation to key myelin proteins such as MBP, MOG, and PLP. Researchers want to find out the exact mechanisms driving autoreactive T cell activation and the factors that trigger this immune response. Bacterial peptides from gut commensals, including from Bacteroides and Bifidobacterium species, have been revealed to share a sequence homology with regions of MBP, providing a molecular basis for their ability to activate autoreactive T cells (Westall, 2006). These microbial peptides not only mimic myelin epitopes but are also accompanied by bacterial adjuvants like N-acetylmuramyl dipeptide, which enhance the immune response, functioning similar as adjuvants used in EAE models (Elsayed et al., 2022).

Viruses can also induce molecular mimicry during MS/EAE, with the influenza virus serving as a promising example. T cell clones derived from MS patients react with both viral hemagglutinin (HA) and myelin-derived peptides (Markovic-Plese et al., 2005), despite minimal sequence similarity (Markovic-Plese et al., 2005). Different from the molecular mimicry of bacteria and myelin proteins as mentioned above, there was no obvious structural overlap found between viral hemagglutinin (HA) and myelin proteins, which shows researchers TCR recognition is actually more flexible than we thought.

Among viruses, EBV stands out as being strongly correlated with MS. EBV is a DNA virus that establishes a lifelong latency in B cells, and an infection in later life has been shown to significantly increase the risk of MS (Libbey et al., 2007). A Study by Lang et al. found that $CD4^+$ T cells from an MS patient could recognize both MBP_{85-99} and an EBV DNA polymerase peptide ($EBV_{627-641}$) (Libbey et al., 2007, Lang et al., 2002). Further structural analyses of MHC-peptide complexes revealed that the TCR contact surfaces for DRB1*1501 MBP_{85-99} and DRB5*0101 $EBV_{627-641}$ were highly similar, implying the TCR cross-reaction is due to molecular mimicry.

Whether gut bacteria, influenza, or the EBV virus, all have shown potential molecular mimicry in activating CNS autoreactive $CD4^+$ T cells in the periphery. This peripheral activation, combined with subsequent CNS infiltration, plays a key role in MS pathogenesis and underscores the complex interplay between environmental factors, immune dysregulation, and genetic susceptibility.

1.6.2.4 CNS Antigen Leak to the Peripheral Activate $CD4^+$ T cells

In addition to the activation of autoreactive T cell through molecular mimicry, there is evidence that even in a healthy state, the CNS is functionally connected to the dcLNs via meningeal lymphatic vessels, providing another pathway for the activation of autoreactive T cells (Louveau et al., 2015). Antigens from the CNS, transported via the glymphatic system and meningeal lymphatics, can be presented in dcLNs under both healthy and inflammatory conditions (Louveau et al., 2015). During inflammation, DCs, who captured CNS antigen in dcLNs may present through MHC-II. This could potentially activate CNS autoreactive T cells. This process has been shown to involve in EAE pathogenesis, as disrupting meningeal lymphatic drainage or removing dcLNs delays the onset of disease (Louveau et al., 2015).

In addition to traditional sites of T cell activation, studies have suggested that early BBB disruptions may also contribute to the peripheral activation of T cells. Two-photon microscopy in EAE models has revealed that transient vessel leakage happens in the CNS vessels shortly after disease induction (Barkauskas et al., 2015). These leakages occur before immune cell infiltration, which shows as a potential way of CNS antigen leakage to the peripheral. However, while these findings suggest a possible link between BBB disruptions and peripheral T cell activation, up to date data cannot provide a clear conclusion. Such events are more likely to exacerbate pre-existing autoimmune responses rather than serve as the primary trigger for autoreactive T cell activation.

1.6.3. Migration of CNS Autoreactive $CD4^+$ T Cells

The second critical step in the onset of MS/EAE is the migration of activated autoreactive $CD4^+$ T cells to the CNS. This process involves two main stages: first, autoreactive T cells phenotypic shift from an activated phenotype to a migratory phenotype; and second, the migration of these cells to the CNS, including rolling, crawling, adhesion, and extravasation. Both experimental and clinical studies have demonstrated that blocking T cell migration to the CNS is an effective strategy to prevent neuroinflammation and delay the onset of neurological symptoms, underscoring the importance of this process in disease pathogenesis.

1.6.3.1 Acquisition of Migratory Phenotype in Peripheral Tissues

In the transfer EAE model induced by MBP-reactive T cells (T_{MBP} cells) for instance, T cells are activated in vitro before transferring into the recipient animals. However, it has been shown that they don't directly migrate to the CNS. The T_{MBP} cells disappear from circulation shortly after injection, only to reappear in large numbers in the blood on around two days post-transfer (Flügel et al., 2001). In this phase, the T_{MBP} cells accumulate in peripheral tissues. For example, T_{MBP} cells transiently localize in the parathymic lymph nodes (ptLNs) within 12-36 hours, subsequently appearing in the spleen by 60 hours. Between 60-80 hours, T_{MBP} cells begin to infiltrate the CNS in large numbers, coinciding with a sharp decline in their numbers in the spleen (Flügel et al., 2001). Interestingly, Ovalbumin (OVA) specific T cells ($T_{OVA\text{-}GFP}$ cells), which are not reactive to CNS antigens, follow a similar distribution pattern initially, but fail to infiltrate the CNS. They instead accumulate in peripheral lymph nodes (LNs) (Flügel et al., 2001). This delay of infiltration occurs at the same time as their accumulation and further modulation in the lung, spleen, and LNs. Among those peripheral organs, spleen and lung, T_{MBP} cells were found to experience significant phenotypic changes, with increased expression of migration-related molecules (Odoardi et al., 2012). For example, the T_{MBP} cells downregulate activation markers such as pro-inflammatory cytokines, co-stimulatory molecules, and cell cycle-related genes, IL-2R (CD25) and OX-40 while expressing MHC class II molecules. Simultaneously, these cells upregulate the genes associated with cell motility, such as chemokine receptors, like C-C chemokine receptor 2 (Ccr2), and migration related GPCRs - sphingosine-1-phosphate receptor 1 (S1pr1), adhesion molecules like Itgb7 and transcription factors Klf2 (Odoardi et al., 2012). This phenotypic shift reduces the inflammatory and proliferative properties of these cells while enhancing their motility and capacity to adhere to endothelial cells, key features required for CNS infiltration (Flügel et al., 2001, Odoardi et al., 2012). Indeed, when spleen- or lung-derived migratory T cells are transferred into naive recipient animals, induce EAE symptoms more rapidly than in vitro-activated T cells. This points out that T_{MBP} cells phenotype

move to migratory phenotype within the spleen and lung (Flügel et al., 2001, Odoardi et al., 2012). However, detailed mechanism of the phenotypic change is still largely unknown.

1.6.3.2 Molecules Associate with T Cell Migration to CNS Blood Vessels

$CD4^+$ T cells exit peripheral organs and enter the bloodstream, followed by reaching the CNS blood vessels. This process is the result of the coordinated function of multiple migration related molecules, including adhesion molecules, chemokines, and sphingosine-1-phosphate (S1p) related molecules. While the exact molecular mechanisms mediating T cell trafficking between peripheral organs and blood circulation in MS/EAE remain unclear, we introduced two important molecules relevant to our study, Ccr7 and S1pr1, about their roles in directing the migration of autoreactive T cells into and out of peripheral organs during the early phase of EAE/MS.

Ccl19/Ccl21 and Ccr7

As the previously described, it was shown that in the initial phase of autoreactive T cell migration during EAE, T cells first accumulate in secondary lymphoid organs (SLOs) before progressing toward the CNS. Ccr7 should be discussed first, as it is the key homing molecule that guides T cell migration into SLOs.

Ccr7 is abundantly expressed on naive T cells and central memory T cells, ensuring their homing and residing in SLOs under homeostatic conditions. Its ligand, Ccl21, is widely found on high endothelial venules (HEVs). HEV is a specialized post-capillary vascular structures within LNs paracortical regions (Masopust and Schenkel, 2013). Ccl21 is immobilized on HEVs by binding to heparin glycosaminoglycans, creating a chemokine gradient that attracts Ccr7-expressing T cells (Masopust and Schenkel, 2013). Upon engaging Ccl21, Ccr7 signaling induces the expression of lymphocyte function-associated antigen 1 (LFA1) on T cells. LFA1 binds to intercellular adhesion molecule 1 (ICAM1) on HEVs, slowing down T cells movement and mediating their rolling which then promote their transmigration into the LNs (Masopust and Schenkel, 2013). Although Ccr7 is a powerful mediator of T cell homing to SLOs, it is not indispensable for all subsets. Alternative pathways involving molecules such as α4β7 integrin, which interacts with mucosal vascular addressin cell adhesion molecule 1 (MADCAM1) in gut-associated SLOs (Bargatze et al., 1995), or CXC-chemokine receptor 4 (Cxcr4), which in some condition replace for Ccr7 function in T cells homing to LNs (Scimone et al., 2004, Okada et al., 2002).

Once inside the SLOs, Ccr7 continues to function on T cells, especially in the T cell zones (Worbs et al., 2007). Within T cell zones, Ccr7 ligands, Ccl19 and Ccl21 are also abundantly present (Okada and Cyster, 2007). Some chemoattractants, when they are without the concentration gradient, can

function to promote immune cells movement through a process known as chemokinesis (Okada and Cyster, 2007). The interaction between Ccr7 on T cells and its ligands within LNs, especially T cell zone as previous described, leads to chemokinesis. This enhances the T cell motility, meaning these T cells have higher ability to scan APCs as well as higher efficiency of antigen recognition (Okada and Cyster, 2007).

In MS, evidence shows that Ccr7 might function in immune surveillance and immune activation as well as lymphocyte migration. For example, while $Ccr7^+$ T cells are found in high abundance in the CSF of MS patients, at the same time the T cells within the parenchymal MS lesions lack Ccr7 expression (Kivisakk et al., 2004). This Ccr7 expression absence on T cells supports those effector T cells to infiltrate into inflammatory lesions, where they execute their pathogenic functions. Therapeutic strategies such as IFN-β treatment have shown the function in modulating Ccr7 expression. By upregulating Ccr7 on lymphocytes, IFN-β treatment redirects their migration from sites of CNS inflammation back to SLOs, reducing the extent of neuroinflammation (Vallittu et al., 2007). Further investigation into Ccr7 in EAE models confirmed its critical role in T cell migration. In active EAE, $CD4^+$ T cells lacking Ccr7 failed to effectively initiate the autoimmune cascade (Belikan et al., 2018). On the contrary, in passive EAE using in vitro activated Ccr7 deficient Th17 cells are still capable to induce EAE with disease onset and severity comparable to those induced by Ccr7 sufficient Th17 cells (Belikan et al., 2018). These results suggest that while Ccr7 is essential for the early activation and priming of T cells, it is dispensable for their subsequent migration and effector functions within the CNS once T cells being primed and released into the circulation. Advanced imaging techniques, such as two-photon laser scanning microscopy, have further clarified the function of Ccr7. Studies tracking Ccr7-deficient and wild-type $CD4^+$ T cells in CNS inflammatory lesions revealed no significant differences in their motility or dynamics (Belikan et al., 2018). This reinforces the conclusion that Ccr7 primary role lies in the initiation of the autoimmune response rather than in the later phases of CNS infiltration and tissue damage (Belikan et al., 2018). In summary, Ccr7 serves as a prominent pathway to mediate T cell migration to SLOs in the early stage of MS/EAE. Additionally, Ccr7 ensures effective interactions with APCs within the SLOs, facilitating the activation of autoreactive T cells, if there is corresponding antigen existing.

S1p and S1pr1

S1pr1 is a GPCR that plays a central role in regulating T cell trafficking by responding to S1p, a bioactive lipid mediator. S1p is distributed in a concentration gradient, with a high concentration in the blood and lymph, and a low concentration in tissues and SLOs, such as LNs (Hla et al., 2008). This

gradient creates directional cues that guide T cell movement, ensuring immune cells patrol around and migrate to sites of inflammation.

The interaction between S1p and S1pr1 provides positive attraction for leaving SLOs, so that T cells could egress from SLOs to blood against Ccl19, Ccl21/ Ccr7 signaling. S1p is synthesized by erythrocytes and endothelial cells through the phosphorylation of sphingosine by sphingosine kinases 1 and 2 (Sphk1/2) (Garris et al., 2014). It is subsequently secreted into the blood plasma, where it is maintained at high concentrations. Within lymphoid tissues, however, S1p levels are kept low due to its degradation by S1p lyase (Breart et al., 2011). In the absence of S1pr1 signaling, lymphocytes fail to exit the thymus or SLOs, as demonstrated in bone marrow chimeric mice using fetal liver from S1pr1 knockout embryos (Matloubian et al., 2004), proving the function of S1p/S1pr1 signaling in regulating immune cell migration.

Expression of S1pr1 is controlled by CD69. Activation through TCR triggers the upregulation of CD69, a surface marker that directly interacts with and inhibits S1pr1 expression on the cell surface (Baeyens et al., 2015). This inhibition counteracts the egress-promoting signals generated by S1p, ensuring that newly activated T cells remain in the SLOs for sufficient time to undergo full activation and differentiation under the effect of APCs. As T cells complete their activation and the expression of CD69 decreased, S1pr1 can be gradually re-expressed on the cell surface (Laidlaw et al., 2019). This recover of surface S1pr1 responsiveness allows T cells to sense the S1p gradient again and guide them to egress from the SLOs and their subsequent entry into the bloodstream. This makes T cell migration to a target organ/ tissue possible.

Once T cells enter the bloodstream, the high concentrations of S1p induce an internalization of S1pr1, temporarily turning the cells unresponsive to S1p signaling to allows T cells to migrate against the S1p concentration gradient to tissues with lower S1p concentrations (Garris et al., 2014). Research using T cell specific S1pr1 knockout mice proved its central role in lymphocyte egress. These mice exhibit lymphopenia, with T cells failing to exit from the thymus (Allende et al., 2004). Similarly, disruption of the S1p gradient, such as inhibiting of S1p lyase, results in impaired T cell migration and a reduction in peripheral T cell counts (Garris et al., 2014). In adoptive transfer EAE models, loss of S1pr1 signaling in T cells significantly reduces disease severity by impairing their ability of exit from the SLOs (Kendirli et al., 2023b).In summary, T cell entry to lymph node and their exit are predominantly regulated by a balance between opposing signals mediated by Ccr7 and S1pr1 (Pham et al., 2008).

The central role of S1pr1 in T cell trafficking from SLOs to blood circulation has made it as an optional target for therapeutic intervention in MS. Fingolimod (FTY720) is the first S1pr1 modulator

approved for MS treatment. Fingolimod acts as a functional antagonist by inducing S1pr1 internalization and degradation (Mackay et al., 2015). This traps lymphocytes within SLOs, preventing their egress into the bloodstream. As a result, fewer lymphocytes are available for the CNS infiltration in MS patients (Cyster and Schwab, 2012). Clinical studies have shown that fingolimod effectively reduces relapse rates and slows disease progression in MS patients (Zecca et al., 2018).

1.6.4. Crawling and Extravasation

Once T cells reach CNS vasculature, the next phase of migration begins. The early interaction between T cells and the vascular endothelium is induced by leukocyte margination, a phenomenon in which leukocytes tend to be positioned closer to the vascular wall than the rapidly flowing center of the vessel (Holman et al., 2011). The following steps of $CD4^+$ T cell migration across the BBB include rolling and crawling on the endothelium, then extravasation. The detail of each step remains unclear during MS. Here, combined insights from general T cell migration mechanisms with MS/EAE-specific studies to describe how $CD4^+$ T cells likely cross the BBB during MS/EAE are discussed.

In general, the earliest molecular contact between T cells and the endothelium is the binding between P-selectin glycoprotein ligand-1 (PSGL-1, which is expressed on T cells), and its receptor P-selectin (expressed on endothelial cells). This step is also referred to as rolling. However, in MS/EAE, the PSGL-1/P-selectin interaction in $CD4^+$ T cells appears to be dispensable. When researchers used $CD4^+$/$CD8^+$ T cells from acute RRMS patients peripheral blood to evaluate their adhesion capacity to the CNS blood vessels in mice, they found that the PSGL-1/P-selectin induce the $CD8^+$ T cell adhesion to the endothelium, but had no effect on $CD4^+$ T cells (Battistini et al., 2003). Furthermore, in the MOG induced active EAE model, knocking out PSGL-1 had no impact on EAE onset (Bill et al., 2011). The dispensability of PSGL-1/P-selectin in $CD4^+$ T cell migration during MS/EAE also explains the absence of rolling behavior in autoreactive T cells within meningeal microvessels. When researchers used intravital fluorescence videomicroscopy to directly observe how autoreactive T cells cross the BBB during EAE, they identified a unique phenomenon, without rolling, autoreactive $CD4^+$ T cells immediately started crawling in the spinal cord white matter microvasculature (Vajkoczy et al., 2001). Similar behavior has been observed in non-inflamed retinal microvessels, where activated T cells stopped abruptly, without reducing their speed by rolling (Xu et al., 2003). It remains unclear whether this phenomenon is unique to the CNS and why it happens.

Crawling is widely recognized as a key step to determine whether T cells can exit the blood vessels, mainly mediated by integrins and their ligands. Integrins such as LFA1 (integrin αLβ2) and very late activation antigen 4 (VLA4; integrin α4β1) are highly expressed in the $CD4^+$ T cells (Bertoni et al., 2018). In general, intracellular signals within T cells can activate integrins on the surface. This leads their conformational changes and aggregation on the cell surface, thereby increasing their affinity for ligands and mediating their cell-to-cell/extracellular matrix adhesion (Ginsberg, 2014). In EAE/MS, an upregulation of ICAM1 (ligand for LFA1) and VCAM1 (ligand for VLA4) were observed on endothelial cells of the BBB (Duan et al., 2013). Moreover, staining around CNS vessels where ICAM1 and VCAM1 were upregulated revealed the presence of inflammatory cells with high LFA1 and VLA4 expression (Engelhardt and Ransohoff, 2012).

Especially VLA4, has been shown to be critical in mediating the infiltration of autoreactive T cells during MS/EAE. Natalizumab, currently used in the clinical therapy of RRMS patients, is a monoclonal antibody against integrin α4 (Itga4, CD49d), a subunit of VLA4 (Hutchinson, 2007). Another subunit that forms VLA4 is integrin β1 (Itgb1, CD29). The genome-wide CRISPR/Cas9 screening results that were previously published by our group further confirmed the critical role of Itga4 in mediating T cell migration into the CNS, as it was the most prominent regulator (Kendirli et al., 2023b). Furthermore, single gene knockout of Itga4 on T_{MBP} completely prevented the onset of adoptive transfer EAE (Kendirli et al., 2023b). Clinical data show that patients treated with Natalizumab only had a low number of $CD4^+$ T cells in their CSF (Stuve et al., 2006), further confirming the essential role of Itga4 and its effect on VLA4 in $CD4^+$ T cell migration to the CNS. It is still unclear what role LFA1 plays in the infiltration of autoreactive $CD4^+$ T cells into the CNS during MS/EAE. LFA1 is formed by integrin αL (ItgaL, CD11a) and integrin β2 (Itgb2, CD18) chains. Although immunological studies have clearly shown that LFA1 is involved in the mechanisms of immune cell crawling on the vascular endothelium, thereby promoting their infiltration into inflammatory tissues (Shi and Shao, 2023). In EAE, the role of LFA1 in T cell pathogenicity through its impact on migration remains controversial (Cannella et al., 1993, Gordon et al., 1995, Wang et al., 2007, Dugger et al., 2009).

In the adoptive transfer EAE model in Lewis rats, two days after T_{MBP} cell injection, these autoreactive cells begin to appear in the leptomeningeal blood vessels, with most exhibiting crawling behavior (Bartholomaus et al., 2009). Further mechanisms were explored in this study by intravenously injecting anti-VLA4 antibodies during T cell crawling on leptomeningeal blood vessels. This treatment caused T_{MBP} cells to rapidly detach from the surface of CNS blood vessels and cease movement within minutes. However, no such effect was observed following the injection of anti-LFA1 antibodies (Bartholomaus et al., 2009). During the crawling process, T cells look for a suitable

exit point. The microvascular endothelial cells of the CNS have a distinct structure compared to those in other organs and tissues. They lack pores and form highly complex, continuous tight junctions (Engelhardt, 2010). People speculate that due to the dense structure of these endothelial cells, the crawling time of T cells before CNS vascular infiltration is significantly longer than the crawling time during an inflammatory infiltration in other parts. How these T cells cross the endothelium after crawling during MS/EAE remains unclear. However, it is clear that only highly activated T cells can penetrate CNS blood vessels. This is the case independent of their ability to recognise CNS-specific antigens (Hickey, 1991, Wekerle et al., 1986). One prevailing hypothesis is that T cells must first induce endothelial activation before extravasation into the perivascular space, which may also explain the prolonged time required for this process (Engelhardt, 2010).

1.6.5. Activation of CNS Autoreactive T Cells after Infiltration

Once autoreactive T cells exit the brain blood vessels, they first enter the perivascular space (Archambault et al., 2005). In the perivascular space, T cells interact with local APCs, including perivascular macrophages and dendritic cells. This interaction is crucial for the reactivation of these autoreactive $CD4^+$ T cells within the CNS. This further advances the local immune reaction and neurodegeneration. By combining intravital imaging combing with calcium-sensing proteins and nuclear factor of activated T cells (NFAT)-based sensors, the activation of autoreactive T cells upon contact with APCs in the perivascular space has been directly visualized (Kyratsous et al., 2017, Pesic et al., 2013). This signaling is antigen-specific, as demonstrated by studies where MBP-specific T cells showed a robust T cell activation which was detected by calcium activity, while OVA-specific T cells in the same region exhibited no such responses (Kyratsous et al., 2017). Furthermore, blocking MHC class II molecules on APCs significantly reduced calcium signaling and EAE severity. This confirms the antigen dependency of these interactions and the importance of the reactivation of T cells to the EAE development (Kyratsous et al., 2017).

Following reactivation, these T cells produce pro-inflammatory cytokines, including TNFα, MIP1α, and MCP1, which recruit additional immune cells such as macrophages, B cells, and endogenous T cells to the CNS (Kawakami et al., 2004). These recruited cells exacerbate inflammation and contribute to tissue damage. Experimental evidence supports the direct link between T cell reactivation and disease severity, as only reactivated T cells in the CNS induce strong EAE (Kawakami et al., 2004).

After activation by perivascular APCs, autoreactive T cells migrate deeper into the CNS, including the meninges and parenchyma (Bartholomaus et al., 2009). The next state of T cells after inducing CNS inflammatory lesion varies. Some T cells, particularly $CD8^+$ T cells, persist as tissue-resident memory T cells, capable of reactivating and inducing inflammation during subsequent immune challenges (Sasaki et al., 2014, Machado-Santos et al., 2018). However, in models such as the Lewis rat EAE model, all autoreactive T cells are eliminated from the CNS during the recovery phase, likely through apoptosis or FasL-mediated mechanisms (Flügel et al., 2001, Kawakami et al., 2005). Despite this clearance, a subset of autoreactive T cells persists in the peripheral organs as memory T cells, retaining the potential to re-initiate inflammation during future episodes (Kawakami et al., 2005).

To summarize this section, the migration and reactivation of T cells within the CNS are critical steps in the pathogenesis of EAE and MS. These processes are orchestrated by intricate interactions between T cells and endothelial cells/APCs, driven by antigen presentation and pro-inflammatory signaling. Targeting key steps in this cascade, such as antigen presentation or cytokine signaling, offers promising therapeutic avenues for controlling CNS autoimmunity. By unraveling the complex dynamics of T cell interaction with other cells such as endothelial cells and CNS APCs, we can gain deeper insights into the mechanisms underlying neuroinflammation and develop more effective treatments for diseases like MS.

1.7. CRISPR/Cas9 Screening Identifies Genes Regulating T Cell Migration during MS/EAE

To investigate the molecular mechanisms of T cell interaction with other cells as potential therapeutic targets for MS, our group, including Dr. Katrin Franziska Lämmle, in collaboration with group of Prof. Kerschensteiner including Dr. Arek Kendirli, performed a genome-wide CRISPR/Cas9 screening using the adoptive transfer EAE models in Lewis rat. First, we generated rat primary $CD4^+$ T_{MBP} cells stably expressing Cas9 and EGFP. Once the functionality and stability of Cas9 were validated, a genome-wide sgRNA library was transduced into these Cas9 expressing T_{MBP} cells. The library comprised 87,690 sgRNAs targeting 21,410 genes and 396 miRNAs (4 sgRNAs per gene), along with 800 non-targeting (NT) control sgRNAs together with BFP for tracking (Kendirli et al., 2023b). The experimental setup ensured that each Cas9 expressing T_{MBP} cell received only one sgRNA by controlling the ratio of retrovirus to T cells, thereby enabling single-gene knockout in individual cells.

After transduction, the Cas9-sgRNA T_{MBP} cells were activated and intravenously injected into recipient rats. According to previous results, the injected T_{MBP} cells begin a massive migration from

the peripheral organ such as the spleen into the CNS via the blood, coinciding with a significant weight loss of the recipient rats with progressive clinical symptoms on day3 after T cells transfer. To analyze the impact of sgRNA on T cell migration, the Cas9-sgRNA T_{MBP} cells were isolated from peripheral compartments, including blood and spleen as well as CNS compartments, such as spinal cord leptomeninges and spinal cord parenchyma. Genomic DNA was extracted from isolated T cells and submitted for next-generation sequencing (NGS) after PCR amplification of sgRNA region. SgRNA counts in each compartment were analyzed using the MAGeCK software, designed to identify significant hits from CRISPR/Cas9 screens (Li et al., 2014, Kendirli et al., 2023b) (Figure 3A). Although many genes are identified as potential regulators of T cell migration into the CNS, the result was noisy presumably due to huge number of sgRNA used. To reduce the noise and increase accuracy, a validation screening was performed with a refined sgRNA library containing 12,000 sgRNAs (6 sgRNAs per gene) targeting 1,950 candidate genes which were selected according to the result from the initial screening (Kendirli et al., 2023b). By comparing sgRNA counts in different compartments, we identified genes that either facilitated or hindered T cell migration into the CNS (Figure 3B) (Lämmle, 2023). The distribution of sgRNA copy numbers between “peripheral compartments” and “CNS compartments” provided insights into the roles of specific genes in regulating T cell migration to the CNS during EAE. Genes with sgRNA enrichment in peripheral compartments compared to CNS compartments were inferred to promote T cell migration to the CNS, whereas genes showing the reverse pattern were suggested to inhibit migration. The effect of sgRNA was analyzed by comparing spleen or blood versus meninges or parenchyma. We have analyzed the mode of action for some genes, including Itga4, Hsp90b1 and Grk2, there are still many genes need to be analyzed. Among the identified genes, I am interested in the transcription factor found to regulate autoreactive T cell migration from the screening result (Figure 3B), Krüppel-like factor 2 (Klf2).

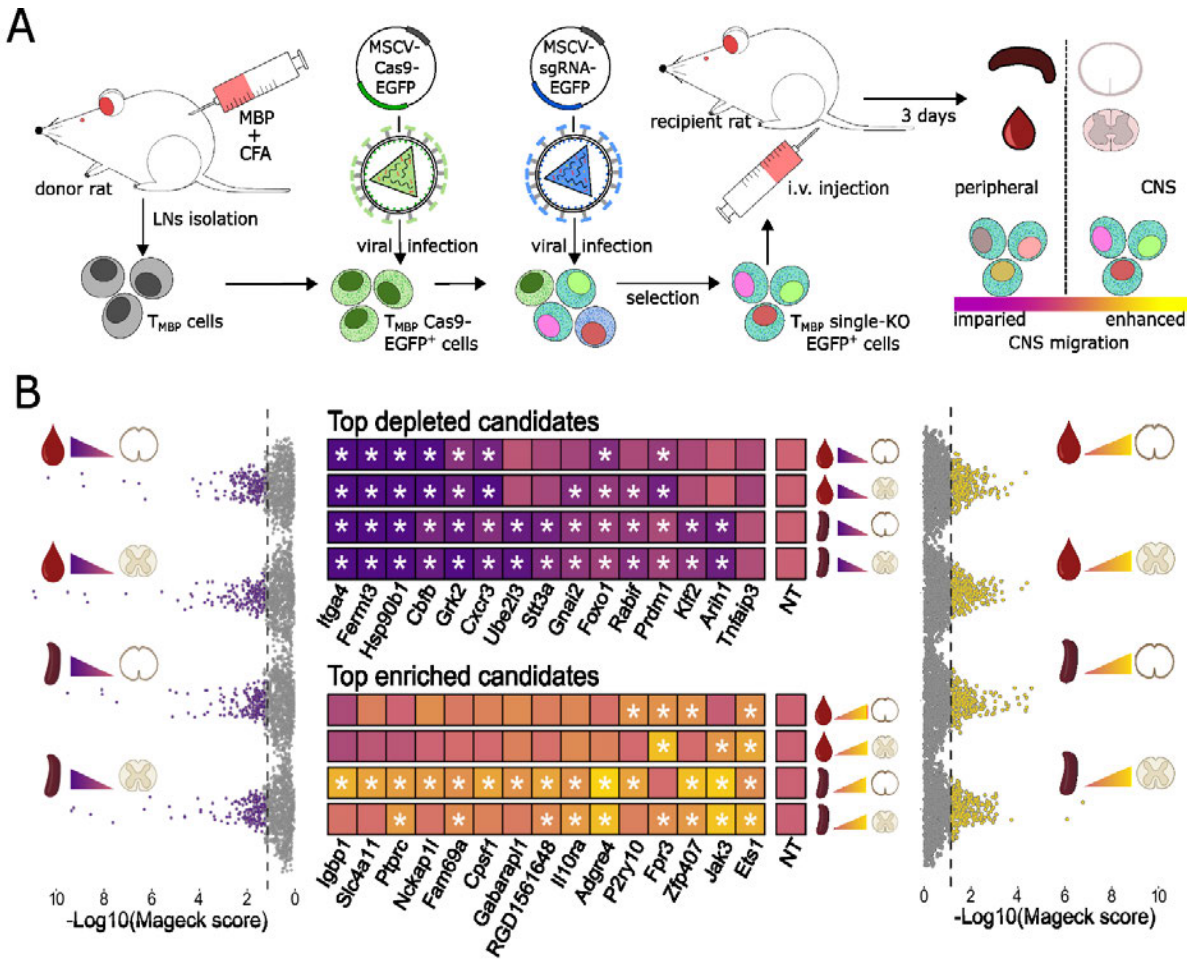

Figure 3 Genome-wide CRISPR/Cas9 Screening of T_{MBP} Cells Migration in the EAE Model
A). Experimental Design. T_{MBP} Cas9-EGFP$^+$ cells by introducing Cas9 nuclease and EGFP coding sequences into rat primary T_{MBP} cells using retroviral transduction. A genome-wide sgRNA library co-expressing BFP was then introduced into these Cas9-EGFP$^+$ cells, creating single-gene knockout (KO) T_{MBP} cells (EGFP$^+$BFP$^+$). These modified cells were injected into rats, and three days post-injection, the rats were sacrificed to isolate the administered T cells from both peripheral compartments (blood and spleen) and CNS compartments (spinal cord leptomeninges and parenchyma). Genomic DNA was then extracted from GFP$^+$BFP$^+$ T_{MBP} cells and analyzed by next-generation sequencing (NGS) to reveal sgRNA distribution. **B). Candidate Genes Influencing T Migration Identified Though Validation CRISPR/Cas9 Screening.** Two-step screenings provided candidates of crucial regulators in T cell migration from the peripheral to the CNS compartments. sgRNAs enriched in the periphery (left, purple) indicated deletion of the gene impaired migration to the CNS, whereas sgRNAs enriched in the CNS (right, yellow) suggested enhanced migration. The heatmap in the center displays the top 15 candidate genes identified based on difference in sgRNA abundance between peripheral and CNS compartments. Stars indicate p-value<0.05. cited from (Lämmle, 2023)

1.8. Krüppel-like Factor 2

Klf2 is a member of the Krüppel-like factor family of transcription factors. In vertebrates, the Klf family includes 17 members. They play essential roles in regulating diverse biological processes, such as cell proliferation, differentiation, survival, and tissue development (Turpaev, 2020, Oishi and Manabe, 2018). Klf proteins are characterized by a conserved C-terminal domain containing three

zinc fingers, each composed of 21-23 amino acids (Turpaev, 2020), that bind GC-rich motifs to regulate the expression of target genes (Turner and Crossley, 1999). The DNA-binding specificity of Klf proteins is determined by the C-terminal domain (Stubbs et al., 2011). In contrast, the N-terminal domains of Klf proteins mediate the interactions with other transcription factors and co-regulators (Pollak et al., 2018).

Klf2, initially named Lung Klf (LKlf) because it was first discovered to be highly expressed in the lung (Kuo et al., 1997). Following research revealed that it is widely expressed in various tissues, including in the spleen, thymus, heart, adipose tissue, skeletal muscle, and vascular endothelium (Turpaev, 2020, Anderson et al., 1995). Efforts to generate Klf2 knockout mice have shown that embryos lacking Klf2 do not survive to birth due to hemorrhaging caused by defective blood vessel formation and abnormalities in the tunica media (Wittner and Schuh, 2021). These findings underscore the critical role of Klf2 in embryonic vascular development and endothelial cell function. Beyond its developmental effect, Klf2 has been also shown to be involved in processes such as mast cell physiology and adipogenesis, as well as in pathological conditions including atherosclerosis, thrombosis, and certain lymphomas such as marginal zone B-cell lymphoma (Wittner and Schuh, 2021). Furthermore, Klf2 is also expressed in various immune cell subsets, including B cells, T cells, NK cells, macrophages, and monocytes. Its expression is closely linked to the differentiation and activation states of these cells, highlighting its pivotal role in regulating immune responses (Wittner and Schuh, 2021).

1.8.1. Klf2 in T Cells

Klf2 expression in T cells is tightly regulated throughout their development, activation, and differentiation. It's function in T cells includes maintaining immune cell quiescence, proliferation, activation, adhesion, and migration (Wittner and Schuh, 2021). More specifically, Klf2 is highly expressed in single-positive $CD4^+$ and $CD8^+$ T cells and remains prominent in naïve and memory T cells (Jha and Das, 2017). However, upon TCR activation, Klf2 expression is rapidly downregulated (Hart et al., 2012). When peripheral T cells lose Klf2, they exhibit spontaneous activation and increased apoptosis (Kuo et al., 1997), directly revealing its role in maintaining T cell quiescence and promoting survival. Meanwhile, forced Klf2 expression in Jurkat T cells kept them in a quiescent state, with reduced cell size, lower protein synthesis, and decreased expression of activation markers (Kuo et al., 1997, Buckley et al., 2001b). Mechanistically, Klf2 achieves this by suppressing the expression of c-Myc. And when T cells lack Klf2, Fas-mediated apoptosis has been identified as the primary pathway that leads to cell death (Kuo et al., 1997).

Klf2 also plays a critical role in regulating the cell cycle and proliferation. By directly binding to the promoter of the cell cycle inhibitor p21WAF1/CIP1, Klf2 induces its expression, thereby halting cell division and enforcing a quiescent phenotype (Wu and Lingrel, 2004). Additionally, Klf2 represses human telomerase reverse transcriptase (hTERT) by binding to CpG-rich sequences in its promoter. This effectively inhibits telomerase activity and maintains T cells in a resting state (Wittner and Schuh, 2021, Mizuguchi et al., 2021). Upon TCR engagement, Klf2 is rapidly downregulated at both the transcriptional and protein levels through a complex signaling cascade involving Akt (protein kinase B), mitogen-activated protein kinases (MAPK), and extracellular signal-regulated kinases (ERK1/2) (Preston et al., 2013). This regulation is mediated by ubiquitination and proteasomal degradation of Klf2, coupled with reduced mRNA expression. Continuous TCR signaling and cytokine stimulation sustain Klf2 downregulation, while the cessation of these signals allows for its re-expression (Preston et al., 2013). In memory T cells, low levels of cytokines such as IL-2, IL-7, and IL-15 restore Klf2 expression, ensuring the survival and readiness of memory T cells for subsequent immune responses (Takada et al., 2011).

1.8.2. Klf2 in T Cell Migration

Another critical regulatory function of Klf2 in T cells is its role in controlling migration by orchestrating the expression of genes that regulate egress, homing, and tissue retention. This begins during T cell development in the thymus and extends to the movement of T cells within peripheral tissues, ensuring that they are properly distributed and responsive to immune challenges. Mature $CD4^+$ and $CD8^+$ single-positive T cells rely heavily on S1pr1 for thymic egress into the bloodstream. S1p, a bioactive lipid mediator, establishes a concentration gradient that guides S1pr1-expressing cells into circulation. During thymocyte maturation, S1pr1 expression increases (Allende et al., 2004), making these cells sensitive to S1p gradients. Chromatin immunoprecipitation (ChIP) assays have demonstrated that Klf2 directly binds to the S1pr1 promoter to regulate its expression (Carlson et al., 2006). When thymocytes lack Klf2, they accumulate in the thymus, and peripheral $CD4^+$ and $CD8^+$ T cells are nearly absent due to impaired S1pr1 expression (Matloubian et al., 2004).

In addition to S1pr1, Klf2 also regulates L-selectin (CD62L), which mediates T cell trafficking to SLOs (Bai et al., 2007). By inducing the expression of both S1pr1 and CD62L, Klf2 coordinates T cell egress from the thymus and migration into lymphoid tissues. However, these two molecules have opposing functions, and the mechanisms how Klf2 selectively regulates their activity remain unclear. Klf2 has also been implicated in the regulation of CXCR3 in $CD8^+$ T cells. When Klf2 is absent, the resulting overproduction of IL-4 leads to the upregulation of CXCR3, enabling T cells to migrate to inflamed

tissues by responding to chemokine gradients such as CXCL10 (Weinreich et al., 2009a). This suggests that Klf2 dysfunction may drive the accumulation of activated T cells in non-lymphoid tissues. Furthermore, Klf2 directly targets the Itgb7 promoter, guiding activated $CD8^+$ T cells to mucosal inductive sites such as Peyer's patches and effector sites like the lamina propria (Wittner and Schuh, 2021).

Through its regulation of adhesion molecules, chemokine receptors, and integrins, Klf2 ensures precise localization and functionality of T cells. In addition, Klf2 enables the transition between quiescent, activated, and memory states while maintaining the spatial and temporal fidelity of immune responses. Despite these advances, the mechanisms by which Klf2 operates in specific T cell subtypes and at specific time points remain incompletely understood, representing a crucial area for future research. These multifaceted roles highlight Klf2's significance as a master regulator of T cell migration and its potential as a therapeutic target in immune-mediated diseases.

OBJECTIVES

The effective treatment of MS remains a global challenge. As a result of increasing knowledge about MS pathogenesis, clinicians now have more effective therapeutic options. Especially the development of disease-modifying therapies (DMTs) has greatly improved the quality of life of MS patients. In general, these therapies are designed to target specific stages of the immune response, thereby reducing immune activity in the CNS of MS patients. However, they cannot solve all problems. To date, no treatment can completely cease MS progression, and the strong immune suppression from DMTs increases the risk of severe infections. Based on the current situations, the ultimate goal of our research is to find potential targets to provide new ideas for improving DMTs. Ideally, these therapies should inhibit the infiltration of autoreactive T cells into the CNS while avoiding broad immune suppression.

In the early stages of MS, $CD4^+$ autoreactive T cells are fundamental for disease onset. These cells are first activated in the periphery, while at the same time also undergoing modifications to acquire migratory capacity, becoming "migratory T cells". Unlike pure "activated T cells," which lack the ability to migrate, migratory T cells rely on multiple molecular mechanisms to move from secondary lymphoid organs into the bloodstream, to reach brain blood vessels, and to undergo crawling and extravasation to infiltrate the CNS. Once inside the CNS, they recognize specific antigens, trigger focal inflammation, and cause tissue damage. How those activated autoreactive $CD4^+$ T cells gain migratory capacity in the periphery remains unclear. Our group previously conducted a genome-wide CRISPR/Cas9 screening in EAE, and revealed genes that influence the migration of $CD4^+$ autoreactive T cells to the CNS. From the screening result, our study is interested in the transcription factors found CRISPR/Cas9 screening data in inducing $CD4^+$ T cell migration to the CNS, since they might be the key reason how autoreactive T cells gain migratory function to the CNS in periphery.

Our first goal is to investigate how these transcription factors influence T cell migration, determine which stage of the migration process they primarily regulate and to uncover the molecular mechanisms involved.

The second goal of our study is to compare the transcription factors we identify, and their downstream effector molecules that regulate $CD4^+$ T cell migration in EAE, with our previous single-cell RNA sequencing data of $CD4^+$ T cells migrating to the CNS in MS patients. This comparison will help us understand whether the discovered targets in the EAE model are also meaningful and effective in MS patients.

2. MATERIAL AND METHODS

2.1. Material

2.1.1. Animals

The Lewis rats used in the experiments were originally obtained from Charles River or Janvier Laboratories and subsequently maintained and bred in the Core Facility Animal Models of the Biomedical Center, LMU. All animal care and experimental procedures were conducted in strict accordance with the Animal Welfare Acts and received approval from the local regulatory authority (Regierung von Oberbayern). The rats were housed under controlled environmental conditions, including stable temperature and humidity, with a fixed light/dark cycle. Both male and female rats were used in the study, with the age of the experimental animals ranging from 5 to 20 weeks.

2.1.2. Solutions, Reagents, and Media

Table 2.1.2.1-Solutions, reagents, and media for cell culture

Medium Name	Component	Concentration	Supplier
EH	DMEM	97.5 % (v/v)	Sigma
	1M HEPES Buffer, PH 7.4	2.5 % (v/v)	Sigma
TCM	DMEM	1L	Sigma
	L-Glutamine solution	2mM	Sigma
	100X Pen/Strep stock	100 µg/ml	Sigma
	L-asparagine (monohydrate)	36 mg/L	Sigma
	100mM Sodium-Pyruvate	1 mM	Sigma
	Non-essential amino acids	10ml/L	Sigma
	β-Mercaptoethanol	4 µl/L	Merck
TCGF medium	TCM	88 % (v/v)	-
	Horse serum	10 % (v/v)	Gibco
	IL-2 enriched supernatant from ConA-stimulated EL4.IL-2 Cells	2% (v/v)	-
RM	TCM	99% (v/v)	-
	Rat serum	1% (v/v)	-
TCM with 10% FBS	TCM	90% (v/v)	-
	FBS	10% (v/v)	Merck
FM	Horse serum	50% (v/v)	Gibco
	EH	40% (v/v)	-
	Dimethyl Sulfoxide solution	10% (v/v)	Sigma
Nycoprep	H_2O	95% (v/v)	-
	Nycodenz	141 g/L	Serumwerk
	NaCl	3 g/L	Roth
	100mM Tricine	5% (v/v)	Sigma
10X PBS (pH 7.4)	H_2O	90 % (v/v)	-
	NaCl	1.4 M	Roth
	Na_2HPO_4	100 mM	Roth

	KCl	27 mM	Merck
	KH_2PO_4	18 mM	Merck
1X PBS	H_2O	90% (v/v)	-
	10X PBS	10% (v/v)	-

Table 2.1.2.2-Solutions, reagents, and media for cell staining

Medium Name	Component	Concentration	Supplier
FACS buffer	1X PBS	99% (v/v)	-
	Rat serum	1% (v/v)	-
	NaN_3	0.05% (v/v)	Roth
2% PFA	H_2O	1L	-
	Paraformaldehyde	20g	Merck
PB Buffer	H_2O	90% (v/v)	-
	10X Permeabilization wash buffer	10% (v/v)	Biolegend

Table 2.1.2.3-Solutions, reagents, and media for bacteria culture and molecular biology experiments

Medium Name	Component	Concentration	Supplier
Lysis Buffer	1M Tris (PH 8.0)	100 µl/ml	Sigma
	3M NaCl	40 µl/ml	Roth
	0.5M EDTA (pH 8.0)	10 µl/ml	Merck
	Tween 20	5 µl/ml	Sigma
10X TAE	Trizma base	48.9 g/L	Sigma
	Acetic acid, ⩾99.8%	11.4 ml/L	Sigma
	EDTA	3.7 g/L	Merck
1X TAE	H_2O	90% (v/v)	-
	10X TAE	10% (v/v)	-
1% Agarose gel	1X TAE	50 ml	-
	Agarose	0.5 g	Biozym
	Midori green advance	3 µl	Nippon genetics
LB medium	H_2O	1 L	-
	Tryptone	10 g	Sigma
	Yeast extract	5 g	Sigma
	NaCl	5 g	Roth
LB plate	LB medium	1 L	-
	Bacto agar	15 g	Fisher scientific
	Ampicillin	100 mg/L	Sigma

2.1.3. Antibodies, cell stimulators and chemoattractant

Table 2.1.3.1-Primary antibodies

Name	Host species, fluorescent	Clone. isotype	Supplier
Mouse isotype control	Mouse, unconjugated	MOPC31C, IgG1	Sigma

Mouse isotype control	Mouse, unconjugated	MG2a-53, IgG2a	Biolegend
Mouse isotype control	Mouse, PE conjugated	MOPC-21, IgG1	BD
Hamster isotype control	Armenian hamster, unconjugated	Ha4/8, IgG2	BD
Goat isotype control	Goat, unconjugated	IgG	Santa Cruz
Rabbit isotype control	Rabbit, unconjugated	RbNP15, IgG	Invitrogen
Anti-rat CD11a	Mouse, unconjugated	Wt.1, IgG2a	Biolegend
Anti-rat CD18	Mouse, unconjugated	Wt.3, IgG1	ThermoFischer
Anti-rat CD25	Mouse, unconjugated	OX39, IgG1	ThermoFischer
Anti-rat CD29	Armenian hamster, unconjugated	HMβ1-1, IgG	Biolegend
Anti-rat CD49d	Mouse, unconjugated	TA-2, IgG1	ThermoFischer
Anti-rat CD134	Mouse, unconjugated	OX40, IgG2b	Serotec
Anti-rat TCRβ	Mouse, unconjugated	R73, IgG1	Serotec
Anti-rat IFNγ	Mouse, unconjugated	DB1, IgG1	eBioscience
Anti-mouse IL-17A	Rat, PE conjugated	TC11-18H10, IgG1	BD
Anti-mouse/rat TNF-α	Armenian hamster, unconjugated	TN3-19.12, IgG	Biolegend
Anti-rat CCR7	Goat, unconjugated	A19, IgG	Santa Cruz
Anti-mouse/rat S1PR1	Rabbit, unconjugated	JM10-66, IgG	Invitrogen
Anti-mouse/rat KLF2	Rabbit, unconjugated	-, IgG	Sigma

Table 2.1.3.2-Secondary antibodies

Name	Host species, fluorescent	Supplier
Anti-mouse IgG (H+L)	Donkey, APC conjugated	Jackson ImmunoResearch
Anti-american hamster IgG (H+L)	Goat, APC conjugated	Jackson ImmunoResearch
Anti-goat IgG (H+L)	Donkey, AF647 conjugated	Jackson ImmunoResearch
Anti-rabbit IgG (H+L)	Goat, AF647 conjugated	Jackson ImmunoResearch

Table 2.1.3.3-Cell stimulators and chemoattractant

Name	Stock Concentration	Supplier
Brefeldin A	5 mg/ml (EtOH)	Biolegend
phorbol 12 myristat 13-acetat (PMA)	1 mg/ml (DMSO)	Sigma
Ionomycin	1 mM (EtOH)	Sigma

CCL5	100 ng/ µl (0.1% BSA)	PeproTech
S1p	100 µM	Tocris Bioscience

2.1.4. Regents and kits

Table 2.1.4.1-Regents and kits for molecular biology experiment

Name	Application	Supplier
TRIzol® Reagenz	RNA extraction	Invitrogen
LunaScript® RT SuperMix Kit	cDNA synthesis	New England Biolabs
2 × qPCRBIO SyGreen Mix Separate-ROX	qPCR	PCRbiosystems
Hard-Shell® 96-well PCR plates	qPCR	Bio-Rad
FastGene® Optima HotStart ReadyMix	PCR	Nippon genetics
FastGene® Gel/PCR Extraction Kit	DNA purification	Nippon genetics
CutSmart™ Buffer	cloning	New England Biolabs
EcoRI-HF™	cloning	New England Biolabs
SacII	cloning	New England Biolabs
T4 DNA Ligase (5 U/µl)	cloning	ThermoFischer
Macherey-Nagel™ NucleoBond™ Xtra Midi EF	Plasmid extraction	Macherey-Nagel
P4 Primary Cell 4D-Nucleofector® X Kit S	Gene edit	Lonza

2.1.5. MBP Antigens

The MBP antigen used for in vitro activation and culture of T_{MBP} cells was prepared from frozen guinea pig brain following the described protocol (Campbell et al., 1973).

2.1.6. Oligonucleotides

Table 2.1.6.1-sgRNA for CRISPR/Cas9 knockout and corresponding primers for TIDE sequencing

Target gene	sgRNA sequence	primer sequence
Itga4	GATGCTGTTGCTGTACTTCG	TGCTGCACTTCATCTCTTGG
		GCGTGGCGTTAAAGTTGAAA
Klf2	TGAGGACCTAAACAGCGTGC	GAAGCGGCCGTGTAGAG
		GTTTTGCCTGGCTTGTTGAC
S1pr1	GCGGCTTCGAGTCCTCACCA	TCTGTCTGCCTCAGTCTTCA
		AGACCTGATCTCCACCCTTC
Foxo1	AGAGAGCGAGGACTTCGCGC	TCTCCTGGTACTCTCTGCTG
		AACTAGCCAACTTCCAAGCC
Ccr7	CAGCGTCCAGATGCCTATAC	AGCAGAAACTCATAGCCAGC
		ACTCACTCAGGGTTTAAGGGA

NT	GCTGCATGGGGCGCGAATCA	-

Table 2.1.6.2-qPCR primers

Target gene	primer sequence
β-actin	CAGGGTGTGATGGTGGGTATGG
	AGTTGGTGACAATGCCGTGTTC
S1pr1	TTCAGCCTCCTTGCTATCGC
	AGGATGAGGGAGATGACCCAG

2.2. Methods

2.2.1. T_{MBP} Cell Culture

Thymocyte Isolation and Inactivation

To prepare APCs for the T_{MBP} cells in vitro activation and culture, thymocytes were isolated from male rats (2–3 months old). The rats were sacrificed, and the thoracic cavity was exposed using sterile surgical scissors and forceps. The thymus was carefully removed with sterile forceps and immediately placed in cold, sterile EH medium.

The extracted thymus was mechanically dissociated by a sterile metal strainer to obtain a single-cell thymocyte suspension in cold EH medium. The suspension was then centrifuged at 400 × g for 5 minutes at 4°C. After centrifugation, the supernatant was discarded, and the pellet was resuspended in 10 mL of cold EH medium. Thymocytes were inactivated by adding mitomycin C to a final concentration of 2.5 µg/mL, followed by incubation in a 37°C water bath for 30 minutes.

To remove residual mitomycin C, thymocytes were washed three times with cold PBS. For each wash, cold PBS was added to fill a 50 mL centrifuge tube, followed by centrifugation at 400 × g for 5 minutes at 4°C. After the final wash, thymocytes were resuspended in 10 mL of EH medium. Cell viability and concentration were assessed using Trypan blue staining and a hemocytometer. The inactivated thymocytes were stored at 4°C and used for in vitro activation and culture of T_{MBP} cells within three days.

T_{MBP} cell culture

T_{MBP} cell clones were previously established in the laboratory from Lewis rats immunized with MBP, as described by (Kawakami et al., 2004). These cell stocks are stored in liquid nitrogen, with each cryovial clearly labeled with the clone number and last culture date.

For T_{MBP} cell culture, fresh RM medium was prepared (valid for up to three days). Frozen T_{MBP} cells were rapidly thawed by brief incubation in a 37°C water bath. The thawed cell suspension was immediately transferred to a centrifuge tube containing 10 mL of EH medium. After cell counting with a hemocytometer, 3.5×10^6 T_{MBP} cells were plated per 6 cm dish along with $70–100 \times 10^6$ mitomycin C-treated thymocytes and MBP antigen at a final concentration of 10 µg/mL, using RM medium as the culture medium and cultured in a 10% CO_2 incubator.

Following activation, the T_{MBP} cells gradually increased in size. On day 2, when T_{MBP} cells exhibited peak activation and maximal cell size, they were either used for intravenous injection into Lewis rats to induce EAE or supplemented with extra TCGF medium, an IL-2-containing culture medium that promotes T cell proliferation. The culture was continued for four additional days in a 10% CO_2 incubator, during which the cell population expanded while cell size gradually decreased. By day 6, T_{MBP} cells reached their smallest size. At this point, cells were harvested for either co-culturing with thymocytes and MBP antigen for the next activation and culture cycle or resuspending in FM medium and transferred to cryovials for short-term storage at -80°C or long-term storage in liquid nitrogen.

2.2.2. Gene Editing

Plasmid preparation

The plasmid pMSCV-IRES-EGFP-neo, generously provided by PD Dr. Naoto Kawakami, was maintained in E. coli DH5α and stored at -80°C. A small amount of E. coli containing the plasmid was taken from the cryotube and transferred into 3 ml of LB medium containing ampicillin. The culture was incubated overnight at 37°C with constant shaking at 180 rpm. Plasmid DNA was subsequently

isolated using the Macherey-Nagel™ NucleoBond™ Xtra Midi EF kit according to the manufacturer's protocol.

S1pr1 overexpression plasmid construction

The S1pr1 cDNA was synthesised through trizol extraction of mRNA from rat splenocyte, followed by cDNA synthesis via using LunaScript® RT SuperMix Kit. After PCR amplification of S1pr1, the PCR product and the plasmid pMSCV-IRES-EGFP-neo was cut with same restriction enzyme. After the complete cutting, T4 DNA Ligase was used to ligate the S1pr1 cDNA with the plasmid. Then the ligated product was transformed to the 5-alpha competent *E. Coli* to get the clone containing pMSCV-IRES-S1pr1-EGFP-neo plasmid. The detail as follow:

restriction enzyme cutting target plasmid

The following form shows the components of the cutting system with the target plasmid, incubate them on 37°C for 3 hours.

pMSCV-IRES-EGFP-neo	5 µg
CutSmart™ Buffer	5 µl
EcoRI-HF™	0.5 µl
SacII	0.5 µl
H_2O	Fill to 50 µl

restriction enzyme cutting insert gene

The following form shows the components of the cutting system with the S1pr1 insert DNA, incubate them on 37°C for 3 hours.

Insert DNA	3 µg
CutSmart™ Buffer	3 µl
EcoRI-HF™	0.3 µl
SacII	0.3 µl
H_2O	Fill to 30 µl

Purify the plasmid and insert DNA separately

After incubation with restriction enzymes, gel electrophoresis was performed at 90V for 30 minutes to separate DNA fragments based on size. Afterwards, The DNA bands were visualized using a UV transilluminator (UVT-22, Herolab). Based on the experimental design, the fully digested plasmid and the inserted fragment were cut at their respective expected lengths. The collected DNA fragments were subsequently purified using the FastGene® Gel/PCR Extraction Kit, following the manufacturer's protocol.

Ligation between digested plasmid and the inserted fragment

The concentration of the purified, fully digested plasmid and target gene was measured using a Nanodrop Spectrophotometer (Nanodrop2000, Thermofisher). Then the ligation reaction was prepared according to the table below and incubated at 22°C for 1 hour.

Digested plasmid (size: 7871 bp)	50 ng
Digested insert DNA (size: 1214 bp)	50 ng
T4 DNA Ligase	0.2 µl
T4 DNA Ligation Buffer	2 µl
H_2O	Fill to 20 µl

Transformation

The ligation reaction was heat-inactivated by incubation at 65°C for 10 minutes. Subsequently, 2.5 µl of the ligated product was added to 50 µl of 5-alpha competent *E. coli* (New England BioLabs, C2987I) and transformed according to the manufacturer's protocol.

Bacterial Colony Selection and Construct Validation

The transformed *E. Coli* was seeded onto a 10 cm LB agar plate containing ampicillin and incubated at 37°C overnight. Six bacterial colonies of appropriate size were then picked from the agar plate and placed in different tubes of LB culture medium containing ampicillin, and shaken at 180 rpm at 37 °C overnight in a shaker. DNA was then extracted using the QIAprep Spin Miniprep Kit, and cut by restriction enzymes as described in the table below. After incubation at 37°C for 1 hour, gel electrophoresis was performed at 90V for 30 minutes to separate DNA to identify the clone which contains desired plasmid.

DNA from picked colonies	2 µl
CutSmart™ Buffer	1 µl
EcoRI-HF™	0.2 µl
SacII	0.2 µl
H_2O	Fill to 10 µl

Plasmid working solution Preparation

A single bacterial colony containing the target plasmid was selected and initially cultured in 3 ml of LB medium supplemented with ampicillin, under 37°C with shaking at 180 rpm overnight. To obtain a higher yield of plasmid DNA, the overnight culture was expanded by transferring it into 300 ml of fresh LB medium containing ampicillin, followed by incubation under the same conditions. Plasmid DNA was then extracted using the NucleoBond® Xtra Midi EF kit according to the manufacturer's protocol. The DNA concentration was measured using a Nanodrop Spectrophotometer (Nanodrop2000, Thermofisher), and the plasmid was diluted in sterile water to a final working concentration of 1 µg/µl.

HEK-293 cell culture

HEK-293 cells were maintained in 10 cm culture dishes using TCM supplemented with 10% FBS in a 10% CO_2 incubator. Once the cells filled the dish, by blowing cells gently detached them from the dish, collected by centrifugation, and resuspended in FM medium at a concentration of 1×10^6 cells/ml and transferred to cryovials for short-term storage at -80°C or long-term storage in liquid nitrogen.

HEK Cell Transfection and Virus Concentration

HEK-293 cells were plated at a density of $1.2x10^6$ HEK293 T cells per 10 cm culture dish and cultured for 24 hours in 10ml TCM with 10 % FBS in a 10% CO_2 incubator. On the next day, which count as first day of HEK cell transfection, the target plasmid was transfected into HEK cells following a two-solution protocol. Solution A and Solution B were prepared according to the below table, incubated separately at room temperature for 5 minutes, and then combined by adding Solution B into Solution A. The mixture was vortexed briefly and incubated for another 20 minutes at room temperature before being added dropwise to HEK cells at a volume of 1 ml per 10 cm dish. The cells were incubated overnight in a 5% CO_2 incubator.

Solution A	*per 100mm dish*
TCM	500 µl
Target plasmid	6 µg

pCL-ECO	3.5 µg
Solution B	
TCM	500 µl
PEI Max	20 µl

On the next day (second day), the culture medium was replaced with 8 ml of fresh TCM with 10% FBS, then the cells were further cultured at 37°C in 10% CO_2 incubator. On the third day, the supernatant was collected, centrifuged at 2000 × g for 10 minutes under room temperature to remove debris, and stored at 4°C. The transfected HEK cells were further cultured with fresh 8 ml TCM with 10% FBS. On the fourth day, the supernatant was again collected, centrifuged at 2000 g for 10 minutes, and pooled with the supernatant from the previous day.
To concentrate the virus, the pooled supernatant was first filtered through a 0.45 µm filter. The virus-containing medium was then processed using Amicon® Ultra – 15 centrifugal filters (Merck Millipore Ltd.) by adding 13 ml per filter unit and centrifuging at 4000 × g for 20 minutes at room temperature. The virus concentrate retained in the upper chamber was collected while the lower filtrate was discarded. This process was repeated until all medium was processed. Finally, the concentrated virus was then stored at -80°C for further use.

T_{MBP} cells purification
To purify T_{MBP} cells from thymocytes, the cells were collected from the culture dish and centrifuged at 400 g for 5 minutes. Then pellet was resuspended in 5 ml of EH medium and the suspension was carefully layered over 3 ml of Nycoprep solution. A well-prepared gradient is indicated by a distinct interface between the clear Nycoprep solution and the red EH suspension before centrifugation. The tube was then centrifuged at 675 × g, 10 minutes at room temperature, using a low acceleration and braking setting. Following centrifugation, a white flocculent layer at the interface contains the purified T_{MBP} cells. This cells layer was collected in a fresh centrifuge tube, then washed once with cold PBS and centrifuged at 400 × g for 5 minutes.

Retroviral transduction of T_{MBP} cells
For retroviral transduction of T_{MBP} cells, purified T_{MBP} cells from Nycoprep separation on the second day of in vitro culture were counted using a hemocytometer. A total of 2×10^6 T_{MBP} cells in 500 µl of TCGF medium supplemented with 8 µg/ml polybrene were plated per well in a 12-well plate. Next, 100 µl of concentrated virus solution was added to each well, followed by centrifugation at 2000 × g for 90 minutes at room temperature to enhance viral uptake. After centrifugation, 1 ml of fresh TCGF medium per well was added, and the plate was incubated in 10% CO_2 incubator for 24 hours. Following incubation, antibiotic selection was applied. On the sixth day of in vitro culture, the transduced T_{MBP} cells were either restimulated and expanded according to experimental requirements or cryopreserved at -80°C or in liquid nitrogen for long-term storage.

CRISPR/Cas9 single gene knockout in T_{MBP} cells
For single-gene knockout in T_{MBP} cells using CRISPR/Cas9, the RNP complex was preassembled in vitro and then introduced into the cells via electroporation. The sgRNAs were designed using the GPP sgRNA designer and synthesized by Integrated DNA Technologies (IDT). The electroporation procedure was performed using the Amaxa 4D-Nucleofector system with the P4 Primary Cell 4D-Nucleofector® X Kit S (Lonza).
To assemble the RNP complex, 0.75 µl of Alt-R CRISPR-Cas9 tracrRNA (200 pmol/µl, IDT) was mixed with 0.75 µl of Alt-R CRISPR-Cas9 crRNA (200 pmol/µl, IDT) specific to the target gene. The mixture was incubated at 95°C 5 minutes, followed by a gradual temperature decrease to 70°C with the

speed of 0.5°C /sec. It was then held at 70°C 1 minute before being cooled to room temperature. Then 7.5 µg of Alt-R S.p. HiFi Cas9 Nuclease V3 (IDT) was added and incubated at room temperature 20 minutes to form the complete RNP complex.
For electroporation, T_{MBP} cells that had been stimulated in vitro for 48 hours were purified via Nycoprep separation. The electroporation buffer was freshly prepared with 18 µl of P4 stock solution, 4 µl of supplement 1, and 1 µl of electroporation enhancer (100 µM, IDT) for each reaction. A total of 21 µl of electroporation buffer was taken and used to resuspend 2×10^6cells per reaction. The prepared T_{MBP} cell suspension was then rapidly mixed with the RNP complex and transferred into a nucleofection cuvette. Electroporation was conducted using the pulse code CM137. Immediately after electroporation, the cells were transferred into 3 ml/well of pre-warmed TCGF medium in a 6-well plate and incubated at 10% CO_2 incubator for later usage.

Tide sequencing
To verify the success of single-gene knockout in T_{MBP} cells, TIDE sequencing was performed. 1×10^6 cell number of T_{MBP} cells processed with RNP-mediated CRISPR/Cas9 editing were collected for analysis on the sixth day of in vitro culture. Then the culture medium was completely removed by washing with PBS. The cells were then lysed by adding 500 µl of lysis buffer per sample, followed by overnight incubation at 56°C. After lysis, the samples were heated to 95°C for 10 minutes and subsequently cooled on ice.
Genomic DNA was then precipitated by adding 350 µl of isopropanol, gently mixing, and incubating at room temperature for 10 minutes. Afterwards, the samples were centrifuged at 16,000 × g for 10 minutes at 4°C. The resulting DNA pellet was washed with 1 ml of 70% ethanol per sample, followed by another centrifugation at 16,000 × g for 5 minutes at 4°C. The supernatant was carefully removed, and the DNA pellet was dried at 56°C until it became transparent. Once fully dried, the DNA was resuspended in 50 µl of nuclease-free water.
For PCR amplification, 1 µl of the gene-specific TIDE sequencing primer working solution, 1 µl of the extracted DNA sample, 8 µl of nuclease-free water, and 10 µl of 2 × Optima PCR HotStart Polymerase (FastGene) were combined to prepare the PCR reaction mix. The PCR products were analyzed by electrophoresis on a 1% agarose gel prepared in 1× TAE buffer. DNA fragments corresponding to the expected size were visualized under UV light and purified using a FastGene® Gel/PCR Extraction Kit. The final DNA volume was adjusted to 20 µl, and the samples were submitted for Sanger sequencing at the LMU Biozentrum sequencing service, following their sample preparation guidelines. The sequencing data were analyzed using the ICE (Inference of CRISPR Edits) v2 software tool (Conant et al., 2022)to determine knockout efficiency.

2.2.3. Quantitative Real-time-PCR

mRNA extraction
In vitro cultured target T_{MBP} cells were purified via Nycoprep separation. A total of 3×10^6 cells per group were transferred to a new tube, washed once with cold PBS and centrifuged at 400 × g for 5 minutes at 4°C. The supernatant was completely discarded, and 1ml of Trizol was added for cell lysis. The cells were thoroughly pipetted and incubated on ice for 5 minutes. After the incubation, 0.2ml chloroform was added on the top, vortexed and centrifuged at 12,000 × g for 15 minutes at 4°C. The colorless upper layer was carefully transferred to a new tube, mixed with 0.5ml isopropanol, vortexed and incubated on ice for 10 minutes. The mixture was then centrifuged at 12,000 × g for 10 minutes at 4°C. The supernatant was removed and the mRNA pellet was washed with 1 ml of 70% ethanol per sample, followed by another centrifugation at 7,500 × g for 10 minutes at 4°C. The supernatant was carefully removed, and the RNA pellet was dried by air. Once fully dried, the mRNA

sample was resuspended in 10 µl of nuclease-free water. Samples were stored on ice for short term and -80°C for long term.

cDNA synthesis
RNA concentration was measured using a Nanodrop Spectrophotometer (Nanodrop2000, Thermofisher), then synthesized cDNA using the LunaScript® RT SuperMix Kit according to the manufacturer's instruction.

qPCR
The cDNA was diluted 1:10, then the qPCR reaction system was prepared according to the table below. Each reaction (20 µl) was added to Hard-shell® 96-well PCR plate, with duplicate wells set for each group.

2 × qPCRBIO SyGreen Mix Separate-ROX	10 µl
gene-specific qPCR primer working solution	0.8 µl
Diluted cDNA	5 µl
H_2O	4.2

2.2.4. Flow Cytometry

Cell surface staining
T cell suspensions designated for staining were transferred into a 96-well V-bottom plate, with wells allocated for unstained controls, isotype controls, and distinct markers staining. Each well contained an adequate number of cells to ensure reliable analysis. Initially, the T cells were resuspended in FACS buffer and incubated on ice for 20 minutes to block nonspecific binding. Following incubation, the cells were centrifuged at 400 × g for 3 minutes at 4°C, the supernatant was discarded, and the cell pellet was resuspended in 100 µl of staining solution containing the primary antibody, diluted at 1:100 in FACS buffer. The cells were incubated on ice for 30 minutes, followed by centrifugation at 400 × g for 3 minutes at 4°C. To remove unbound antibodies, the cells were washed three times with FACS buffer with the same centrifugation conditions.
Subsequently, the cells were resuspended in 100 µl of secondary antibody solution, prepared at a 1:500 dilution in FACS buffer, and incubated on ice in the dark for 45 minutes. After incubation, the cells were centrifuged at 400 × g for 3 minutes at 4°C, and the secondary antibody solution was discarded. The samples were then washed once with FACS buffer, followed by two additional washes with ice-cold PBS, with centrifugation at 400 × g for 3 minutes at 4°C for each step. Finally, the stained cells were resuspended in 100 µl of ice-cold PBS and kept on ice in the dark until flow cytometry analysis was performed using a CytoFlex S flow cytometer (Beckman Coulter).

Cytokine staining
T cell suspensions were transferred into 96-well V-bottom plates, with separate wells designated for unstimulated and stimulated groups. Each group included a negative control, isotype control, and distinct cytokines staining. The cells were centrifuged at 400 × g for 3 minutes at room temperature, and the supernatant was removed. The unstimulated group was resuspended in 100 µl RM medium containing 5 µM Brefeldin A (Sigma Aldrich), ensuring thorough mixing. In the stimulated group, cells were resuspended in RM medium supplemented with 100 ng/ml phorbol 12-myristate 13-acetate

(PMA), 100 nM ionomycin, and 5 µM Brefeldin A. The cells were then incubated at 10% CO_2 incubator for 4 hours. After incubation, the cells were centrifuged at 400 × g for 3 minutes at 4°C, the supernatant was discarded, and the cells were resuspended in 150 µl of 2% paraformaldehyde (PFA). The samples were incubated on ice for 15 minutes to fix, followed by another centrifugation under the same conditions. The cells were then resuspended in 150 µl PBS and stored at 4°C until further staining, which was always performed within three days.
For intracellular staining, the fixed cells were first washed with PB buffer (Biolegend) and resuspended in 150 µl PB buffer per well. The samples were incubated on ice for 15 minutes to permeabilize the membrane, followed by centrifugation at 400 × g for 3 minutes at 4°C. After discarding the supernatant, the cells were resuspended in 100 µl of primary antibody solution, prepared by diluting the antibody at 1:100 in PB buffer. If the primary antibody was conjugated with fluorescence, all subsequent steps were performed in the dark. The cells were incubated on ice for 30 minutes and then washed three times with PB buffer to remove unbound antibodies.
Next, the secondary antibody was added at a 1:500 dilution in PB buffer (100 µl per well) and incubated on ice in the dark for 45 minutes. After incubation, the cells were washed once with PB buffer, followed by two additional washes with PBS, using centrifugation at 400 × g for 3 minutes at 4°C for each step. The stained cells were then resuspended in PBS, kept on ice in the dark, and analyzed using a CytoFlex S flow cytometer (Beckman Coulter).

2.2.5. Transwell Chemotactic Assay

For the transwell chemotaxis assay, T_{MBP} cells activated and cultured for six days were used. On the sixth day, T cells were collected and purified using Nycoprep gradient centrifugation. The purified cells were counted using a hemocytometer, and specific gene knockout (KO) $T_{MBP\text{-}GFP}$ cells were mixed with NT control $T_{MBP\text{-}BFP}$ cells in a 1:1 ratio. The final cell suspension was prepared at a concentration of 1.3 × 10^6 T cells/ml in TCM medium, ensuring that each 75 µl medium contained 0.1 × 10^6 T cells.
The assay was performed using a 96-well transwell chamber with a 5 µm pore size (Corning). First, 75 µl of the prepared T cell mixture was carefully added to the upper chamber of each transwell insert. The plate was incubated at 10% CO_2 incubator for 30 minutes to allow the T cells to settle at the bottom of the upper chamber. During this time, the lower chamber remained empty.
After the settling period, 235 µl of TCM medium containing either no chemoattractant (negative control), 30 ng/ml recombinant CCL5 (positive control), or S1p at 100 nM, 50 nM, or 10 nM was added to the lower chambers. Additionally, a reference well was set up by adding the mixed cell suspension directly into the lower chamber to determine the original GFP/BFP ratio before migration. The plate was then incubated at 10% CO_2 incubator for 4 hours without disturbance.
Following incubation, the medium from the lower chambers was carefully collected and transferred into a 96-well V-bottom plate. The collected cells were centrifuged at 400 × g for 3 minutes at 4°C, the supernatant was discarded, and the cells were resuspended in 50 µl of cold PBS per well. The samples were kept on ice until analysis by using a CytoFlex S flow cytometer (Beckman Coulter).

2.2.6. Rat EAE model

Adoptive transfer EAE
T cells that had been in vitro activated for 48 hours were collected from culture dishes, and their numbers were determined using a hemocytometer. A total of 1 × 10^6 T cells per rat were moved to

new centrifuge tube and were centrifuged at 400 × g for 5 minutes at room temperature. The supernatant was discarded, and the cell pellet was then resuspended in 1 ml of pre-warmed EH medium per rat.
The prepared T cell suspension was administered to recipient rats via intravenous injection through the tail vein. The body weight of each rat was recorded immediately after injection as the baseline measurement. Following cell transfer, body weight and EAE score were monitored daily to assess disease progression.
EAE score was according to the following scale: 0 - no observable clinical symptoms, 0.5 - mild tail weakness, 1 - complete tail paralysis, 1.5 - unsteady gait or difficulty in righting reflex, 2 - Hind limb paresis, 2.5 - Hind limb paresis with dragging of one foot, 3 - complete hind limb paralysis

In vivo Migration assay
To analyze the in vivo migration of gene-modified T cells, specific gene-knockout $T_{MBP\text{-}GFP}$ cells and NT control $T_{MBP\text{-}BFP}$ cells were collected after 48 hours of in vitro activation. The cell number was determined using a hemocytometer, and a mixture containing 3×10^6 $T_{MBP\text{-}GFP}$ and 3×10^6 $T_{MBP\text{-}BFP}$ cells per animal was prepared. The mixed cells were injected as described above.
Three days post-injection, the rats were sacrificed for tissue collection and analysis of T cell distribution. Blood (6 ml) was drawn via cardiac puncture using a heparin-pretreated syringe. Cerebrospinal fluid (CSF) was collected from the foramen magnum (0.1 ml). The spleen, parathymic lymph nodes, spinal cord leptomeninges, and spinal cord parenchyma were carefully dissected and placed in cold EH buffer on ice for further processing.

In vivo Migration assay tissue/organ processing and T_{MBP} cell isolation
The collected blood was diluted 1:1 with room-temperature PBS and carefully layered onto 3 ml Nycoprep. Each rat required two Nycoprep gradient tubes for blood processing (a total of 12 ml diluted blood). Gradient centrifugation was performed at 800 × g for 30 minutes with slow acceleration and deceleration settings. Following centrifugation, the white cell layer was collected, washed with PBS (400 × g, 5 min, 4°C), resuspended in 3 ml EH medium and placed on ice for subsequent analysis.
The collected CSF was diluted with an equal volume of PBS and stored on ice for further analysis.
Spleen and parathymic Lymph Nodes were processed into a single-cell suspension using sterile metal strainer. The resulting suspension was centrifuged at 400 × g for 5 minutes at 4°C. The supernatant was discarded, and the splenocyte pellet was resuspended in 5 ml ACK lysis buffer and incubated at room temperature for 2 minutes to remove red blood cells. The sample was then washed by filling the tube with PBS and centrifuging at 400 × g for 5 minutes at 4°C. The final cell suspension was prepared in 10 ml EH medium, filtered through a 40 µm cell strainers (Greiner Bio-One GmbH) to remove debris, and stored on ice until analysis. For parathymic lymph nodes sample, the supernatant was discarded, and the cells were resuspended in 1 ml EH medium and stored on ice until analysis.
The leptomeninges and spinal cord parenchyma were processed separately into single-cell suspensions using sterile metal strainers. The spinal cord parenchyma cell suspensions were placed on ice until analysis, and the leptomeninges cell suspensions were centrifuged at 400 × g for 5 minutes at 4°C. The supernatant was removed, and the cells were resuspended in 1 ml EH buffer and stored on ice.
Following tissue processing, the proportions of GFP^+ and BFP^+ T cells in each sample were analyzed using a CytoFlex S flow cytometer (Beckman Coulter).

2.2.7. Intravital Two-photon Imaging

Animal Model and Surgical Procedures

The EAE model used for two-photon intravital imaging followed the same protocol as the in vivo migration assay. Activated Klf2-KO $T_{MBP\text{-}GFP}$ and NT control $T_{MBP\text{-}BFP}$ cells were intravenously injected into recipient rats at an amount of 3×10^6 cells per group, in total 6×10^6 cells per animal. Body weight and EAE scores were recorded daily to monitor disease progression. On the third day post-injection, when a significant reduction in body weight was observed, intravital two-photon imaging was performed to analyze T cell migration in the leptomeninges.

The surgical procedures were conducted as previously established in our laboratory (Bartholomaus et al., 2009). Anesthesia was induced by intramuscular injection of MMF (2 mg/kg Midazolam, 150 µg/kg Medetomidine, and 5 µg/kg Fentanyl). Once the animals were stabilized under anesthesia, a catheter was inserted into the tail vein for the intravenous administration of 100 µg Texas-Red conjugated to 70 kDa dextran (Invitrogen/ThermoFisher) to visualize the blood plasma.

A tracheotomy was performed following a midline incision of the neck, and mechanical ventilation was initiated to maintain stable respiration and remained anesthetized with continuous delivery of 1.5–2.0% isoflurane. To expose the leptomeninges, the animals were placed in a prone position on a platform. A 3 cm midline incision was made at the Th12/13 vertebral level, and the paraspinal muscles were carefully dissected. To minimize movement artifacts during imaging, three vertebrae were stabilized bilaterally using a custom-made fixation platform, and the rat was gently elevated. A dental drill (Foredom) was used to thin and remove the dorsal portion of a vertebra.

For imaging stabilization, low-melting-point agarose was carefully applied around the exposed area, forming a containment ring. The cavity was then filled with PBS to maintain tissue hydration during imaging. The spinal cord leptomeninges was imaged in vivo using a Leica SP8 two-photon microscope equipped with a water-immersion 25× objective lens (N.A.: 1.00, WD: 2.6 mm). A pulsed laser (InSight DS+ Single, Spectra Physics) was tuned to 840 nm to excite BFP and EGFP fluorescence. Following emission signals were detected, BFP: 400-463nm, GFP: 505nm-567nm, and Texas Red: 578nm-644nm Image acquisition covered a field of around 440 µm × 440 µm, with a resolution of 512 × 512 pixels and a Z-stack depth of ~60 µm, using 1–2 µm intervals.

Image acquisition and analysis

Time-lapse image sequences were recorded using LAS X software (Leica) and processed using ImageJ (NIH). A Gaussian blur filter (1-pixel cutoff) was applied before generating maximum Z-projections. When required, background subtraction was performed to enhance contrast. Fluorescence intensity adjustments were made through linear contrast and brightness corrections.

2.2.8. Bioinformatic Analysis

The bioinformatics analysis and graphical representation of the results (Figure 18) in this study were conducted by Clara de la Rosa del Val. The analytical methods employed were consistent with those previously described in the publication by Dr. Arek Kendirli and Clara de la Rosa del Val (Kendirli et al., 2023b).

2.2.9. Statistical Analysis

Flow cytometry data were analyzed using FlowJo (version 10+), statistical analyses and corresponding figures were processed using GraphPad Prism 7. Specific statistical methods applied in the analyses are detailed in the respective figure legends. Data are presented as mean ± standard deviation (SD), with statistical significance indicated by p-values as follows: * $p<0.05$, ** $p<0.01$, *** $p<0.001$, **** $p \leqslant 0.0001$, and NS for non-significant differences.

3. RESULTS

3.1. Genome-wide CRISPR/Cas9 Screening of T_{MBP} Cells Migration in EAE Model

As described above, crucial regulators influence T cell migration were identified from genome-wide CRISPR/Cas9 screening. From those candidate genes, we need further validation of their actual effect in T cell migration and related mechanisms. Since the ultimate goal was to find potential therapeutic targets for MS treatment, we focused on genes whose deletion reduces T cell migration into the CNS (Figure 3B). This analysis identified several key genes, including Itga4, Hsp90b1, Grk2, Cxcr3, and Gnai2, which were further validated that these genes are indeed crucial regulators of T cell migration into the CNS (Kendirli et al., 2023b). In addition, we revealed the mechanism of action. Specifically, the deletion of Hsp90b1 led to reduced surface expression of Itga4, as Hsp90b1 is required for transporting Itga4 from the Golgi to the cell membrane. Given that Itga4 is essential for T cell adhesion to endothelial cells (Holman et al., 2011), the loss of either Itga4 or Hsp90b1 impaired T cell migration into the CNS and subsequently reduced EAE development.

Among these expanded candidates, the Foxo1 and Klf2 related signaling pathway emerged as an interesting topic of exploration. Foxo1, a member of the forkhead box O (Foxo) transcription factor subfamily, is known for its critical role in regulating genes associated with T cell memory. For instance, Foxo1 enhances T cell factor (Tcf) expression, which mediates the development of central memory T cells in mice (Doan et al., 2024). Specific deletion of Foxo1 in T cells leads to an accumulation of single-positive thymocytes and dramatic reduction in $CD4^+$ and $CD8^+$ T cells in the peripheral blood circulation (Gubbels Bupp et al., 2009). Transcriptomic analyses of Foxo1-deficient T cells have revealed downregulation of key trafficking molecules, including L-selectin (Sell), S1pr1, Klf2, and Ccr7 (Gubbels Bupp et al., 2009). These changes explain the impaired migration of Foxo1-knockout (KO) T cells exit from the thymus to the peripheral circulation.

Klf2 was identified as a critical regulator of T cell migration and was also reported to function downstream of Foxo1 (Kerdiles et al., 2009). Previous findings by Odoardi et al. demonstrated that Klf2 is the most upregulated gene in T cells with a migratory phenotype, the T cells which are ready to migrate into the CNS, at the transcriptomic level (Odoardi et al., 2012). Alongside the Klf2, other migration-associated genes, including S1pr1, Itgb7, Ccr2, Sytl1, and Rhoh, were also upregulated in the T cells with migratory phenotype, with S1pr1 and Itgb7 being under the transcriptional control of Klf2 (Odoardi et al., 2012). These results position Klf2 as a key marker of migratory $CD4^+$ T cells.

3.2. CRISPR-Cas9 Klf2 Knockout does not Alter Activated T Cell Activation and Function

Although two rounds of CRISPR/Cas9 screening identified Klf2 as a candidate gene significantly influencing T_{MBP} cell migration to the CNS during EAE (Figure 3B), the possibility of false-positive results remains possible. Reduction in T_{MBP} cell migration to the CNS sometimes may not only due to the impaired migration-associated mechanisms but also from changes in T cell activation and proliferation. To further discuss how Klf2 functions, we established Klf2-KO T_{MBP} cells to test their exact role in T cells during EAE. For accurate and efficient genome editing, we employed transient delivery of Cas9 protein complexed with Klf2 sgRNA, known as the ribonucleoprotein (RNP) system (Zhang et al., 2021). This method minimizes cell stress compared to double-viral transduction systems that require in vivo transcription and translation of Cas9, which can disrupt normal cellular functions and prolong in vitro culture. The RNP approach also has been proven could reduce off-target effects, insertional mutagenesis, and immune responses while maintaining high editing efficiency (Zhang et al., 2021).

To be able to track these edited cells in animals, T_{MBP} cells were first transduced with EGFP for experimental T cells and BFP for control T cells. RNP-mediated CRISPR/Cas9 genome editing was then applied to generate Klf2-KO $T_{MBP\text{-}GFP}$ cells and control $T_{MBP\text{-}BFP}$ cells which were transfected with non-targeted sgRNA (NT) (Figure 4A). Knockout efficiency was validated using TIDE sequencing, and the KO score was above 60% (Figure 4B), meaning successful Klf2-KO in the majority of the cell population.

To evaluate the impact of Klf2 deficiency on T cell proliferation and phenotype, we compared Klf2-KO and NT T_{MBP} cells number under standard in vitro culture conditions. In this system, rat primary T_{MBP} cells were activated using mitomycin C-treated thymocytes (as antigen presenting cells, APCs) and MBP protein. The first two days of culture, termed the "restimulation phase" represents the activation period of our rat primary T_{MBP} cells. Especially on the day 2 of culture, the cells exhibit peak protein synthesis and the largest observed cell size. This phase was followed by the "expansion phase" (from day 3 to day 6), during which IL-2 was supplemented to promote proliferation (Nelson and Willerford, 1998). While Klf2-KO and NT T_{MBP} cells exhibited comparable numbers during the restimulation phase, Klf2-KO cells displayed a slightly enhanced proliferative capacity after entering the expansion phase, with cell numbers reaching approximately 1.5-fold that of NT controls by day 4 (Figure 4C).

About the activation status, we analyzed classic T cell surface activation markers expression on our Klf2-KO cells, including CD25 (IL-2 receptor alpha chain), CD134 (OX40 receptor), and the TCRβ (T cell receptor beta chain). By day 2 of activation, when T cells were at their peak activation state, Klf2-KO

T_{MBP} cells expressed CD25 and CD134 at levels comparable to NT controls. TCRβ expression was slightly elevated in Klf2-KO cells, but the difference did not reach statistical significance (Figure 4D, F).

Beyond evaluating activation markers, we also tested integrin expression to initially explore whether Klf2 deficiency influences T cell adhesion and migration. Integrins are critical mediators of T cell trafficking, as they facilitate interactions with endothelial cells and coordinate responses to chemokines and antigenic signals, thereby regulating cellular motility and tissue infiltration (Bertoni et al., 2018). Considering their central role in immune cell localization, any dysregulation in integrin expression could significantly impact T cell function.

Flow cytometric analysis of key integrins, integrin α4 (CD49d) and integrin β1 (CD29), which form the VLA4 complex, as well as integrin αL (CD11a) and integrin β2 (CD18), components of the LFA1 complex, revealed no significant differences in expression levels between Klf2-KO and NT T_{MBP} cells (Figure 4E, F). Therefore, in vitro Klf2 deletion does not obviously influence the integrin expression.

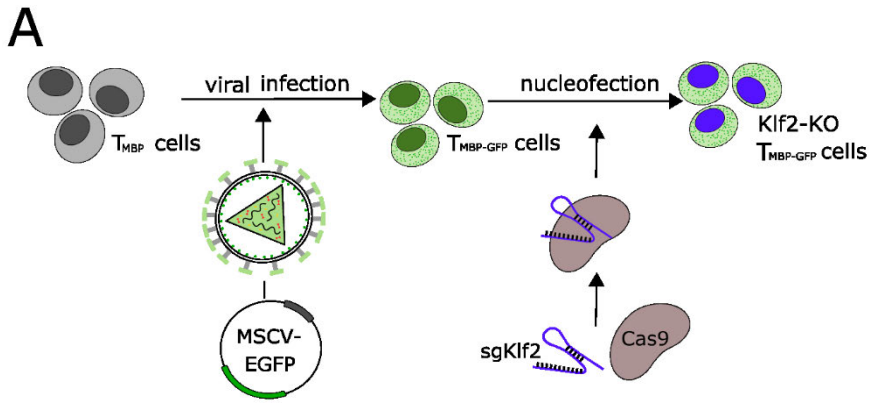

B

Status	Guide Target	PAM Sequence	Indel %	Model Fit (R^2)	Knockout-Score	Nuclease
Succeeded	TGAGGACCTAAACAGCGTGC	TGG	88	0.93	80	spcas9

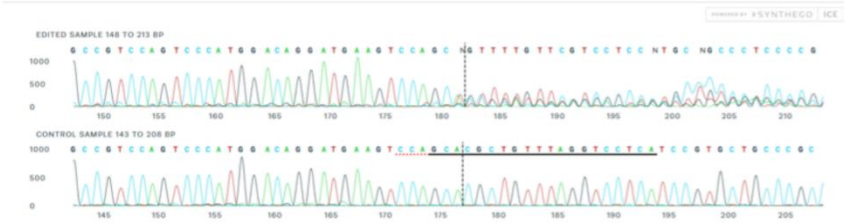

Figure continues on next page

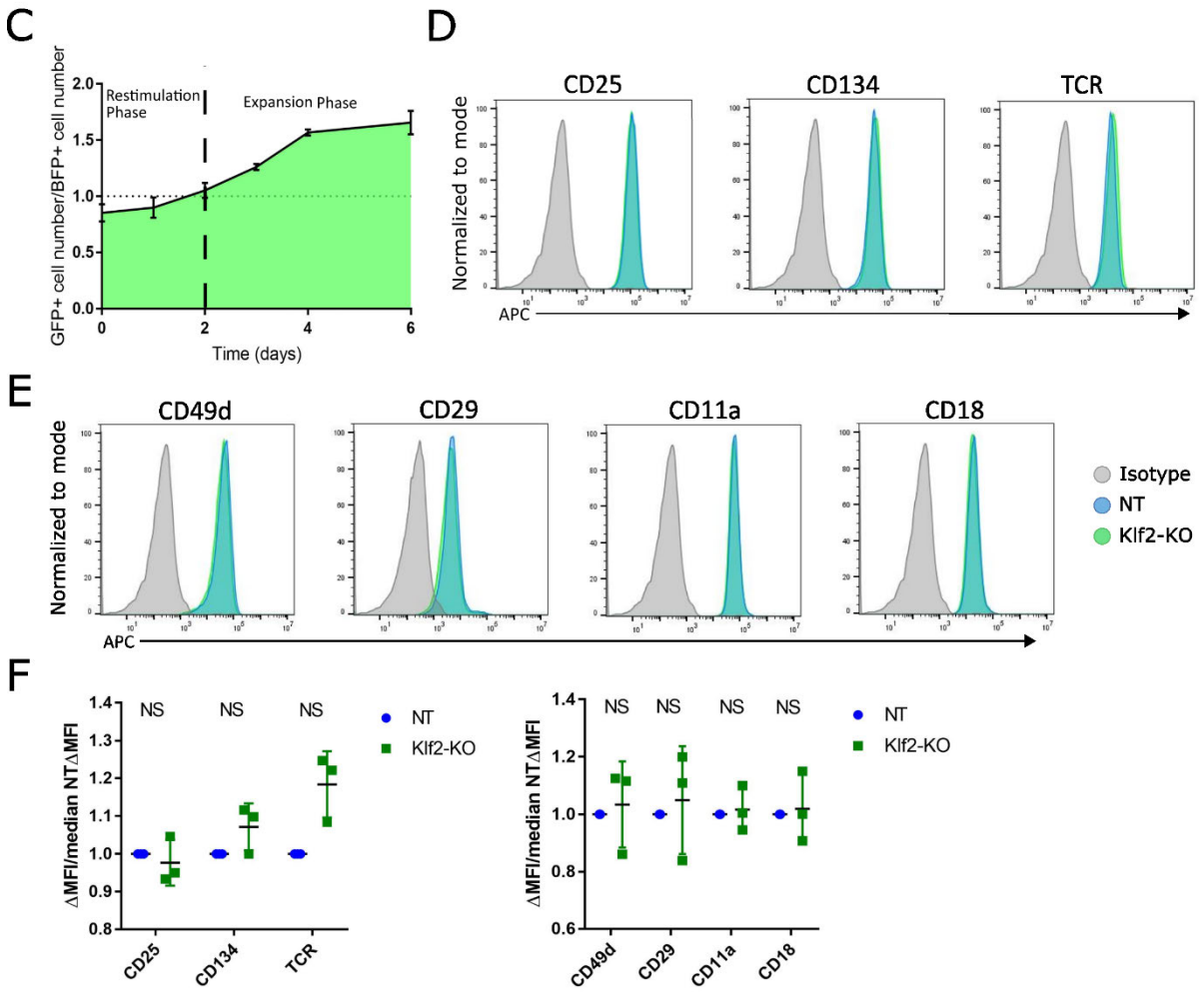

Figure 4 Activated Klf2-KO T_{MBP} Cells Proliferation, Activation and Adhesion in vitro

A). CRISPR/Cas9-mediated Klf2-KO. Rat primary T_{MBP} cells were first transduced with a retroviral vector encoding EGFP. Then further introduced Cas9 and Klf2 sgRNA to $T_{MBP\text{-}GFP}$ cells by electroporation to achieve RNP-mediated CRISPR/Cas9 genome editing. B). TIDE Sequence Result. DNA sequence of the Klf2-KO and NT T_{MBP} cells including KO intervention area was compared by ICE (Inference of CRISPR Edit) approach. C). Klf2-KO T Cells Proliferation. Klf2-KO and NT T_{MBP} cells were co-cultured and their cell number was counted daily using flow cytometry from day 0 to day 6 under standard T_{MBP} in vitro culture condition. Day 0 to 2 are considered as the restimulation phase of T_{MBP} cells, and day 2 to 6 are extension phase. The ratio of Klf2-KO T cells to NT T_{MBP} cells was then calculated. Data represent N=2 independent experiments. D,E). Activation (D) and Adhesion (E) Markers Expression in Klf2-KO T Cells. Flow cytometry plots show the surface expression of activation and adhesion markers in Klf2-KO and NT T_{MBP} cells on day 2 post-activation. Gating strategy: lymphocytes →single cells → BFP+ or GFP+ populations. The expression was assessed using APC fluorescence. F). Quantification of Activation and Adhesion Markers Expression in Klf2-KO T Cells. The activation markers and adhesion molecules level were quantified by calculating the ΔMFI (MFI- MFI of isotype control) and normalizing it to the ΔMFI of NT control cells. MFI values were obtained using FlowJo. Statistical analysis was performed using two-way ANOVA with multiple comparisons. Data is presented as mean ± SD (N = 3).

3.3. Klf2 KO T_{MBP} Cells Fails to Induce EAE and Accumulate in the SLOs

From the in vitro phenotype and proliferation analysis, Klf2-KO T cells displayed a mild increase in proliferative capacity and a comparable activation status as NT controls cells, proving that they were functionally able to induce EAE. This raised the question of whether Klf2 deletion affected their migratory ability in vivo. To answer this, we adoptively transferred Klf2-KO T_{MBP} cells into rats and monitored clinical scores and body weight over time. As a reference, NT T_{MBP} cells were injected in parallel to establish a standard EAE model. We also compared Klf2-KO T_{MBP} cells EAE induction ability with Itga4-KO T_{MBP} cells EAE induction, which has been already published (Kendirli et al., 2023). Surprisingly, Klf2-KO T_{MBP} cells failed to induce any signs of EAE, similar with the outcome observed with Itga4-KO cells (Figure 5A). Rats injected with Klf2-KO cells showed no weight loss or neurological symptoms, indicating a complete inability to trigger the disease. Combing with the slightly enhanced Klf2-KO cells proliferation under in vitro culture condition, we could conclude that their failure to induce EAE was not due to intrinsic functional defects or proliferation impairment but rather to an impaired ability to reach the CNS.

Although both Klf2-KO and Itga4-KO T cells resulted in an absence of EAE symptoms, their underlying migration behaviors were markedly different, as revealed by our genome-wide CRISPR/Cas9 screen (Figure 3B). Itga4-KO prevented T_{MBP} cells from migrating into the CNS from both the blood and spleen. While Klf2-KO specifically impaired migration from the spleen to the CNS. Although our screening did not directly assess how Klf2-KO affects T_{MBP} cells trafficking between the spleen and blood, the statistical analysis showed no significant difference in Klf2-KO T_{MBP} cell amount between the blood and CNS (Figure 3B). This implies that in the absence of Klf2, T_{MBP} cells may have a stronger tendency to remain in the spleen than circulating in the blood.

For a more detailed look at the distribution pattern of Klf2-KO T cells in our adoptive EAE model and to determine which migration step Klf2 primarily regulates, we performed adoptive transfer EAE model to observe Klf2-KO cells in vivo distribution patterns (Figure 5B). Klf2-KO $T_{MBP\text{-}GFP}$ cells and NT $T_{MBP\text{-}BFP}$ cells were activated in vitro for two days. At the time point of their peak activation, the cells were mixed at a 1:1 ratio and intravenously injected into the same recipient rat. By day 3 post-injection, when NT T_{MBP} cells had begun infiltrating the CNS, evidenced by obvious weight loss in the host, we harvested and analyzed cell distribution across multiple compartments, including peripheral blood, spleen, ptLNs, CSF, spinal cord leptomeninges, and spinal cord parenchyma (Figure 5B).

Klf2-KO T_{MBP} cells exhibited a unique regionally concentrated distribution pattern, characterized by a significant accumulation in SLOs, particularly in the ptLNs, where their numbers were nearly ten-fold higher than NT T_{MBP} cells (Figure 5C, D). Also, their accumulation in the spleen was elevated,

approximately two to four-fold compared to control cells (Figure 5C, D). The accumulation in the spleen was notably less pronounced than in the ptLNs. Only a small fraction of Klf2-KO cells successfully entered the CNS, and their distribution among the spinal cord leptomeninges, CSF, and parenchyma showed no difference (Figure 5D).

These findings suggest that Klf2 might play a role in facilitating T cell egress from SLOs. Unlike Itga4, which primarily mediates adhesion-dependent trafficking (Kendirli et al., 2023), Klf2 appears to be more likely to function in the T cells traffic between SLOs and bloodstream.

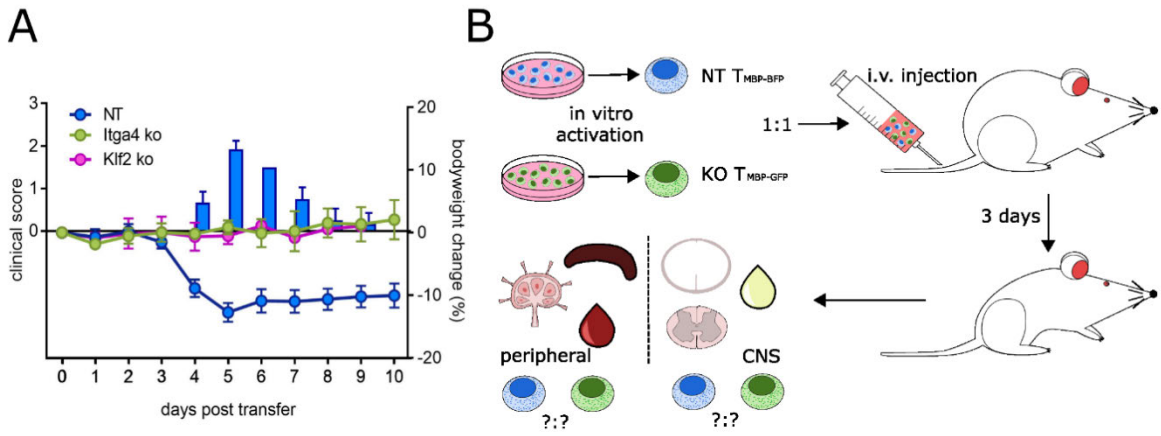

Figure continues on next page

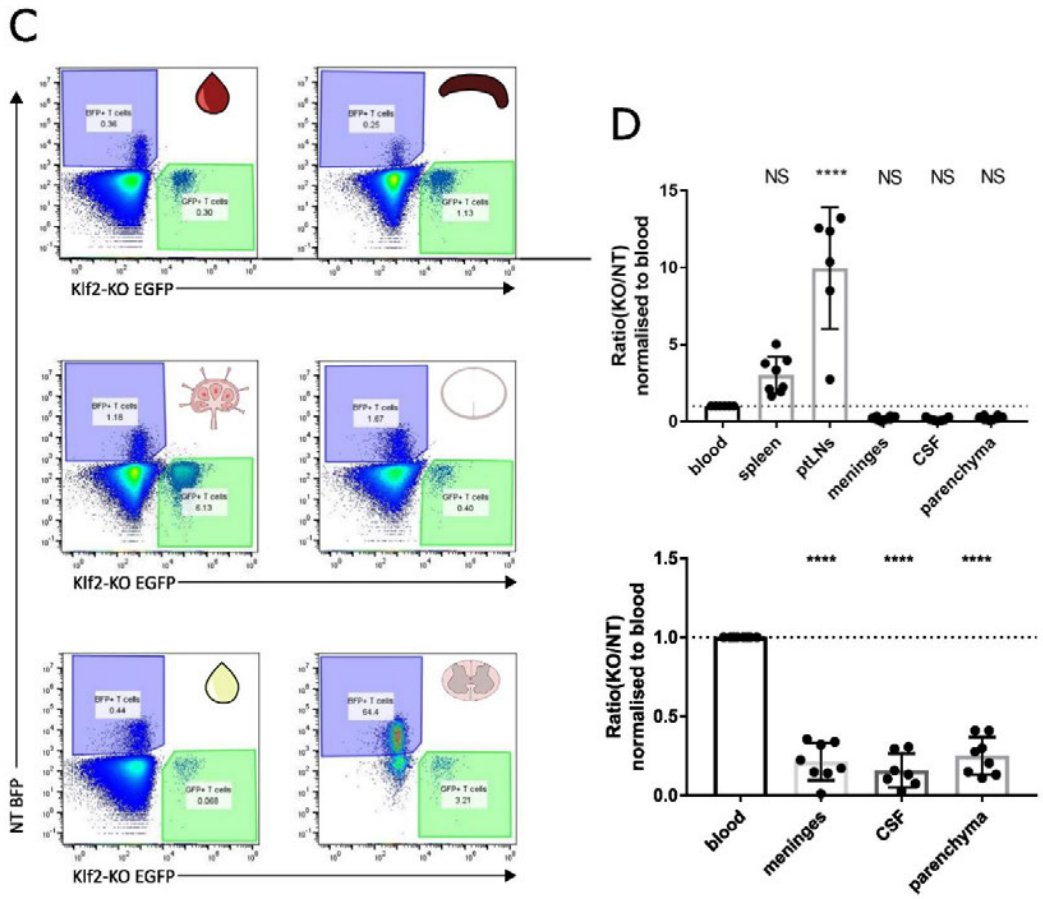

Figure 5 Klf2-KO T_{MBP} Cells EAE Model and in vivo Distribution Pattern

A). EAE clinical course by Klf2-KO and NT T_{MBP} Cells. Clinical scores (bars) and relative body weight changes (lines) were monitored in rats following NT (blue), Itga4-KO (green) or Klf2-KO (pink) T_{MBP} cell injection, body weights are normalized to day 0 (pre-injection). Each group: N = 3, mean ± SD. For comparison, the Itga4-KO T_{MBP} cell data is included (Kendirli et al., 2023b). B). Setting of the Klf2-KO T_{MBP} Cell in vivo Distribution Pattern. NT $T_{MBP-BFP}$ cells and Klf2-KO $T_{MBP-GFP}$ cells were activated in vitro, mixed at a 1:1 ratio, and intravenously injected into rats. Clinical scores and body weight were monitored daily post-injection. On day 3, when significant weight loss was observed, rats were sacrificed, and organs/compartments were harvested, including peripheral compartments (spleen, ptLNs, and blood) and CNS compartments (CSF, spinal cord leptomeninges, and spinal cord parenchyma). Tissues were homogenized, and the ratios of GFP^+ and BFP^+ cells in different compartments were analyzed by flow cytometry. C). Flow Cytometry Analysis of NT and Klf2-KO T_{MBP} Cell Distribution. Flow cytometry plots depict the proportion of Klf2-KO $T_{MBP-GFP}$ and NT $T_{MBP-BFP}$ cells across different organs and compartments on day 3 post-injection. Gating strategy: lymphocytes →single cells →BFP^+ or GFP^+ populations. BFP+ cells are gated in blue, and GFP^+ cells in green. D) Quantification of Klf2-KO T_{MBP} Cell Distribution in Organs. Cell counts for GFP^+ and BFP^+ populations were obtained via FlowJo analysis. To account for inter-individual variability, the upper bar chart shows GFP^+/BFP^+ ratio in all compartments examined. The lower chart only shows the cell ratio in CNS compartments. The GFP^+/BFP^+ ratio in each compartment was all normalized to the ratio in the blood of the same animal. A value of 1 indicates equal distribution between blood and the respective compartment, values >1 indicate Klf2-KO GFP^+ cell accumulation in that compartment compared to blood, and values <1 indicate reduced presence relative to blood. Statistical analysis was performed using one-way ANOVA with multiple comparisons. Data is presented as mean ± SD (N = 8).

3.4. Klf2 KO cells Exhibits High Activation Status in the SLOs

To further explore the mechanisms underlying the preferential retention of Klf2-KO T_{MBP} cells in SLOs, we first examined their activation status and cytokine production. GFP^+ (Klf2-KO) and BFP^+ (NT) T_{MBP} cells from the spleen and ptLNs on day 3 post-intravenous administration in a Klf2-KO $T_{MBP\text{-}GFP}$/NT $T_{MBP\text{-}BFP}$ 1:1 co-transfer EAE model, were used for flow cytometry analysis (Figure 6A). TCR expression, the central receptor that induce $CD4^+$ T cell activation via antigen recognition, was slightly upregulated in Klf2-KO T cells compared to NT T cells. In addition, the analysis of CD25 and CD134 expression revealed that CD25 expression was significantly upregulated in Klf2-KO T_{MBP} cells than in NT control cells within ptLNs. Meanwhile their CD134 expression were not changed compared to control (Figure 6B, C). Both CD25 and CD134 serve as activation markers for T cells, as their expression levels increase upon T cell activation. However, their upregulation depends on different mechanisms. For instance, CD134 expression upregulation strictly regulated by TCR signaling (Redmond et al., 2009), CD25 expression upregulation can be induced by either TCR or IL-2 induced STAT5 signaling way (Shatrova et al., 2016). Additionally, previous research from Dr. Kawakami revealed that in our rat primary T_{MBP} cells model, TCR expression downregulates when T cells get activated in an antigen dependent manner (Aboul-Enein et al., 2004).

Beyond activation markers, we assessed cytokine production, focusing on IFN-γ, IL-17A, and TNF-α, key effector molecules of Th1 and Th17 cells. Detecting cytokine expression is essential for understanding the functional properties of autoreactive T cells. Flow cytometry allows us to compare cytokine production between GFP^+ (Klf2-KO) and BFP^+ (NT control) T cells in tissue suspensions from the spleen and ptLNs. However, it is difficult to detect under standard intracellular staining protocols, as newly synthesized cytokines are rapidly secreted. Also, the overall amount of cytokines produced by each T cell is relatively low, making it difficult to detect subtle changes in expression.

To overcome these limitations, we cultured cells ex vivo in the presence of brefeldin A, with or without additional stimulation by PMA and ionomycin. The analysis without stimulation shows baseline cytokine production, while one with stimulation reveal the potential to secrete cytokines. Brefeldin A was used to inhibit intracellular protein transport, ensuring that newly synthesized cytokines remained within the cells during the culture period, thereby reaching detectable levels (Schuerwegh et al., 2001). PMA and ionomycin, which activate the nuclear transcription factor-kappa B (NF-κB) and NFAT signaling pathways (Lee et al., 2023), were included to amplify cytokine production. Cells cultured with only brefeldin A were designated as the “unstimulated”, while those exposed to brefeldin A along with PMA and ionomycin were classified as “stimulated”.

Klf2-KO cells from both the spleen and ptLNs exhibited slightly elevated levels of IFN-γ and IL-17A under unstimulated condition compared to NT cells, suggesting mildly heightened inflammatory phenotype. When extra stimulation was performed, T_{MBP} cells isolated from both organs (ptLNs and the spleen) showed four distinct population based on IFN-γ and IL-17A staining: IFN-γ^-IL-17A^- (nonpolarized), IFN-γ^+IL-17A^- (Th1), IFN-γ^-IL-17A^+ (Th17), and IFN-γ^+IL-17A^+ (dual Th1/Th17) (Figure 6D).

PMA and ionomycin stimulation enhanced production of cytokines in general, but Klf2-KO T_{MBP} cells displayed significantly increased IFN-γ and IL-17A production compared with NT controls. Another interesting result is despite their heightened production of IFN-γ and IL-17A, Klf2-KO T_{MBP} cells did not exhibit any bias toward either the Th1 or Th17 lineage, maintaining a Th1/Th17 distribution similar to NT control cells (Figure 6D, E). Additionally, the expression of TNF-α upregulated only in the Klf2-KO cells collected from the ptLNs (Figure 6F), which is different than the IFN-γ and IL-17A production change. TNF-α has been widely admitted as a strong pro-inflammatory factor, which is secreted by inflammatory immune cells. Study also revealed that TNF-α is not only a product synthesized by $CD4^+$ T cells, but also function as shaping Th1/Th17 polarization (Pesce et al., 2022). With the stimulation of TNF-α more cells differentiated to Th17 phenotype, alongside an enhanced capacity of in Th1 cells (Pesce et al., 2022).

Taken together, we revealed that Klf2-KO T cells exhibited higher CD25 expression compared with NT control T cells in SLOs during EAE induction, which is different with the activation phenotype observed during standard in vitro culture. At the same time, Klf2-KO T cells produce more IFN-γ, IL-17A and TNF-α compared to NT T cells, especially in ptLNs, where Klf2-KO T cells were highly accumulated during EAE. Despite showing marked pro-inflammatory profile in SLOs, Klf2 deficiency did not alter the Th1/Th17 differentiation. Considering the absence of MBP antigen in rat SLOs as well as a different upregulation between CD25 and CD134 as described before, high pro-inflammatory profile in Klf2-KO T cells seem due to a failure to downregulate the pro-inflammatory function as control cells.

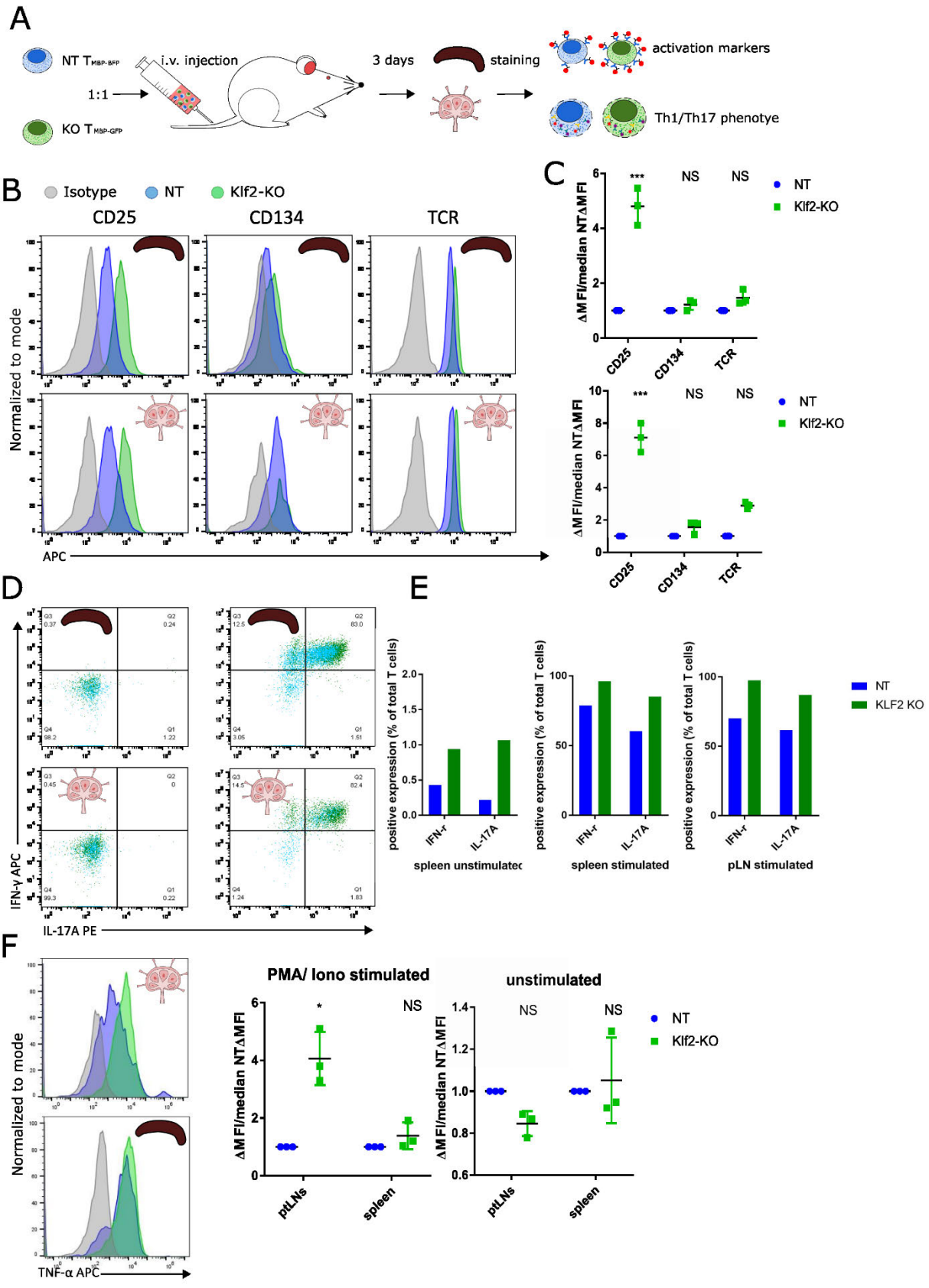

Figure 6 Phenotypic Analysis of Klf2-KO T_{MBP} Cells in Spleen and ptLNs at the Onset of EAE

A). Experimental Design for Phenotypic Analysis of Klf2-KO T_{MBP} Cells. NT $T_{MBP-BFP}$ and Klf2-KO $T_{MBP-GFP}$ cells were activated in vitro, mixed at a 1:1 ratio, and intravenously injected into rats. Three days post-injection, when significant weight loss was observed, rats were sacrificed, and GFP^+/BFP^+ T_{MBP} cells were isolated from the spleen and ptLNs. Flow cytometry was performed to assess the expression of activation markers and cytokines. **B). Activation Profile of Klf2-KO T_{MBP} Cells.** Flow cytometry plots depict the expression of surface activation markers on Klf2-KO T_{MBP} cells (green) and NT T_{MBP} cells (blue) in the spleen (top row) and ptLNs (bottom row). Gating strategy: lymphocytes → single cells → BFP^+ or GFP^+ populations → APC fluorescence detection. **C). Quantification of Surface Activation Marker Expression.** ΔMFI values (MFI - MFI isotype control) of surface activation markers in Klf2-KO T_{MBP} cells were normalized to NT T_{MBP} control cells. Statistical significance was determined using two-way ANOVA with multiple comparisons. Data is presented as mean ± SD (N = 3). **D). IFN-γ and IL-17A Production in Klf2-KO T_{MBP} Cells.** Flow cytometry plots illustrate IFN-γ and IL-17A expression in Klf2-KO (green) and NT T_{MBP} cells (blue) from the spleen (top) and ptLNs (bottom). Left: cytokine expression in unstimulated group. Right: cytokine expression following ex vivo PMA/Ionomycin stimulation. Gating strategy: lymphocytes → single cells → BFP^+ or GFP^+ populations → APC and PE fluorescence detection. **E). Quantification of IFN-γ^+ and IL-17A$^+$ Populations.** The percentage of IFN-γ^+ and IL-17A$^+$ cells was quantified (N = 1). **F). TNF α Production in Klf2-KO T_{MBP} Cells.** Flow cytometry plots in the left illustrate TNF-α production in Klf2-KO (green) and NT T_{MBP} cells (blue) from the spleen (top) and ptLNs (bottom) under ex vivo PMA/Ionomycin stimulation. Gating strategy: lymphocytes → single cells → BFP^+ or GFP^+ populations → APC fluorescence detection. Right dot plots show the quantified TNF-α production level with (left) and without (right) ex vivo PMA/Ionomycin stimulation. Quantification was performed by calculating the ΔMFI (MFI- MFI of isotype control) and normalizing it to the ΔMFI of NT control cells. MFI values were obtained using FlowJo. Statistical analysis was performed using two-way ANOVA with multiple comparisons. Data is presented as mean ± SD (N = 3).

3.5. Klf2 KO T_{MBP} Cells Exhibits Distinct Ccr7 Expression in SLOs

For answering the question of why Klf2-KO T_{MBP} cells stopped migrating into the CNS and instead accumulated in the SLOs, we first examined the key homing molecule Ccr7. Up to date, Ccr7 has been well-established as a classic homing molecule that induce both T cell entry into and retention within lymphoid nodes (Masopust and Schenkel, 2013). Ccr7, expressed on the surface, guides T cells to high endothelial venules (HEVs) where the Ccl21 (ligand of Ccr7) is abundantly expressed. It induces conformational changes in integrins expressed on T cells, enabling their interaction with ligands presented by HEVs, thereby further promoting the entire migration process into the LNs (Masopust and Schenkel, 2013). Within the LNs, especially in the T cell zone, Ccl19 (another ligand of Ccr7) and Ccl21 are highly abundant and act as the T cells retaining signals.

During in vitro culture, the Ccr7 expression was comparable between Klf2-KO and NT T_{MBP} cells (Figure 7A). When we quantified the expression levels by calculating ΔMFI values (Figure 7C), Klf2-KO T_{MBP} cells showed a slight increased Ccr7 expression, but no statistical difference. Upon entering SLOs during adoptive transfer EAE, T_{MBP} cells undergo a phenotypic transition, shifting from an activated state to a migratory phenotype characterized by upregulation of integrins and chemokine receptors required for CNS infiltration (Flügel et al., 2001). To test whether deletion of Klf2 change the expression of Ccr7 in migratory T cells, we next examined the Ccr7 expression in Klf2-KO and NT

T_{MBP} cells isolated from the spleen and ptLNs by the third day post-intravenous injection in a 1:1 co-transfer EAE model. Flow cytometry analysis revealed a pronounced increase in Ccr7 expression in Klf2-KO T_{MBP} cells within the ptLNs. In the spleen, Ccr7 expression was also slightly upregulated, with the increase reaching statistical significance (Figure 7B, C). This increase expression of Ccr7 in ptLNs and the spleen happened together with their preferential retention of Klf2-KO cells in these organs. Combining with the previously described function of Ccr7, our results lead to the hypothesis that the overexpression of Ccr7 is a reason of Klf2 deficient T_{MBP} cells highly accumulate in the SLOs.

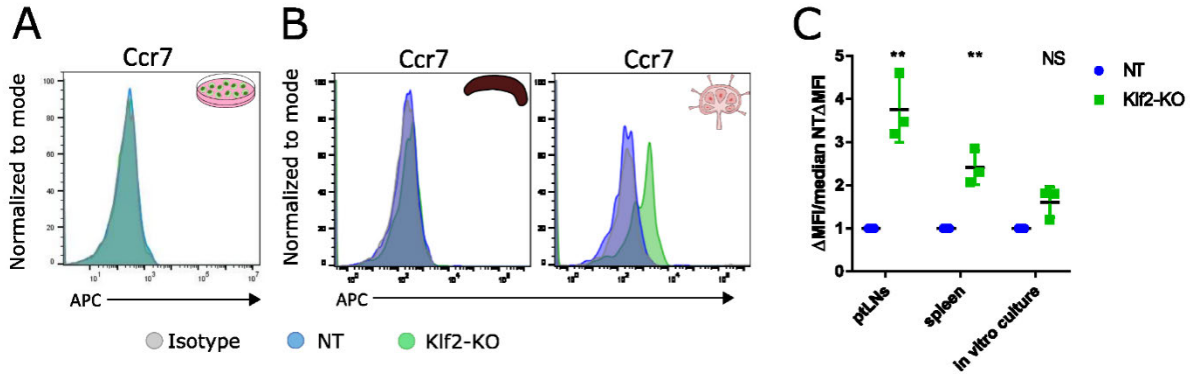

Figure 7 Expression of Ccr7 in Klf2-KO T_{MBP} Cells

A). Ccr7 Expression in vitro. Flow cytometry plots illustrate the expression of Ccr7 in Klf2-KO T_{MBP} cells (green) compared to NT T_{MBP} cells (blue) at day 2 of standard in vitro culture conditions. **B). Ccr7 Expression in Klf2-KO T_{MBP} Cells During EAE**. Ccr7 expression in Klf2-KO T_{MBP} cells (green) and NT T_{MBP} cells (blue) from the spleen (left) and ptLNs (right) by the third day post-intravenous injection in a co-transfer EAE model. **C). Quantification of Ccr7 Expression**. ΔMFI values (MFI - MFI isotype control) of Ccr7 in Klf2-KO T_{MBP} cells, normalized to NT T_{MBP} control cells in different experimental conditions. Statistical analysis was performed using two-way ANOVA with multiple comparisons. Data is presented as mean ± SD (N = 3).

3.6. Ccr7 Function in the T Cell Migration

To confirm the hypothesis in the previous chapter and to investigate the function of Ccr7 in T_{MBP} cells induced EAE model, we generated Ccr7-KO T_{MBP} cells by applying the same RNP-mediated CRISPR/Cas9 genome editing approach as used for generating Klf2-KO T_{MBP} cells. Knockout efficiency was validated using TIDE sequencing, and the KO score was above 60% (Figure 8A), confirming successful Ccr7-KO in the majority of the cell population. Afterwards, we conducted an adoptive transfer EAE model examining Ccr7-KO T_{MBP} cells distribution in organs especially to SLOs. The overall process is shown as below (Figure 8B), after in vitro activation, Ccr7-KO $T_{MBP\text{-}GFP}$ cells were co-transferred at a 1:1 ratio with NT $T_{MBP\text{-}BFP}$ control cells into recipient rats. On day 3 post-injection, a time point when rats began to significant loss weight, we harvested peripheral and CNS organs/compartments and analyzed the distribution of GFP^+ and BFP^+ cells (Figure 8B).

By Flow cytometric analysis, we found that Ccr7-KO T_{MBP} cells appear obviously less in the ptLNs compared to NT T_{MBP} control cells, while their distribution in the spleen is comparable to the control

(Figure 8C, D). The unbalanced distribution between ptLNs and spleen from this experiment clearly pointed out that Ccr7 is specifically required for T cell recruitment into ptLNs, but dispensable for entering the spleen. It is also worth mentioning that Ccr7-KO T_{MBP} cells exhibited no significant effect on T cell migration into the CSF, spinal cord leptomeninges, or parenchyma compared to NT controls (Figure 8C, D). Hence Ccr7 expression on the T cell surface appears essential for T cell migration to ptLNs, but has no influence on guiding/inhibiting T_{MBP} cells to enter the spleen and the further infiltration into the CNS.

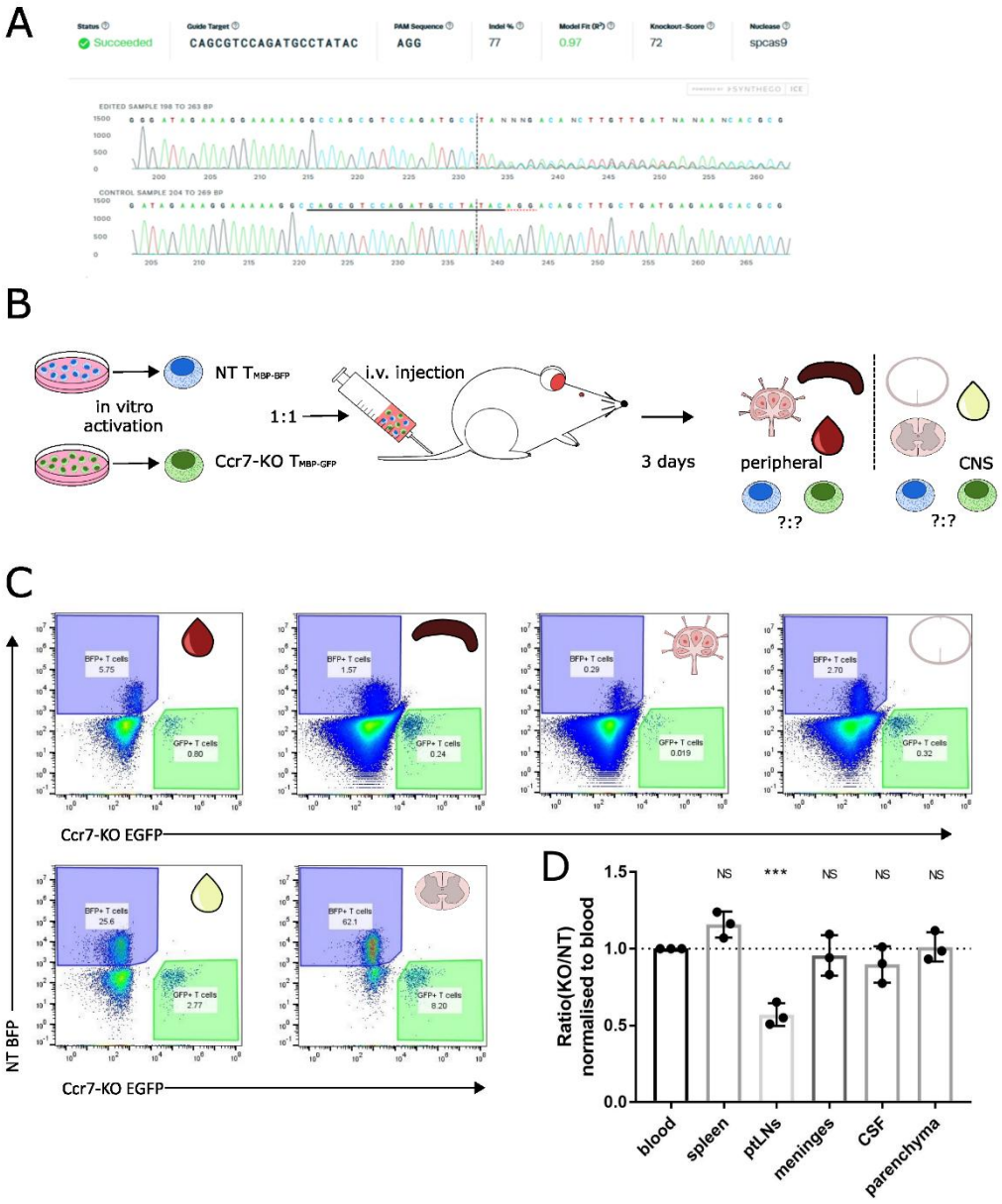

Figure 8 in vivo Distribution Pattern of Ccr7-KO T_{MBP} Cells in the EAE Model
A). TIDE Sequence Result. DNA sequence of the Ccr7-KO and NT T_{MBP} cells including KO intervention area was compared by the ICE (Inference of CRISPR Edit) approach. B). Experimental Design for Ccr7-KO T_{MBP} Cell in

vivo Distribution Pattern. NT $T_{MBP-BFP}$ and Ccr7-KO $T_{MBP-GFP}$ cells were activated in vitro, mixed at a 1:1 ratio, and intravenously administered into rats. Clinical scores and body weights were recorded daily. On day 3 post-injection, rats were sacrificed, and tissues including peripheral compartments (spleen, ptLNs, and blood) and CNS compartments (CSF, spinal cord leptomeninges, and spinal cord parenchyma) were collected. The distribution of GFP^+ and BFP^+ cells was assessed by flow cytometry. c). Flow Cytometry Analysis of Ccr7-KO T_{MBP} Cell Distribution. Representative flow cytometry plots show the distribution of Ccr7-KO $T_{MBP-GFP}$ and NT $T_{MBP-BFP}$ cells across various compartments on day 3 post-injection. Gating strategy: lymphocytes → single cells → BFP^+ or GFP^+ populations. BFP^+ cells are gated in blue, and GFP^+ cells in green. D). Quantitative Assessment of Ccr7-KO T_{MBP} Cell Distribution in Organs. Numbers of GFP^+ and BFP^+ T cells in each organ were quantified by using FlowJo and used to calculate GFP^+/BFP^+ ratios in each organ. To correct for inter-individual variability, the GFP^+/BFP^+ ratio in each compartment was normalized to the ratio in blood. A value of 1 indicates proportional distribution relative to blood, values >1 denote enrichment in the given compartment, and values <1 suggest a lower presence compared to circulation. Statistical analysis was conducted using one-way ANOVA with multiple comparisons. Data is presented as mean ± SD (N = 3).

3.7. Ccr7 Causes Klf2 KO T cells to Accumulate in the Lymph Nodes

We revealed that T cells lacking Ccr7 fail to migrate to the ptLNs in the EAE model. To determine whether the abnormally high Ccr7 expression in Klf2-KO T cells is the exact reason of their accumulation in ptLNs, we generated a double knockout model targeting both Klf2 and Ccr7 in the same T_{MBP} cell population. Via RNP-mediated CRISPR/Cas9 approach, we transiently delivered Klf2 sgRNA together with Cas9 into pre-established Ccr7-KO $T_{MBP-GFP}$ cells (Figure 8A, 9A). Afterwards Klf2 KO efficiency was validated at the DNA level, with knockout scores exceeding 60%, ensuring effective deletions conducted in both genes (Figure 9B).

In the next step the migration ability of Ccr7&Klf2-KO $T_{MBP-GFP}$ cells was examined by using the similar adoptive transfer EAE model to observe gene edited T_{MBP} cell distribution in organs as previously described. In this experiment, Ccr7&Klf2-KO $T_{MBP-GFP}$ cells and NT $T_{MBP-BFP}$ cells were activated in vitro, mixed at a 1:1 ratio, and intravenously injected into rats. On day 3 post-injection, when rats started obvious weight loss, we collected organs and compartments to test the distribution of GFP^+ and BFP^+ cells in both peripheral and CNS compartments (Figure 9C, D). To better understand the changes after Ccr7 deletion in Klf2-KO T_{MBP} cells, we compared the distribution results of Ccr7&Klf2-KO T_{MBP} cells with the previously described distribution patterns of Klf2-KO $T_{MBP-GFP}$ cells (Figure 9E). Ccr7&Klf2-KO T_{MBP} showed a striking shift of the distribution pattern compared to Klf2-KO $T_{MBP-GFP}$ cells. Ccr7 deficiency leads Klf2-KO cells to no longer accumulate in ptLNs. In contrast, the accumulation in the spleen was not affected by the absence of Ccr7, where Ccr7&Klf2-KO and Klf2-KO $T_{MBP-GFP}$ cells numbers were at a similar level above the NT control cells (Figure 9E). These results confirmed that high expression of Ccr7 indeed is an important cause for Klf2-KO cells accumulating in ptLNs. The number of Klf2-KO T cells in CNS compartments showed only a slight increase after Ccr7 deletion (although not statistically significant), suggesting that the reduced migration of Klf2-KO

cells in the CNS is not primarily due to high Ccr7 expression (Figure 9E) and additional unknown pathways contribute to inhibiting T cells infiltration into the CNS in the absence of the Klf2 transcription factor.

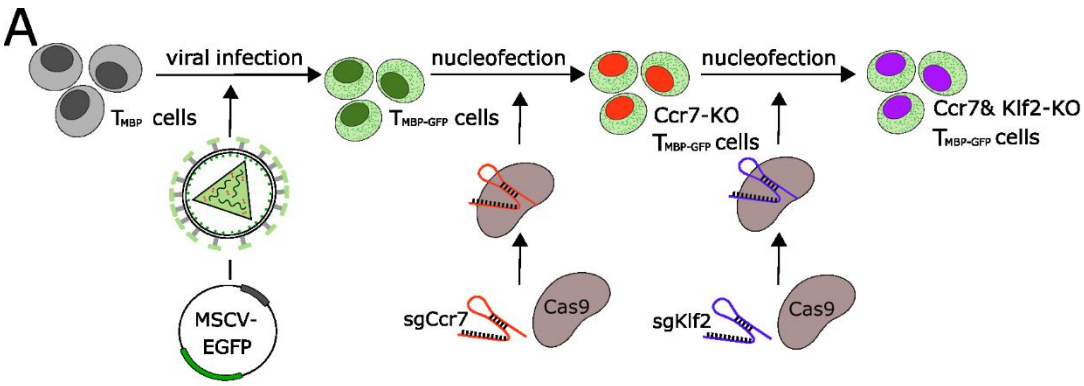

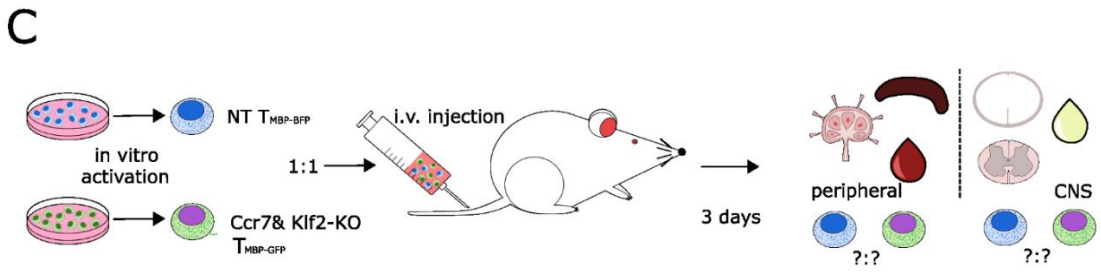

Figure continues on next page

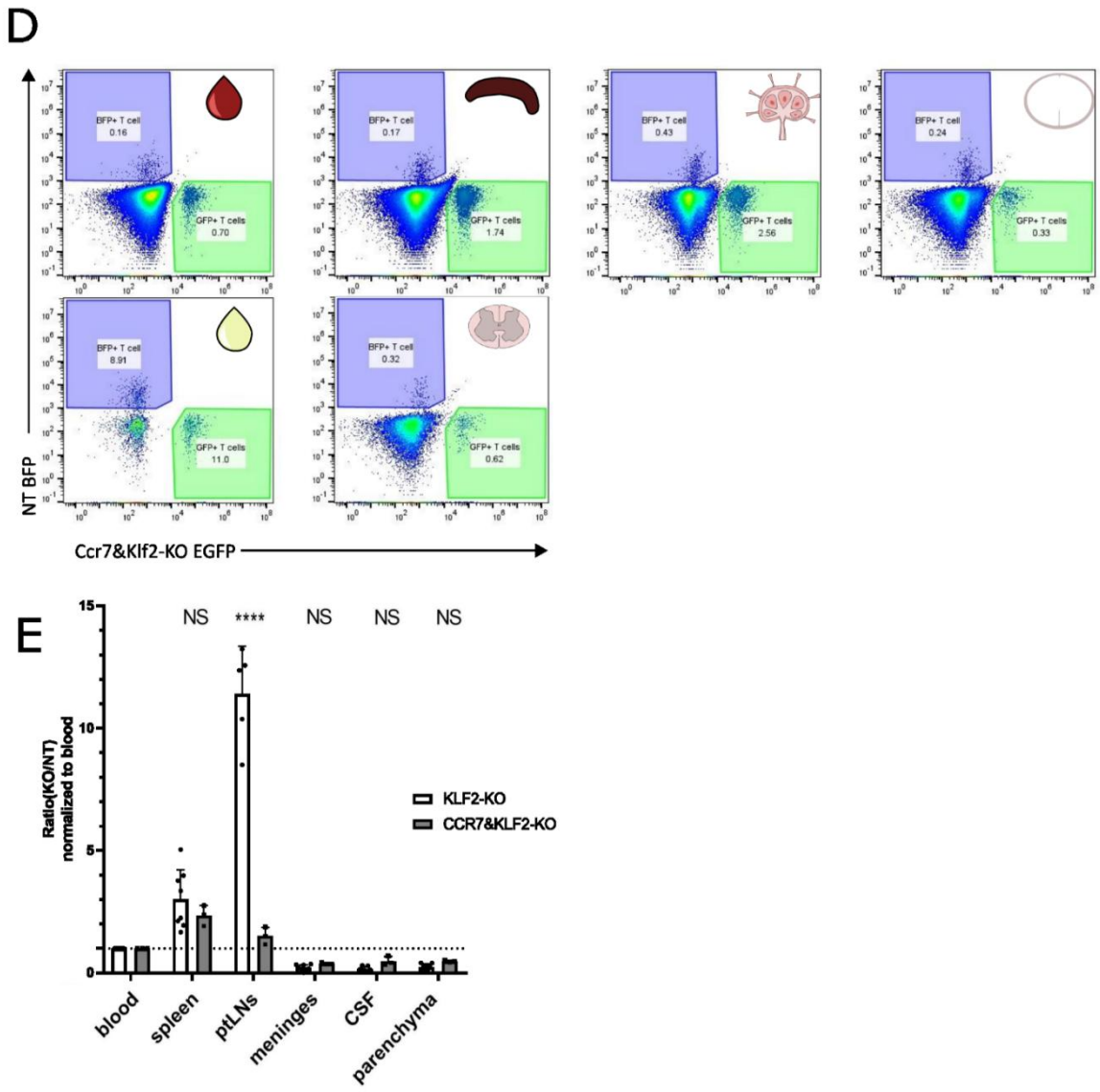

Figure 9 Ccr7& Klf2-KO T_{MBP} cells in vivo Distribution Pattern in EAE Model

A). Generation of Ccr7& Klf2-KO $T_{MBP-GFP}$ Cells. Rat primary T_{MBP} cells were first transduced with a retroviral vector encoding EGFP, yielding $T_{MBP-GFP}$ cells. To generate Ccr7-KO $T_{MBP-GFP}$ cells, Cas9 and sgKlf2 RNA were transiently introduced via RNP-mediated CRISPR/Cas9 genome editing (Ccr7-KO efficiency shown in Figure 8A). Following six days of in vitro culture, these Ccr7-KO $T_{MBP-GFP}$ cells were reactivated with fresh deactivated thymocytes and MBP. On day 2 post-activation, a second round of CRISPR/Cas9 editing was performed using sgKlf2 RNA, effectively knocking out Klf2 in the Ccr7-deficient $T_{MBP-GFP}$ cells. B). TIDE Sequence Result. DNA sequence of the Ccr7&Klf2-KO and NT T_{MBP} cells including Klf2-KO intervention area was compared by the ICE (Inference of CRISPR Edit) approach. C). Experiment Design. NT $T_{MBP-BFP}$ cells and Ccr7& Klf2-KO $T_{MBP-GFP}$ cells were activated in vitro, mixed 1:1, and intravenously injected into rats. Clinical scores and body weights were monitored daily. On day 3, when significant weight loss was observed, rats were sacrificed, and peripheral (spleen, ptLNs, blood) and CNS (CSF, spinal cord leptomeninges, parenchyma) compartments were collected for flow cytometry analysis. D). Flow Cytometry Analysis of Ccr7& Klf2-KO T_{MBP} cells Distribution. Representative flow cytometry plots show distribution of Ccr7& Klf2-KO $T_{MBP-GFP}$ cells (green gate) and NT $T_{MBP-BFP}$ cells (blue gate) across different compartments on day 3. Gating strategy: lymphocytes → single cells → BFP^+ or GFP^+ populations. E). Quantification of Ccr7& Klf2-KO T_{MBP} Cell Distribution in Organs. GFP^+/BFP^+ cell counts were normalized to the ratio in the blood of the same animal. Also the cells in vivo distribution pattern

between Ccr7&Klf2-KO T_{MBP} cells and Klf2-KO T_{MBP} cells was compared. A value of 1 indicates equal distribution, >1 reflects accumulation in the compartment, and <1 denotes reduced presence. Statistical analysis: one-way ANOVA with multiple comparisons. Data shown as mean ± SD (N = 3).

3.8. S1pr1 Signaling Pathway in the Klf2-KO Cells

Although elevated Ccr7 expression explains the preferential retention of Klf2-KO T cells in ptLNs, it could not explain for their accumulation in the spleen or their impaired migration ability into the CNS. Therefore, we turned our attention to another key molecule, S1pr1. S1pr1 is a GPCR that function as a strong driver for T cell to exit from lymphoid tissues into the blood circulation (Matloubian et al., 2004). Previous research has identified that Klf2 is the direct upstream transcription factor which promotes S1pr1 expression (Carlson et al., 2006). The way S1pr1 mediates cell migration relies on the concentrations difference of S1p among different tissues/organs. When the surrounding around T cells includes low concentration of S1p, S1pr1 present on the cell surface, mediating T cell migration towards high S1p concentration areas. When reaching the site with high S1p concentration (for example blood plasma), S1p immediately binds with S1pr1, mediating its internalization (Drouillard et al., 2018). Due to the high dynamics of S1pr1 localization between cell surface and cytoplasm as described, and the difficulty in finding anti-rat S1pr1 specific antibodies for staining, it is difficult to directly detect the level of S1pr1 expression on the T cells by flow cytometry staining in our study. Therefore, we conducted the transwell chemotaxis assay as compensatory experiments to indirectly validate the function of S1pr1 in T cell migration and to evaluate its expression level on different T cell groups.

First, to prove the role of S1pr1 in T cell migration as well as establish the transwell chemotaxis assay, we performed the assay with S1pr1-KO T_{MBP} cells. The S1pr1-KO T_{MBP} cells were generated by Dr. Lämmle using RNP-mediated CRISPR/Cas9 genome editing, following the same method used to establish Klf2-KO and Ccr7-KO T cells, as described previously (Kendirli et al., 2023b). The transwell system includes three parts, an upper chamber to seed testing cells, a lower chamber containing corresponding chemoattractants, and a microporous membrane functioning as the separation between two chambers and to avoid cells passing through due to gravity but allowing the gradual diffusion of chemoattractants and permitting the cells active migration in response to chemotactic gradients (Figure 10A). Since massive S1p exist in serum, under standard serum-rich culture conditions, S1pr1 is always staying in an internalized condition in cells. As only S1pr1 expressed on the cell surface could respond to S1p concentration gradient, we had to recover its surface expression before the transwell chemotaxis assay.

Hence, we mixed S1pr1-KO $T_{MBP\text{-}GFP}$ cells and NT $T_{MBP\text{-}BFP}$ cells at a 1:1 ratio and seeded them in the upper chamber of a transwell system with serum-free medium. After a one-hour recovery incubation, different chemoattractants were added to the lower chamber. The cells were then left undisturbed for four hours, afterwards the ratio of GFP^+ to BFP^+ cells in the lower chamber was quantified by flow cytometry (Figure 10A). Compared to BFP^+ NT control T cells, GFP^+ S1pr1-KO T cells exhibited a markedly reduced response to S1p in a dose dependent manner (Figure 10B). This result confirmed the effectiveness of the transwell chemotaxis assay in evaluating the molecular function of S1pr1 in T cells.

Therefore, in next step, we applied the transwell chemotaxis assay with Klf2-KO T_{MBP} cells by mixing them with NT $T_{MBP\text{-}BFP}$ cells at a 1:1 ratio and placing them in the upper chamber. In the lower chamber we added a different concentration of S1p, after four hours incubation, same as the result with S1pr1-KO $T_{MBP\text{-}GFP}$ cells (Figure 10C). Compared to the BFP^+ control T cells, GFP^+ Klf2-KO T cells showed a remarkably reduced reaction for S1p chemotaxic signal. In contrast, GFP^+ Klf2-KO T cells and BFP^+ control T cells migrate similarly against the CCL5 chemotaxis gradient (Figure 10C). This significantly weakened responsiveness to S1p in Klf2-KO T cells, combined with the notably low S1pr1 mRNA expression under standard in vitro culture conditions (Figure 10D), strongly confirms that Klf2 deficiency leads to a marked reduction in S1pr1 expression. This might further explain their massive accumulation in SLOs during EAE.

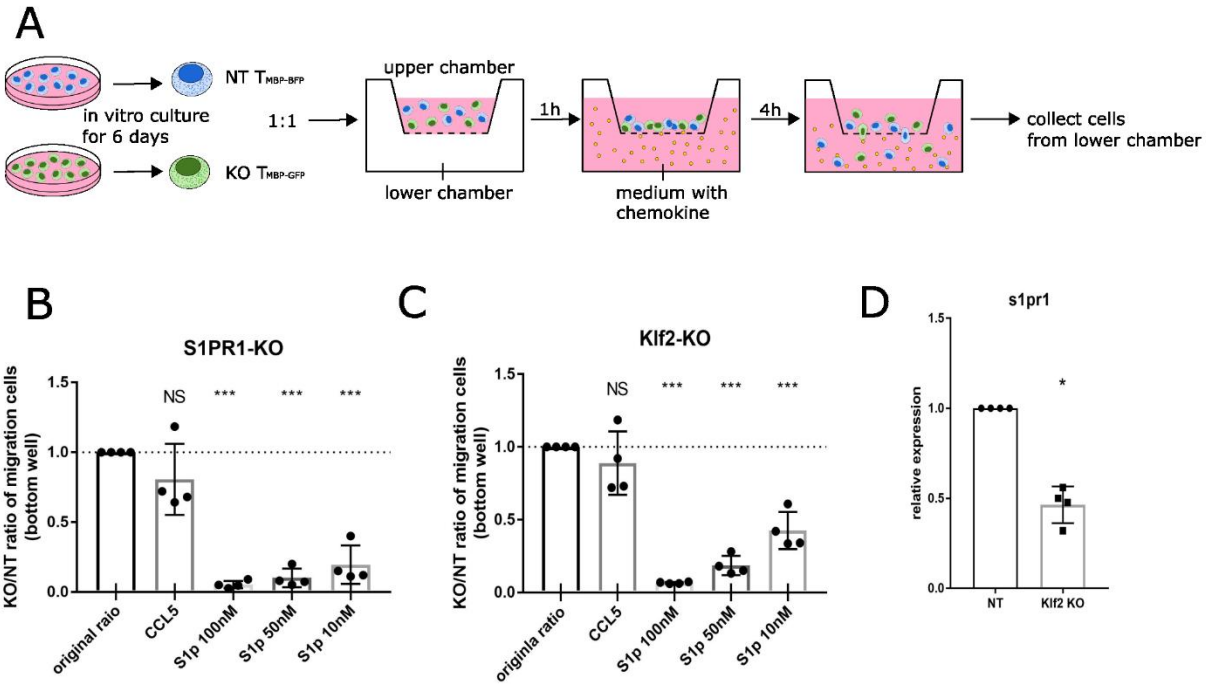

Figure 10 S1pr1 Expression and Functional Assessment in Klf2-KO T_{MBP} Cells

A). Experiment Design of the Transwell Chemotactic Assay. KO $T_{MBP\text{-}GFP}$ and NT $T_{MBP\text{-}BFP}$ cells were cultured in vitro for six days after their stimulation, mixed at a 1:1 ratio, and plated in the upper chamber of a transwell system. Cells were incubated in advance for 1 hour in serum-free medium to allow S1pr1 reappear on the

surface. The lower chamber contained either no chemoattractant (negative control), CCL5 (positive control), or varying concentrations of S1p. An additional "original ratio" control group was included by directly adding the mixed cell suspension into the lower chamber. After four hours, the proportion of GFP^+ and BFP^+ cells migrating into the lower chamber was quantified via flow cytometry. **B, C). Quantification of S1pr1-KO T_{MBP} Cells (B) and Klf2-KO T_{MBP} Cells (C) in vitro Migration.** GFP^+/BFP^+ ratios in the lower chamber were normalized to their respective baseline ratios from the "original ratio" group. A value of 1 indicates equal distribution, >1 signifies enhanced migratory capacity of GFP^+ cells, and <1 reflects impaired migration. Statistical analysis was performed using one-way ANOVA with multiple comparisons. Data is presented as mean ± SD (N = 4). **D). S1pr1 mRNA expression in Klf2-KO T_{MBP} Cells.** Relative mRNA expression of S1pr1 in Klf2-KO T_{MBP} cells is normalized to NT T_{MBP} controls. Statistical analysis was performed using unpaired t test. Data is presented as mean ± S.E.M (N = 4).

3.9. S1pr1 Overexpression Reduces Klf2 KO T Cell Accumulation in the Lymph Nodes

Klf2-KO T cells display impaired responsiveness to S1p chemotaxis, coupled with a significant reduction in S1pr1 mRNA levels, which firmly proved that S1pr1 expression is indeed visibly reduced. Given that S1pr1 is essential for T cell egress from lymphoid tissues, the expression deficiency likely contributes to their accumulation in SLOs. Therefore, to further validate the involvement of S1pr1 deficiency in the reason of Klf2-KO T cells being trapped in the SLOs, we generated a retroviral construct encoding S1pr1 along with an EGFP reporter (Figure 11A). After the retroviral transduction to T_{MBP} cells and selection of successfully transduced T cells with antibiotic, we obtained $S1pr1^{OE}$ (overexpressed) $T_{MBP\text{-}GFP}$ cells. In next step we knocked out Klf2 in $S1pr1^{OE}$ $T_{MBP\text{-}GFP}$ cells using RNP-mediated CRISPR/Cas9 genome editing, generating $S1pr1^{OE}$ Klf2-KO $T_{MBP\text{-}GFP}$ cells (Figure 11A). Unfortunately, the highest Klf2 Knockout efficiency we could get in $S1pr1^{OE}$ Klf2-KO $T_{MBP\text{-}GFP}$ cells is only around 27% (Figure 11B). Nevertheless, we performed the transwell chemotaxis assay to confirm that S1pr1 overexpression restores its expression in Klf2-deficient T cells, similar as previously described (Figure 10A). Indeed, the $S1pr1^{OE}$ Klf2-KO $T_{MBP\text{-}GFP}$ cells shows as similar responsiveness to the chemotactic effect of S1P as NT control $T_{MBP\text{-}BFP}$ cells, which indirectly confirms the S1pr1 expression was successfully recovered (Figure 11C).

Considering that around 27% of T cells still exhibit Klf2 deficiency, but S1pr1 expression has been fully recovered, we decided to still proceed with the in vivo migration assay to assess any changes in the distribution pattern. $S1pr1^{OE}$ Klf2-KO $T_{MBP\text{-}GFP}$ cells were mixed with NT $T_{MBP\text{-}BFP}$ cells in a 1:1 ratio and intravenously injected into the rat. Three days after injection, we compared the distribution of GFP^+ cells and the BFP^+ cells across various peripheral and CNS compartments (Figure 11D). Additionally, to provide a clearer assessment of how S1pr1 overexpression influences migratory behavior, the migration profile of $S1pr1^{OE}$ Klf2-KO $T_{MBP\text{-}GFP}$ cells was compared to the previously

shown Klf2-KO T_{MBP} as well as the S1pr1-KO T_{MBP} cells, which our group already published (Kendirli et al., 2023a) (Figure 11E).

Compared to NT control T_{MBP} cells injected into the same individual, $S1pr1^{OE}$ Klf2-KO $T_{MBP\text{-}GFP}$ cells showed a slightly higher number of cells in the spleen and ptLNs, while slightly fewer cells were distributed in the CNS compartment (Figure 11E).

It is difficult to directly compare the $S1pr1^{OE}$ Klf2-KO $T_{MBP\text{-}GFP}$ cells distribution pattern with Klf2-KO cells due to differences in Klf2-KO efficiency. However, when comparing the distribution patterns of S1pr1-KO cells and Klf2-KO T_{MBP} cells, we observe that S1pr1 primarily facilitates T cells egress from the ptLNs rather than from the spleen. The S1pr1-KO cells distribute in the spleen remains in the same level as that of NT control T cells (Figure 11E).

As for the CNS infiltration, although the Klf2 KO efficiency is low, $S1pr1^{OE}$ Klf2-KO $T_{MBP\text{-}GFP}$ cells still exhibited reduced infiltration compared to NT control cells in the same individuals, even after S1pr1 surface expression was restored (Figure 11E). This indicates that S1pr1 deficiency is not the main reason for Klf2-deficient T cells to fail to infiltrate the CNS. Instead, another pathway is likely responsible for this impairment.

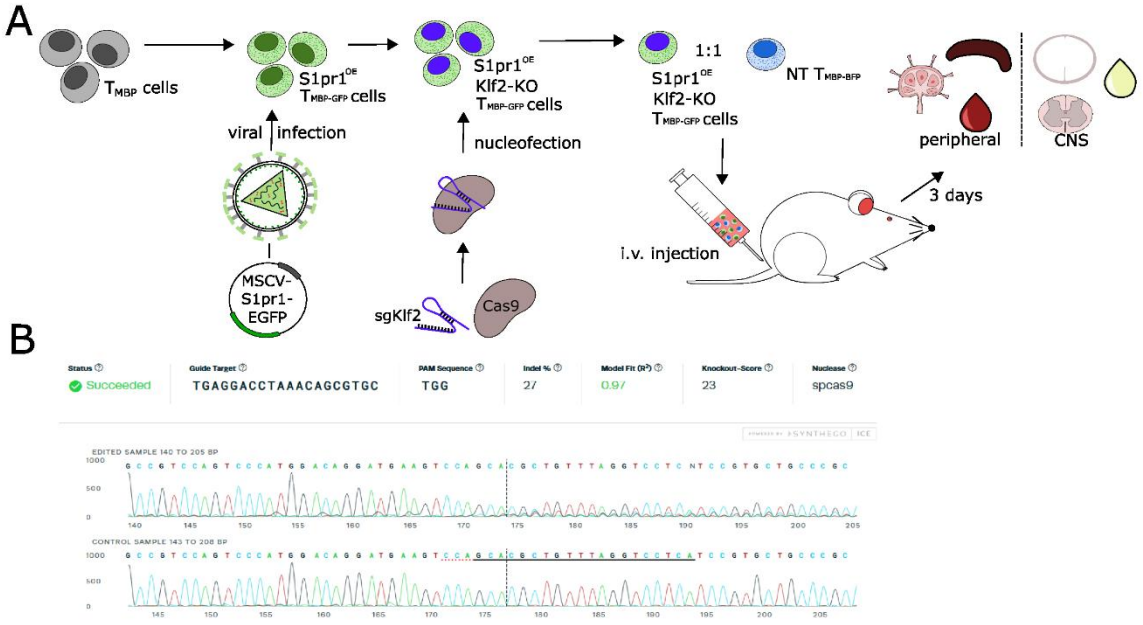

Figure continues on next page

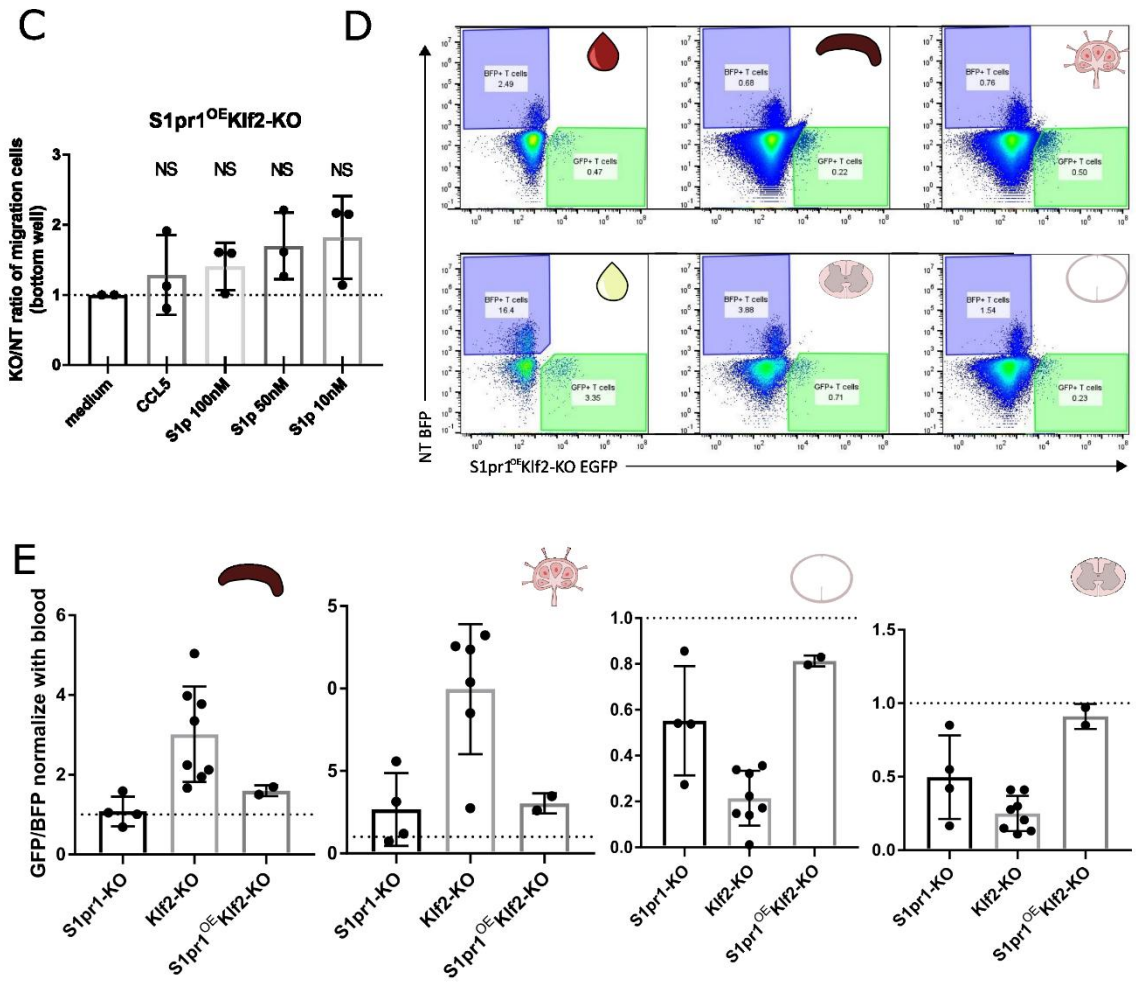

Figure 11 S1pr1^{OE} Klf2-KO T_{MBP} Cells Distribution Pattern in the EAE Model

A). Generation of S1pr1^{OE} Klf2-KO T_{MBP} cells and Further in vivo Distribution Pattern Evaluation. Rat primary T_{MBP} cells were transduced with a retroviral vector encoding both S1pr1 and EGFP, generating S1pr1$^{OE}T_{MBP\text{-}GFP}$ cells. Klf2 knockout was then induced via RNP-mediated CRISPR/Cas9 genome editing, followed by Tide sequence validation. After activation with fresh deactivated thymocytes and MBP, cells were mixed 1:1 with NT $T_{MBP\text{-}BFP}$ cells and intravenously injected into rats. Three days post-transfer, GFP$^+$ and BFP$^+$ cell distributions were analyzed across peripheral and CNS compartments. **B). TIDE Sequence Result.** DNA sequence of the S1pr1^{OE}Klf2-KO and NT T_{MBP} including Klf2-KO intervention area was compared by the ICE (Inference of CRISPR Edit) approach. **C). S1pr1 Overexpression Validation.** By Transwell Chemotactic Assay, same as Figure 10A, it was confirmed that S1pr1^{OE}Klf2-KO $T_{MBP\text{-}GFP}$ express functional S1pr1 on the surface, control cells are NT $T_{MBP\text{-}BFP}$ cells. GFP$^+$/BFP$^+$ ratios in the lower chamber were normalized to their respective baseline ratios from the "original ratio" group. Statistical analysis was performed using one-way ANOVA with multiple comparisons. Data is presented as mean ± SD (N = 3). **D). Distribution of S1pr1^{OE} Klf2-KO T_{MBP} Cells in vivo.** Flow cytometry plots depict the localization of S1pr1^{OE} Klf2-KO T_{MBP} cells (green) and NT $T_{MBP\text{-}BFP}$ cells (blue) across different compartments on day 3. Gating: lymphocytes → single cells → BFP+ or GFP+ populations. **E). Quantification of S1pr1^{OE} Klf2-KO T_{MBP} Cells Distribution in Organs.** GFP$^+$/BFP$^+$ ratios were calculated in each organ and normalized to one in the blood within the same animal. Values >1 indicate compartmental accumulation, while values <1 reflect reduced migration. Statistical analysis: one-way ANOVA with multiple comparisons. Data presented as mean ± SD (N = 3).

3.10.Klf2 Affects T Cells Transmigration

Although our results suggest that Klf2 deficiency led to a reduced S1pr1 expression and an enhanced Ccr7 expression, which were the two main reason for massive accumulation of Klf2-KO cells in SLOs. In addition, we also revealed that less Klf2-KO T cells migrate from blood to CNS compared to NT T cells (Figure 5D). To analyze which steps of T cell migration through the BBB is inhibited, we applied intravital two-photon imaging. With this method, we can directly visualize the process of how T cells slow down within the blood vessels of the leptomeninges in the rat spinal cord, gradually break through the BBB and infiltrate the CNS (Kawakami and Flügel, 2010). To this end, we injected a 1:1 mixture of Klf2-KO $T_{MBP\text{-}GFP}$ cells and NT $T_{MBP\text{-}BFP}$ cells intravenously. On the third day post-injection, we imaged the dynamic changes in the presence, distribution, and movement of Klf2-KO $T_{MBP\text{-}GFP}$ cells and control NT $T_{MBP\text{-}BFP}$ cells within the leptomeninges blood vessels of the spinal cord (Figure 12A).

The result unfortunately was not satisfactory and failed to undoubtedly answer the question. During imaging, large numbers of both NT $T_{MBP\text{-}BFP}$ cells and Klf2-KO $T_{MBP\text{-}GFP}$ had already infiltrated the CNS, with only a few cells remaining in the leptomeninges blood vessels (Figure 12B). We speculate the main reason for observing so few GFP^+ and BFP^+ cells in the intraluminal space is that the imaging time point was too late. Nevertheless, from the imaging data, we identified only one Klf2-KO $T_{MBP\text{-}GFP}$ cell crawling along the intraluminal surface. This cell began crawling at the start of the recording (0 min) and continued until 16 min but ultimately failed to cross the BBB. Instead, it ceased crawling, detached from the intraluminal surface, and remained within the blood vessel (Figure 12B). Additionally, we observed several Klf2-KO T_{MBP} cells that remained within blood vessel area, while only one BFP+ NT control cell was found in there. The presence of more GFP^+ Klf2-KO cells in this area compared to BFP^+ control cells, combined with the observed dynamic movement of a GFP^+ T cell on the intraluminal surface of the vessel (Figure 12B), suggests that Klf2 deficiency may impair the transmigration of T cells. However, given the limitations of the current imaging data, we plan to repeat this experiment in the future. As a supplementary approach, we have also analyzed the expression of integrins in these cells to evaluate their migratory capacity.

A

Figure continues on next page

B

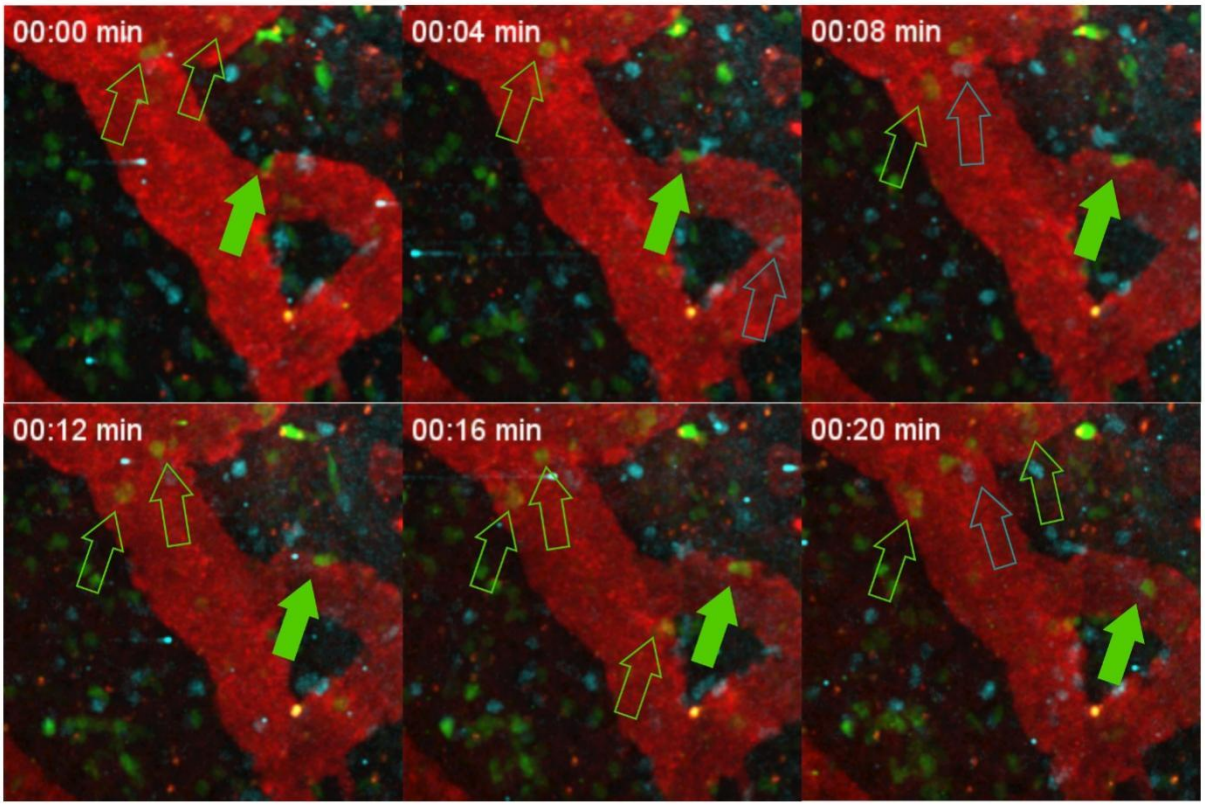

Figure 12 Leptomeningeal imaging following co-transfer of T_{MBP} Klf2-KO cells
A) Experimental design. T_{MBP} Klf2-KO and T_{MBP} NT cells were in vitro restimulated and were injected in a 1:1 mix into rats. After three days intravital 2-photon imaging was performed. B) Time-lapse Images Tracking T_{MBP} cells along the Meningeal Vasculature. Cyan indicates BFP^+ T_{MBP} NT cells, green indicates GFP^+ T_{MBP} Klf2-KO cells, solid arrows point to cells crawling on the intraluminal surface, and hollow arrows point to cells found in the blood vessels area.

Since our result showed that Klf2-KO cells failed to migrate into the CNS, we further studied integrin expression on the Klf2-KO cells. If integrin expression is altered on the surface of the Klf2-KO cells, it could explain the infiltration impairment. Since T cells get phenotypical changes after being injected into the rats, we isolated them from the rat and further analyzed integrin expression as similar as those for detecting the activation of Klf2-KO cells (Figure 6A). On the third day after intravenous injection of a 1:1 mixture of Klf2-KO T_{MBP} cells and NT $T_{MBP-BFP}$ cells, the expression of key integrin components (CD49d, CD29, CD11a and CD18) in the spleen and ptLNs was tested in both GFP^+ and BFP^+ T cells. We found a significant reduction in CD49d expression in Klf2-KO $T_{MBP-GFP}$ cells across both the spleen and ptLNs compared to NT $T_{MBP-BFP}$ cells in the same organs. Similarly, CD29 expression was also decreased, particularly in ptLNs, though to a lesser extent than CD49d (Figure 13). CD49d and CD29 together form the VLA4 complex, which mediate immune cell firm adhesion to VCAM1 on endothelial cells (Martin-Blondel et al., 2015). The downregulation of VLA4 lead to the

impairment of the adhesion-dependent trafficking ability, as we published that Itga4-KO T_{MBP} cells no longer migrate to the CNS compartments (Kendirli et al., 2023b). Conversely, CD11a and CD18 were significantly upregulated in Klf2-KO T_{MBP} cells compared to NT controls (Figure 13). These two integrins form LFA1, another integrin mediating the looser interaction of immunce cells with endothelial cells, and proven to not be necessary for T cells extravasation into the CNS (Dominguez et al., 2015, Schläger et al., 2016).

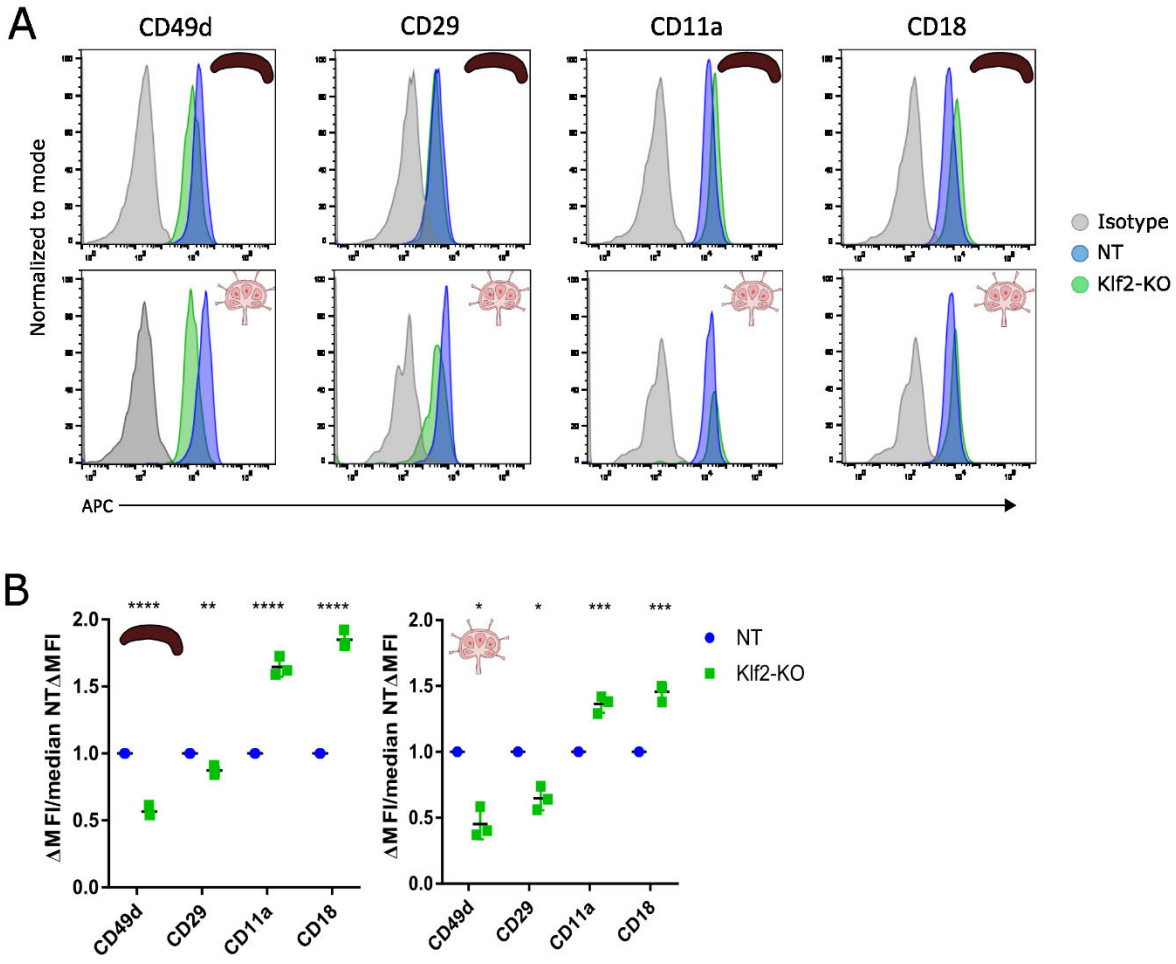

Figure 13 Integrins Expression in Klf2-KO T_{MBP} Cells During EAE

A). Expression in Klf2-KO T_{MBP} Cells in vivo. Integrins expression in Klf2-KO T_{MBP} cells (green) and NT T_{MBP} cells (blue) from the spleen (top) and ptLNs (bottom) by the third day post-intravenous injection in a co-transfer EAE model. B). Quantification of integrins Expression. ΔMFI values (MFI - MFI isotype control) of CD49d, CD29, CD11a and CD18 in Klf2-KO T_{MBP} cells, normalized to NT T_{MBP} control cells in different experimental conditions. Statistical analysis was performed using two-way ANOVA with multiple comparisons. Data is presented as mean ± SD (N = 3).

3.11. Foxo1 Regulates T Cell Migration

Our above-described findings revealed that Klf2 is a critical transcription factor in regulating autoreactive T cell migration to the CNS, especially in their trafficking between SLOs and the

bloodstream during the early phase of EAE. Revisiting our CRIPR/Ca9 screening data (Figure 3B), we noticed another transcription factor, Foxo1, which also appears to play a role in T cell migration during EAE. Notably, Foxo1 has been reported as an upstream transcription factor inducing Klf2 expression (Gubbels Bupp et al., 2009). When T cells are stimulated through the activation of TCR, cytokine receptors and chemokine receptors, the PI3K-AKT signaling pathway is activated (Han et al., 2012). Phosphorylated AKT then enters the nucleus and induce Foxo1 phosphorylation, causing Foxo1 to exit the nucleus and relocate to the cytoplasm, thereby inhibiting its transcriptional activity (Han et al., 2012). During the steady states, Foxo1 promotes the expression of Klf2, Il-7ra, Tcf7, Ccr7 and Sell (L-selectin) (Gubbels Bupp et al., 2009). Among these, Klf2 has been revealed as a key regulator of T cell migration into the CNS, while Ccr7 plays crucial role in promoting T cells retention in the lymph nodes, as shown in our study. Il-7ra encodes the IL-7 receptor α chain, which plays a crucial role in maintaining T cells survival by inhibiting the mitochondrial apoptotic pathway (Azizi et al., 2024). Tcf7 encodes T cells factor 1 (Tcf1), which has been linked to MS pathogenesis (Escobar et al., 2020). Research has shown that Tcf1 helps to suppress T cell differentiation towards Th1 cells, a key pathogenic T cells subtype in MS/EAE (Escobar et al., 2020). Meanwhile, L-selectin (encoded by Sell) is essential for T cell migration to the SLOs and it facilitates T cells rolling along the vascular endothelium in an inflamed area (Venturi et al., 2003). Given these background studies on Foxo1, we proposed Foxo1 as a strong regulator of autoreactive T cell migration in EAE. Therefore, to determine its exact role in T cell migration, uncover the related molecular mechanisms, and compare Foxo1 with Klf2 to identify the most potent target for regulating T cell migration in EAE, we used RNP-mediated CRISPR/Cas9 single-gene knockout technology to generate Foxo1-KO $T_{MBP\text{-}GFP}$ cells.

At first, we adoptively transferred Foxo1-KO T_{MBP} cells into rats and monitored their clinical scores and body weight over time. Unlike Itga4-KO and Klf2-KO T_{MBP} cells, which failed to induce significant weight loss or neurological symptoms (Figure 5A), Foxo1-KO T_{MBP} cells still induce EAE (Figure 14A). However, the onset of significant weight loss occurred approximately one day later than in NT T_{MBP} cell-induced EAE. Similarly, neurological symptoms appeared with a one-day delay and were milder compared to those induced by NT control cells.

For further understanding the detailed Foxo1-KO T_{MBP} cells distribution in different organs during adoptive transfer EAE, we performed a co-transfer experiment in rats (Figure 14B). In this setup, in vitro activated Foxo1-KO $T_{MBP\text{-}GFP}$ cells were mixed with NT $T_{MBP\text{-}BFP}$ cells at a 1:1 ratio and then intravenous transferred into recipient rats. On day 3 post-injection, we harvested both peripheral and CNS compartments and tested the distribution of GFP^+ (Foxo1-KO) and BFP^+ (NT) cells by flow cytometry (Figure 14B). Compared with NT control cells, Foxo1 deficiency led to increased T cell

accumulation in the SLOs, particularly accumulation in the ptLNs showed statistically significant (Figure 14C, D left). In the spleen, Foxo1-KO T_{MBP} cell numbers were slightly higher than NT cells, though the difference was not statistically significant. Another point to note is that Foxo1 deficiency did not affect T cell migration into the CNS. Across all tested CNS compartments, including CSF, spinal cord leptomeninges, and spinal cord parenchyma, Foxo1-KO T_{MBP} cell numbers were comparable to those of control cells.

Since Klf2 expression has been reported to be regulated by Foxo1, and Foxo1-KO cells exhibited a distribution pattern similar to Klf2-KO T_{MBP} cells (Figure 5D), we generated a bar chart to further compare their distribution patterns in adoptive transfer EAE (Figure 14D right). Overall, Foxo1 deficiency resulted in a much milder retention of T_{MBP} cells in the SLOs compared to Klf2-KO cells, and their infiltration into the CNS was higher than T cells with Klf2 deficiency. To explain this weaker retention effect, we propose two possibilities: either Foxo1 is not a major regulator of Klf2 in autoreactive rat T_{MBP} cells, or Foxo1 controls additional migration-related molecules. In the latter case, Foxo1 depletion may have disrupted the expression of other key regulators of T cell migration, counteracting the retention effect caused by Klf2 deficiency and allowing more T cells to enter the bloodstream.

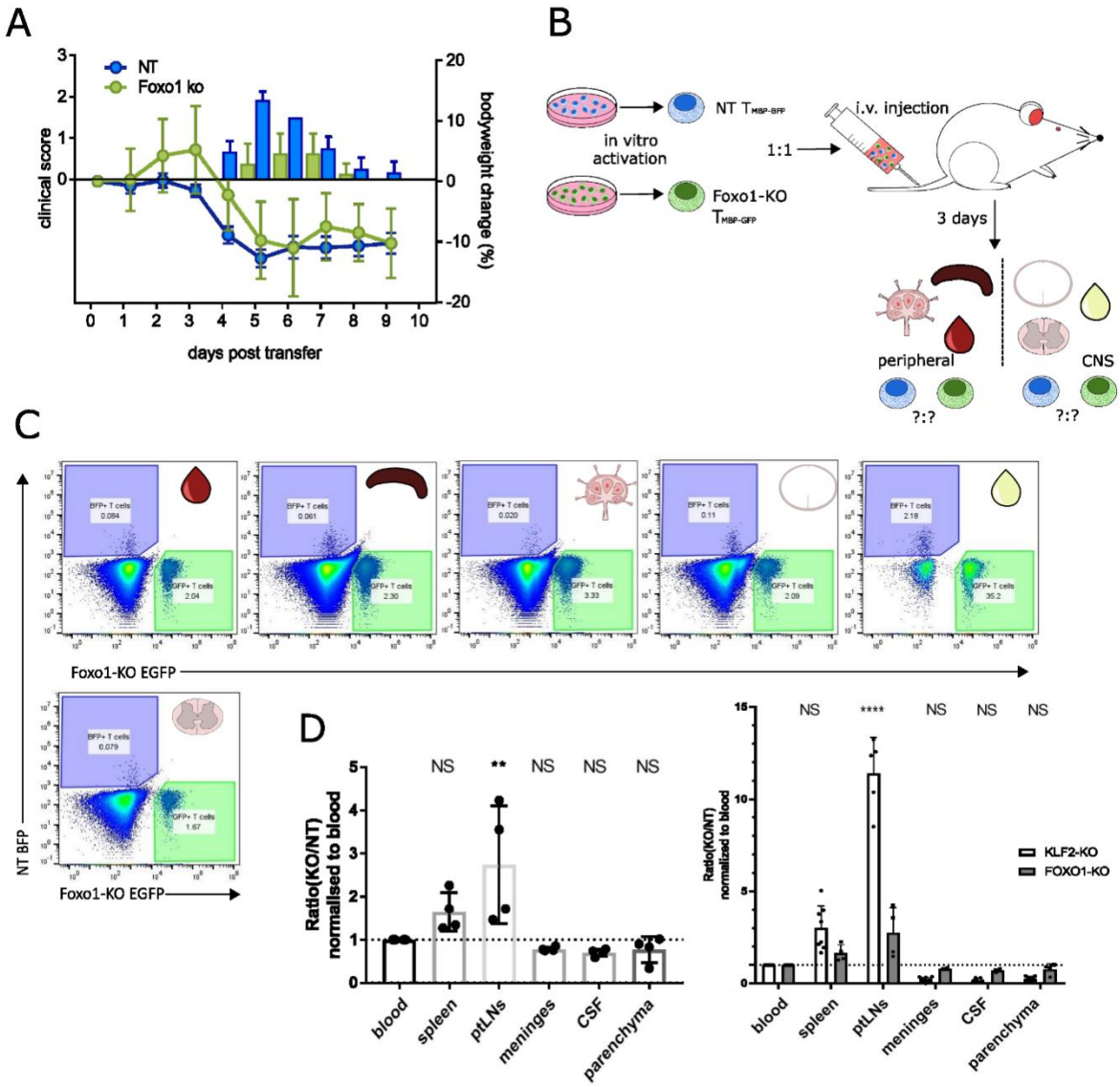

Figure 14 Foxo1-KO T_{MBP} cells EAE Model and in vivo Distribution Pattern

A). EAE clinical course by Foxo1-KO and NT T_{MBP} Cells. Clinical scores (bars) and relative body weight changes (lines) were monitored in rats following NT (blue) and Foxo1-KO (green) T_{MBP} cells injection, body weights are normalized to day 0 (pre-injection). Mean ± SD (N=4). B). Experiment Design. NT $T_{MBP-BFP}$ cells and Foxo1-KO $T_{MBP-GFP}$ cells were activated in vitro, mixed 1:1, and intravenously injected into rats. Clinical scores and body weights were monitored daily. On day 3, when significant weight loss was observed, rats were sacrificed, and peripheral (spleen, ptLNs, blood) and CNS (CSF, spinal cord meninges, parenchyma) compartments were collected for flow cytometry analysis. C). Foxo1-KO T_{MBP} Cells Distribution. Representative flow cytometry plots show distribution of Foxo1-KO $T_{MBP-GFP}$ cells (green gate) and NT $T_{MBP-BFP}$ cells (blue gate) across different compartments on day 3. Gating strategy: lymphocytes → single cells → BFP^+ or GFP^+ populations. D). Quantification of Foxo1-KO T_{MBP} Cell Distribution in Organs. GFP^+/BFP^+ cell counts were normalized to the ratio in blood of the same animal (left chart). Also compared the cells in vivo distribution pattern between Foxo1-KO T_{MBP} cells and Klf2-KO T_{MBP} cells (right chart). A value of 1 indicates equal distribution, >1 reflects accumulation in the compartment, and <1 denotes reduced presence. Statistical analysis: one-way ANOVA with multiple comparisons. Data shown as mean ± SD (N = 4).

3.12.Foxo1 not only Regulates the Klf2 Expression, but also Ccr7

To explore why Foxo1-KO cells exhibit only mild accumulation in SLOs despite it being a direct regulator of Klf2, we first examined the impact of Foxo1 deficiency on Klf2 expression. The Klf2 transcription factor highly expressed in naive T cells and memory T cells (Endrizzi and Jameson, 2003). When T cells are activated through TCR, downstream signaling pathways involving protein kinase B and the MAP kinases ERK1/2 lead to the downregulation of Klf2 expression (Preston et al., 2013). Therefore, unlike previous analyses of activation phenotypes among in vitro cultured T cells, which typically uses the second day of culture as the peak activation time point, we chose to examine Klf2 expression on the sixth day of the in vitro T_{MBP} cell culture. At this stage, the T_{MBP} cells in our experiment exhibited the lowest activation levels, making Klf2 expression more detectable. As expected, Klf2 expression in Foxo1-KO T_{MBP} cells at the day 6 under standard in vitro culture condition was lower than in control T_{MBP} cells (Figure 15A). This confirms that Foxo1 positively regulates Klf2 expression in the T_{MBP} cell. This is consistent with previous reports identifying Foxo1 as an upstream transcriptional activator of Klf2 (Kerdiles et al., 2009).

However, if Klf2 were the sole effector downstream of Foxo1 in controlling T cell migration, Foxo1-KO T_{MBP} cells would be expected to exhibit a distribution pattern similar to Klf2-KO T_{MBP} cells. Instead, our results show that Foxo1 deficiency leads to a much milder impairment in migration compared to Klf2 deficiency (Figure 14D right). Foxo1-KO cells, while also partially trapped in SLOs, were less restricted than Klf2-KO cells and maintained a greater CNS infiltration capacity. This discrepancy suggests that Foxo1 influences T cell migration through additional pathways in addition to its regulation of Klf2.

A study has reported that Foxo1 directly regulates Ccr7 expression, with Foxo1-KO T cells showing reduced Ccr7 at both the mRNA and protein levels (Kerdiles et al., 2009). Combined with the findings in our study that the massive accumulation of Klf2-KO T cells in the ptLNs was driven by Ccr7 overexpression, a Ccr7 expression reduced due to a Foxo1 deficiency could explain why Foxo1-KO cells exhibit only a mild retention in the ptLNs compared to Klf2-KO cells. Therefore, to verify this hypothesis, we examined the Ccr7 expression in rats three days after co-injecting Foxo1-KO and NT control cells.

As previously described, Itga4 (CD49d) is a crucial marker for T cell infiltration into the CNS and was the top hit in our CRISPR/Cas9 screening (Figure 3B). Therefore, we analyzed CD49d expression with same approach.

Unlike Klf2-KO T_{MBP} cells, which showed an increased Ccr7 expression in the retained SLOs, Foxo1 deficient T_{MBP} cells did not exhibit any upregulation of Ccr7 in either the spleen or ptLNs (Figure 15B).

Foxo1 is observed to be an upstream regulator of Klf2 expression, as Foxo1-KO leads to a reduced Klf2 expression in T cells (Figure 15A). When T cells lose Klf2, from our above-described data, Ccr7 expression was upregulated. However, the Ccr7 expression stays comparable to control T cells in Foxo1 depleted T cells. This can be explained by a potential upregulating effect directly between Foxo1 and Ccr7.

In addition, Foxo1 deficient T cells showed no change in CD49d expression in the spleen and a slightly reduced expression in the ptLNs (Figure 15C). Overall, through the Foxo1-KO T cells model, we found it is not only the upstream transcription factor of Klf2, but it also induces Ccr7 expression, and without obvious effect on the T cell CD49d expression.

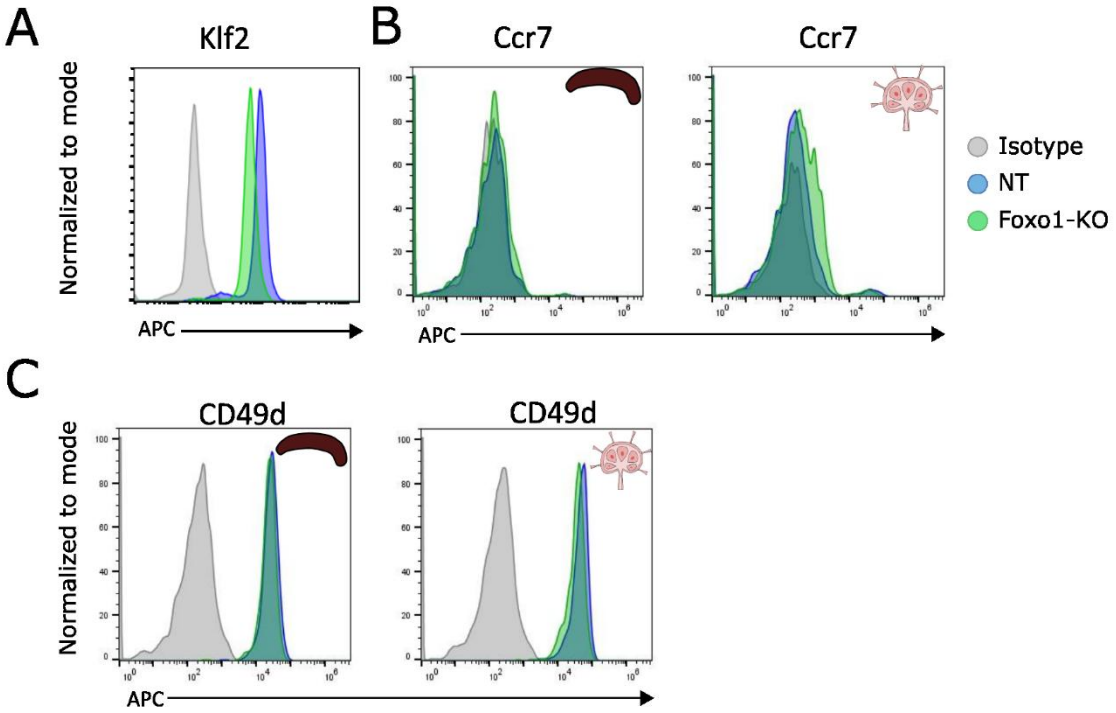

Figure 15 Foxo1-KO T_{MBP} Cells Expression of Klf2, Ccr7, and CD49d in the EAE Model
A). Klf2 Expression. Flow cytometry plots compare Klf2 expression in Foxo1-KO $T_{MBP\text{-}GFP}$ (green) and NT $T_{MBP\text{-}BFP}$ (blue) cells under in vitro culture condition. B). Ccr7 Expression. Ccr7 expression in Foxo1-KO $T_{MBP\text{-}GFP}$ and NT $T_{MBP\text{-}BFP}$ cells from spleen and ptLNs. C). CD49d Expression. CD49d expression in Foxo1-KO $T_{MBP\text{-}GFP}$ and NT $T_{MBP\text{-}BFP}$ cells from spleen and ptLNs.

3.13.Activation and Migration are a Complex Balance

When we observed that Klf2 deficiency led to the loss of the migratory ability in T_{MBP} cells, including down regulation of S1pr1, causing them to be retained in SLOs, we also noted that these cells exhibited a significantly higher activation status, characterized by CD25, compared to NT T_{MBP} control cells. The heightened activation status of Klf2-KO cells was observed only in vivo within the peripheral organs where they were retained (Figure 5,6). Additionally, the extent of CD25

upregulation varied depending on the degree of local cell accumulation. Therefore, we propose that an intrinsic link exists between migration impairment and heightened activation status.

To understand how Klf2 regulates T cell activation, we found a study demonstrating that Klf2 inhibits nearly all downstream targets of nuclear factor-κB (NF-κB) in monocytes, including IL-1, IL-8, TNF, MCP-1, MIF, MIP, and CD40L (Das et al., 2006). NF-κB plays the role of a key proinflammatory transcription factor in T cells, which is activated through TCR signaling, and further promotes T cells proliferation, activation and differentiation (Liu et al., 2017). CREB binding protein (CBP)/p300 is widely recognized as a critical co-activator of NF-κB (Sheppard et al., 1999). Some studies have reported that Klf2 competitively binds with CBP/p300, enhancing its own transcriptional activity (Song et al., 2002) while inhibiting NF-KB transcriptional activity (SenBanerjee et al., 2004). These findings align with our results, suggesting that the absence of Klf2 might result in more CBP/p300 being available to interact with NF-κB, leading to increased NF-κB transcriptional activity. This, in turn, results in elevated CD25 expression and enhanced production of proinflammatory cytokines, including TNF-α, IFN-γ, and IL-17 (Figure 17).

In the T cells model, there is no direct evidence that Klf2 regulate T cell activation. It remains unclear whether Klf2 is directly involved in T cell activation pathway, potentially inhibiting NF-κB as hypothesized above, or its regulatory role occurs through its downstream target S1pr1, its upstream regulator Foxo1, or Ccr7, which is upregulated in Klf2-KO cells. To investigate this, we analyzed the expression of activation markers (CD25, CD134) as well as TCR in Foxo1-KO, S1pr1-KO, and Ccr7-KO T cells in vivo. Following the same approach used to analyze activation marker expression in Klf2-KO T cells in vivo (Figure 6A), we mixed Foxo1-KO, S1pr1-KO, and Ccr7-KO $T_{MBP\text{-}GFP}$ cells with NT control $T_{MBP\text{-}BFP}$ cells respectively at a 1:1 ratio and injected them into separate rats. After three days, we assessed their expression levels in the peripheral organs.

Flow cytometric analysis showed that S1pr1-KO T_{MBP} cells displayed lower expression of activation markers CD25 and CD134 in ptLNs, where they were largely retained, with a slight reduction in activation levels also observed in the spleen (Figure 16A). Although S1p/S1pr1 signaling pathway is crucial for guiding T cells exit from LNs, it has also been revealed to activate NF-κB activity and amplify immune responses in epithelial cells and cardiac fibroblasts through PKCα-dependent phosphorylation (Yang et al., 2020, Tian et al., 2024) (Figure 17). Therefore, S1pr1-KO T cells exhibited opposite change of activation markers compared with Klf2-KO T cells.

Unlike Klf2-KO and S1pr1-KO T cells, Ccr7-KO $T_{MBP\text{-}GFP}$ cells exhibited activation marker expression comparable to NT $T_{MBP\text{-}BFP}$ cells (Figure 16B). Specifically, there were no differences in CD25 (IL-2 receptor α-chain) or CD134 (OX40 receptor) expression, suggesting that Ccr7 deficiency does not

affect the activation state of T_{MBP} cells. In both ptLNs and the spleen, Foxo1-KO T_{MBP} cells also displayed an activation profile similar to NT control cells, with no major differences in activation marker expression (Figure 16C). Although statistical analysis showed a significant difference in CD134 and TCR expression in Foxo1-KO T_{MBP} cells within the spleen, this effect was likely due to low baseline expression levels and highly consistent values among replicates, which resulted in a statistically significant but functionally insignificant difference. Flow cytometry plots confirmed that Foxo1-KO cells did not exhibit any meaningful difference in activation status.

Taken together, these findings demonstrate that Klf2 deficiency leads to increased T cell activation, whereas its downstream effector S1pr1 has the opposite effect, with S1pr1-KO T_{MBP} cells displaying reduced activation marker expression. The regulation effect of Klf2 and S1pr1 is potentially related to their regulation on NF- κB transcription activity (Figure 17), which need further validation and discussion. In contrast, Foxo1, as an upstream regulator of Klf2, and Ccr7, as a downstream molecule of Foxo1, appear to have no direct influence on T cell activation status in the T_{MBP} EAE model, as their deficiency did not alter CD25 or CD134 expression levels.

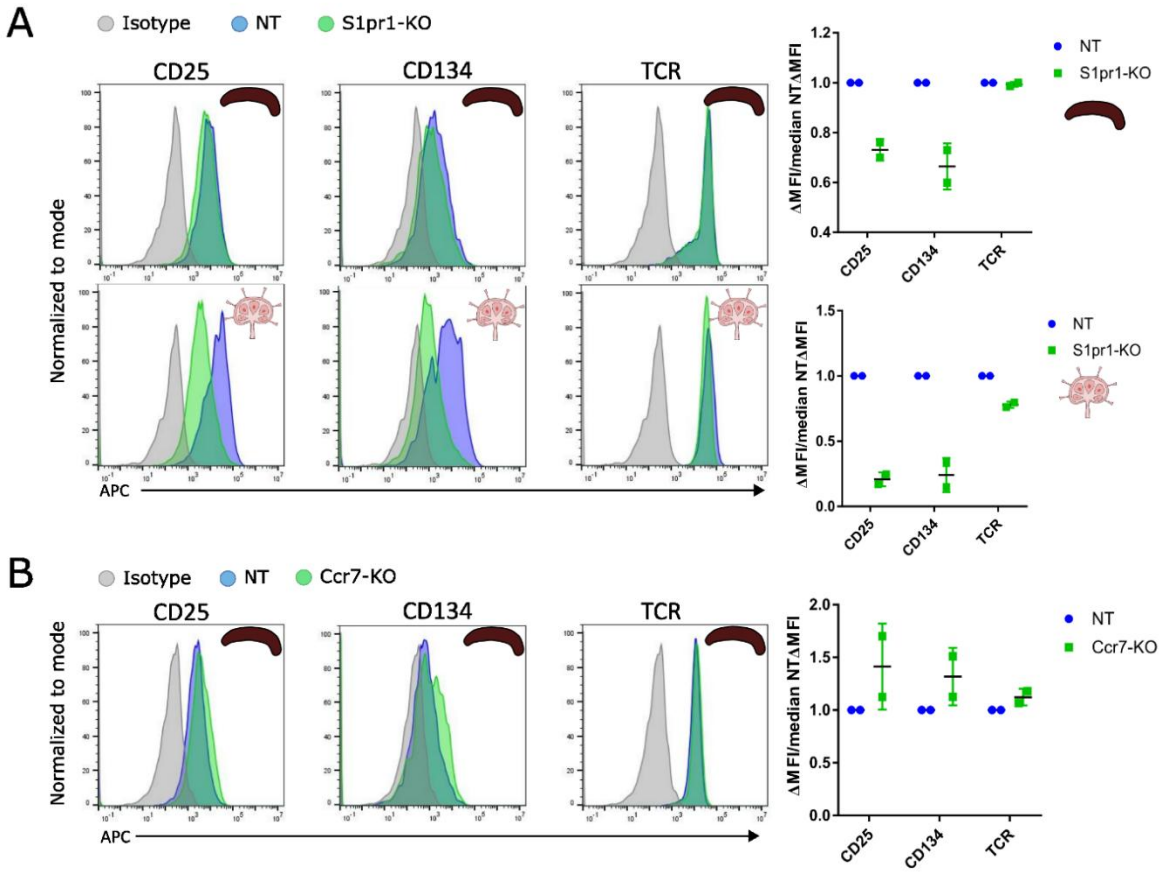

Figure continues on next page

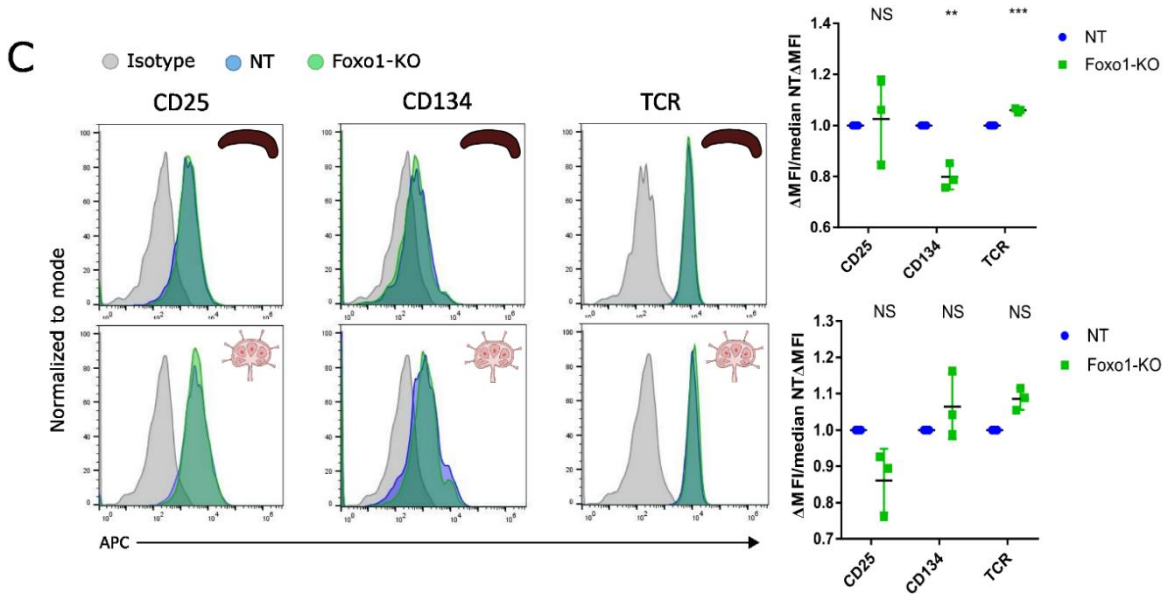

Figure 16 Activation Profiles of S1pr1-KO, Ccr7-KO, and Foxo1-KO T_{MBP} Cells

Activation Markers in S1pr1-KO (A), Ccr7-KO (B) and Foxo1-KO (C) T_{MBP} Cells. Flow cytometry analysis of CD25, CD134, and TCR expression in KO T_{MBP} cells (green) versus NT T_{MBP} cells (blue) from the spleen (top row) and ptLNs (bottom row) on day 3 post-intravenous injection in a co-transfer EAE model. ΔMFI values (MFI - isotype control MFI) were used to quantify marker expression, normalized to NT T_{MBP} control cells from the spleen (top, right) and ptLNs (bottom, right). Statistical Analysis: Two-way ANOVA with multiple comparisons. Data are presented as mean ± SD (N = 3)

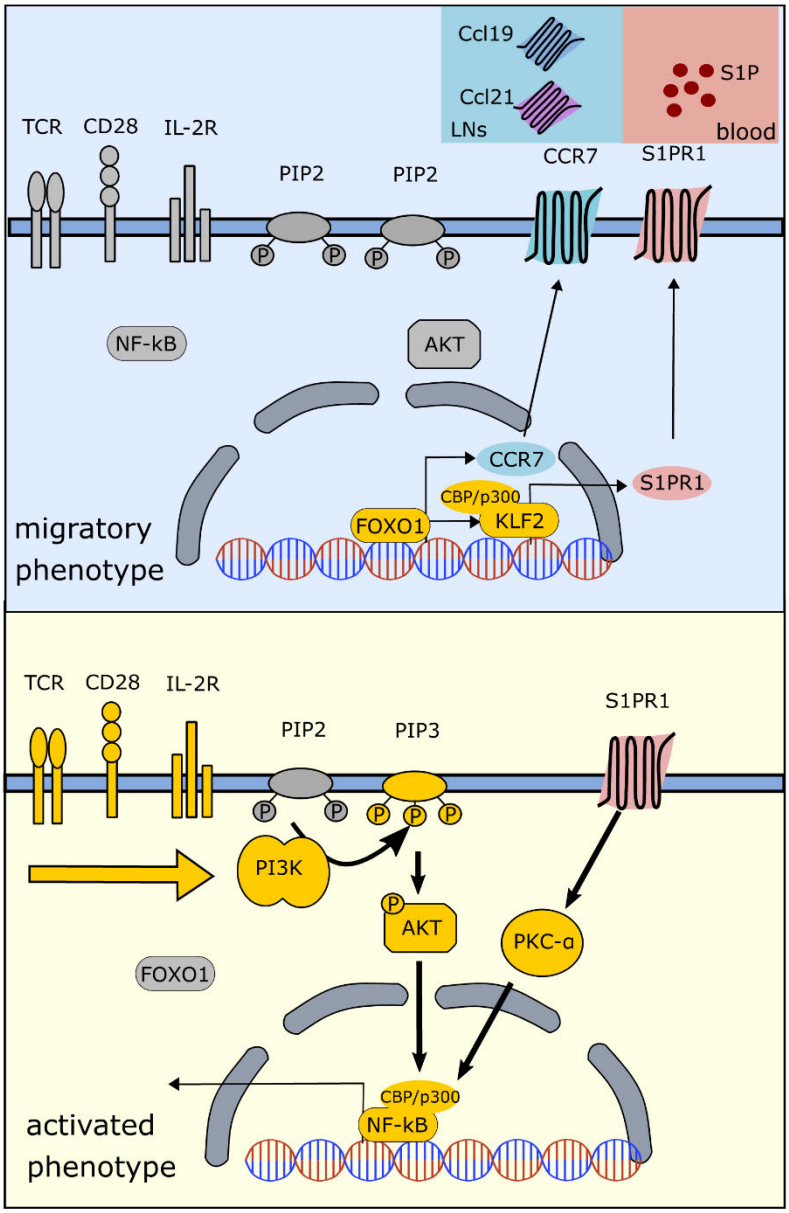

Figure 17 Potential Molecular Mechanisms in the Migratory and Activated Phenotypes of Autoreactive CD4⁺ T Cells

During steady-state conditions, the Foxo1 transcription factor remains highly active, promoting the expression of Klf2 and Ccr7 (Figure 15). Klf2, downstream transcription factor of Foxo1, drives S1pr1 expression (Figure 10). Additionally, CBP/p300 binds to Klf2, further enhancing its transcriptional activity. On the cell surface, Ccr7 and S1pr1 play opposing roles in T cell migration. Ccr7, which interacts with its ligands Ccl19/21, abundant in LNs, signals T cells to retain in the LNs (Figure 9). In contrast, S1pr1, which binds to S1p, promotes migration toward areas of high S1p concentration, such as the bloodstream (Figure 11). The balance between Ccr7 and S1pr1 ultimately determines whether CD4⁺ T cells stay in the LNs or enter circulation. Upon TCR/CD28 or cytokine (like IL-2) stimulation, the PI3K-AKT signaling pathway is activated. Phosphorylated AKT induces NF-κB activation and Foxo1 phosphorylation. Phosphorylated Foxo1 translocates from the nucleus to the cytoplasm. With Foxo1 inactivated, Ccr7 and Klf2 expression decreases. As a result, the reduced availability of Klf2 releases CBP/p300, which then binds to NF-κB, further enhancing its

transcriptional activity. Additionally, the S1p/S1pr1 signaling pathway activates the PKCα pathway, further amplifying NF-κB activity.

3.14. Foxo1, Klf2, and Their Downstream Molecules in T Cell Migration in Human MS

To evaluate whether Foxo1, Klf2, and their downstream effector molecules contribute to T cell migration in human MS, we reanalyzed transcriptomic data from people with MS previously published by our group (Kendirli et al., 2023a). This dataset included samples from four untreated MS patients and four individuals diagnosed with idiopathic intracranial hypertension (IIH) as controls (Kendirli et al., 2023a). Peripheral blood and cerebrospinal fluid (CSF) samples were collected from all participants, followed by the isolation of antigen-experienced $CD4^+$ T cells. In total, 70,594 antigen-experienced $CD4^+$ T cells were obtained from the peripheral blood of untreated MS patients, while 16,575 $CD4^+$ T cells were isolated from the CSF of both MS and IIH participants (Kendirli et al., 2023a) (Figure 18A).

By Single-cell RNA sequencing (scRNA-seq), we classified those antigen-experienced $CD4^+$ T cells into 12 distinct cell clusters (T1–T12) (Figure 18B). To further characterize T cell migration during MS, we compared TCR sequences between $CD4^+$ T cells from peripheral blood and CSF, identified cells with overlapping TCRs as cells with higher possibility to migrate (Kendirli et al., 2023a). This approach enabled us to investigate whether the migration-associated transcriptional regulators we identified in the EAE model fit in human MS. Klf2 and its downstream effector molecule Itgb7 (Ise et al., 2025) appeared positively correlated with T cell migration in MS patients (Figure 18C), consistent with our findings in rats. CD69 showed negative correlation in MS patients (Figure 18C). This Further confirmed the Klf2 role in promoting T cell migration during MS, since CD69 is agonists of S1pr1, and appears upregulated in Klf2 depleted T cells (Weinreich et al., 2009b). Ccr7, which showed inverse correlation to Klf2 expression in our finding (Figure 7), appears to also negatively correlate with T cell migration in MS patients (Figure 18C). Overall, human MS scRNA-seq data confirms that Klf2 and its related molecules, including Ccr7, CD69, and Itgb7, influence T cell migration in MS. Their role in migration aligns with our findings in the rat EAE model.

When analyzing the effect of Foxo1 and its downstream effector molecules, including Tcf7, Il7r, and Sell (Gubbels Bupp et al., 2009), on T cell migration, we obtained results that were different with what we observed in rat EAE. In MS patient scRNA-seq data, $CD4^+$ T cell clusters with higher TCR overlap showed lower Foxo1 expression, suggesting that Foxo1 may negatively regulate T cell migration (Figure 18C). Similar effects were also observed in the Foxo1 downstream molecules, Tcf7, Il7r and Sell. However, in the Foxo1-KO T cells adoptive transfer EAE model described above, Foxo1-

deficient CD4⁺ T cell accumulated in the ptLNs with a slight reduction in CNS infiltration (Figure 14). The opposing trends between human MS and rat EAE suggest that the relationship between T cell migration and Foxo1 gene expression differs between rat autoreactive CD4⁺ T cells and CD4⁺ T cells in MS patients. One major difference between the rat adoptive transfer EAE model and human MS lies in how autoreactive CD4⁺ T cells become activated.

In the rat EAE model, CD4⁺ T cells are first activated in vitro using CNS-related antigens and APCs, then transferred into the rats as fully activated cells. These cells initially migrate into the SLOs, undergo a phenotypic shift towards a migratory state, characterized by reduced activation marker expression and increased integrin and chemokine receptor expression. These autoreactive CD4⁺ T cells with migratory phenotype could reappear in the bloodstream and further infiltrate into the CNS. When Foxo1 is knocked out in this model, activated T cells may struggle to transition into a migratory phenotype.

However, in MS patients, although the exact mechanisms remain unclear, the prevailing view is that autoreactive T cells acquire activation and migratory capacity simultaneously. Whether Foxo1 plays the same inhibitory role in promoting a migratory phenotype in this context remains uncertain. Based on human MS data, we speculate that it does not and further investigating is need for uncover their more detailed role in T cell migration during MS/EAE.

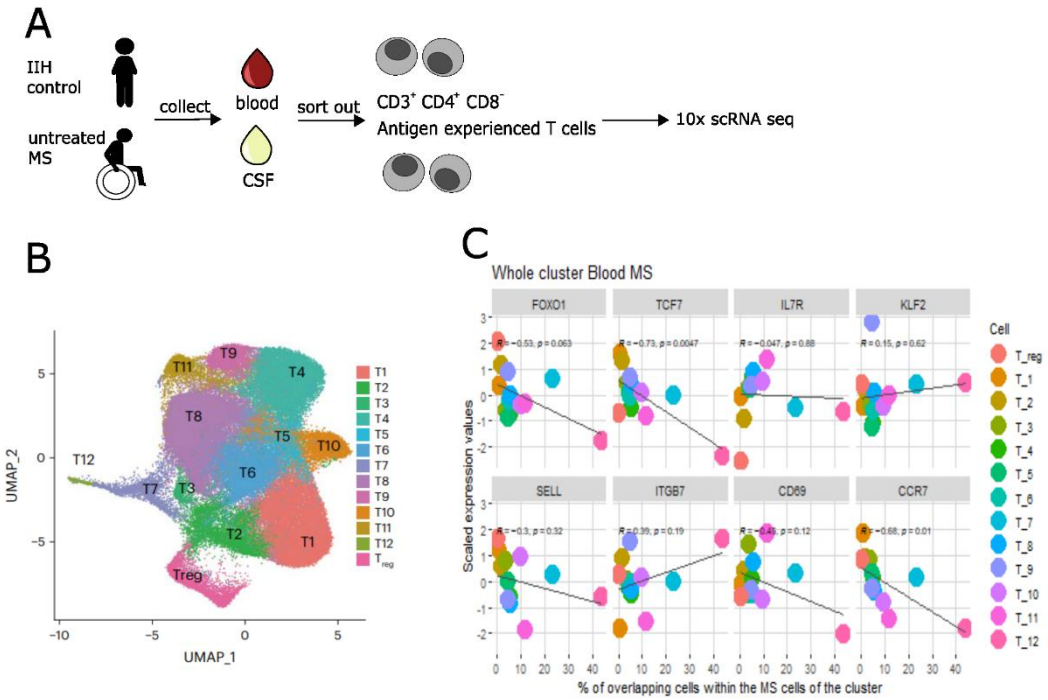

Figure 18 Expression of Foxo1 and Klf2 Associated Effector Molecules in T Cells from Human MS

A). scRNA-Seq Experimental Design. Blood and cerebrospinal fluid (CSF) samples were collected from untreated MS patients and Idiopathic Intracranial Hypertension (IIH) controls. Antigen-experienced $CD4^+$ T cells were isolated from both compartments and analyzed via single-cell RNA sequencing (scRNA-seq). B) UMAP Plot. scRNA-seq data from whole $CD4^+$ T cells cluster of both untreated MS patients and IIH controls. (Kendirli et al., 2023b). C). Correlation Between Gene Expression and TCR Overlap in MS Patients. A subset analysis was performed exclusively in MS patients to examine how Foxo1, Klf2, and their downstream effectors correlate with TCR-overlapping cells between peripheral blood and CSF. Statistical Analysis: Pearson correlation; $P < 0.05$ considered significant.

4. DISCUSSION

4.1. Klf2 as the Critical Transcription Factor Mediates T Cell Migration

In our study, we discovered the role of Klf2 regulating proliferation, activation, and migration of encephalitogenic T cells, especially focusing on molecular mechanisms during the initiative phase of EAE.

Previous studies showed the function of Klf2 in T cells. For example, it was firmly proven that Klf2 plays a role in maintaining T cell quiescence by suppressing c-Myc, which in turn reduces protein production, limits cell growth, and lowers activation marker levels (Buckley et al., 2001a, Rabacal et al., 2016, Chen et al., 2024). When Klf2 is missing, this inhibitory effect disappears, leading to faster cell division and increased T cell numbers (Buckley et al., 2001a). More directly, Klf2 is highly upregulated in encephalitogenic T cells with migratory phenotype (Odoardi et al., 2012).

Our CRISPR/Cas9 screening identifies Klf2 as a regulator of T cell infiltration into the CNS (Figure 3B). Consistent with previous findings, we showed that Klf2 restricts cell proliferation, while Klf2 deficient T cells showed slightly increased cell number under standard in vitro culture conditions (Figure 4C), although this did not seem to be linked to their migration defects. Activation markers and integrin levels also remained unchanged in Klf2 deficient cells in vitro (Figure 4D-F). Moreover, our flow cytometry data suggest that Klf2-KO T cells and NT control T cells have the same phenotype at the time of injection (Figure 4D-F). These results led us to further study how Klf2 regulates T cell migration in vivo.

4.1.1. Animal Model to Study the Role of T Cell Migration in vivo

In our model, intravenously injected T_{MBP} cells follow a stable time kinetic on their migration: they rapidly disappear from the blood and enter the lungs within hours, accumulate in the ptLNs within in 12-36 hours, appear in the spleen around 60 hours, and re-enter circulation as well as infiltrate the CNS between 60-80 hours (Flügel et al., 2001). The ptLNs, which receive drainage from the thymus, peritoneal cavity, and liver via internal thoracic lymph channels (Tilney, 1971), differ anatomically from the spleen. Although the spleen functions as a SLO in the immune system, it lacks afferent lymphatic vessels and instead collects immune cells directly from the blood through open circulation in the red pulp (Bronte and Pittet, 2023). It is important to note that the T cell appearance in different organs in the adoptive transfer EAE model follows strict sequence of time, but may not completely equal to their actual migration route. For example, the ptLNs are not the direct drainage lymph nodes of the lungs, and the T cell numbers declining in the ptLNs while increasing in the spleen may not imply direct migration between these two organs. Since these organs are located

deep within the thoracic cavity, current technical limitations make it challenging to track individual T cells in real-time. However, it was shown that T_{MBP} cells with migratory phenotype isolated from lung or spleen can migrate into the CNS directly (Odoardi et al., 2012). The role of Klf2 on T cell migration in vivo was analyzed after injection of mixed in vitro activated Klf2-KO $_{TMBP\text{-}GFP}$ and NT control $T_{MBP\text{-}BFP}$ cells at a 1:1 ratio (Figure 5B). We chose day 3 post-injection as the target time point, and then analyzed the distribution of GFP^+ and BFP^+ cells across different organs and compartments. Indeed, day 3 post-injection is a time point when T_{MBP} cells have acquired a migratory phenotype in peripheral SLOs, re-entered the blood circulation, and begun accumulating in the CNS (Flügel et al., 2001).

During data analysis, we observed that T cell numbers varied significantly across different batches of T cells and individual rats, making direct comparisons challenging. Calculating the GFP/BFP ratio within each organ/compartment helped stabilize the data by accounting for injection ratio differences, but variability in T cell migration behavior within batches and immune responses among individual rats still influenced the results. To eliminate these effects, we normalized the GFP/BFP ratio in each organ/compartment to the ratio in the blood, which optimized individual differences and improved consistency across experiments. Afterwards, we found that Klf2 deficient T cells had obvious difficulty in exiting from SLOs and returning to circulation (Figure 5D). Similarly, we also observed that Klf2-KO T cells faced challenges trafficking from blood to CNS tissues (Figure 5D), independent of their retention in peripheral organs.

4.1.2. T Cell Entry to and Exit from Parathymic Lymph Nodes

We found that Klf2-KO T cells accumulate in the ptLNs but not in the spleen (Figure 5D). Apart from the anatomical differences between the ptLNs and spleen, T cells also rely on different molecular mechanisms for entry and exit in these organs. In the ptLNs, T cells follow classical lymph node trafficking pathways, entering via HEVs through integrin-mediated rolling and crawling, followed by Ccr7-dependent migration. Ccr7 not only facilitates T cell entry but also serves as a retention signal, keeping T cells within the lymph node. Over time, Ccr7 expression gradually decreases, allowing another key signaling pathway, S1p/S1pr1, to take over. $CD4^+$ T cells typically reside in lymph nodes for 10–12 hours (Gasteiger et al., 2016). When S1pr1 signaling becomes dominant, T cell starts to egress into the blood circulation. Our findings directly showed that Ccr7 and S1pr1 function as opposing regulators that determine whether T cells remain in the LNs or enter the bloodstream. The Ccr7 signal leads T cell retention in the LNs, while S1pr1 promotes migration into the circulation. Klf2 acts as a critical switch in this balance. In Klf2-deficient T cells, Ccr7 remains persistently high, while S1pr1 expression is significantly reduced (Figure 7,10). As a result, the retention signal from Ccr7 is

too strong, and the egress signal from S1pr1 is nearly absent, causing T cells to be trapped in the ptLNs. When Ccr7 was deleted in Klf2-KO T_{MBP} cells using CRISPR/Cas9 single gene knockout technology, this retention effect disappeared (Figure 9), confirming that excessive Ccr7 expression is the primary cause of Klf2 deficient T cell accumulation in the ptLNs.

4.1.3. T Cell Entry to and Exit from the Spleen

In contrast, T cell migration into and from the spleen follows a more complex pattern due to the unique structure. Unlike in lymph nodes, Ccr7 is not required for the initial entry of T cells into the spleen (Sharma et al., 2015, Chauveau et al., 2020). During entering via the blood, T cells are released into the red pulp and marginal zone (MZ) through central arterioles. From there, they must actively migrate toward the white pulp, where antigen presentation and T cell activation takes place. A study reported that Ccr7 plays a key role in this process by guiding T cells into the T cell zones of the white pulp along perivascular pathways (Chauveau et al., 2020).

Although our study did not specifically analyse the distribution of T cells within the red pulp and white pulp, Ccr7-KO T cell still migrate to the spleen and Ccr7 expression levels on T cells we observed (Figure 7, 8) were consistent with previous findings (Sharma et al., 2015, Chauveau et al., 2020). Our results showed that Klf2 deficient T cells in the spleen exhibited lower Ccr7 expression than those in ptLNs, though still higher than control cells (Figure 7). Knocking out Ccr7 in Klf2-KO T cells did not affect their accumulation in the spleen (Figure 9), confirming that T cells retention mechanisms in the spleen differ from those in ptLNs, which does not rely on Ccr7 mechanism. In our EAE model, the injected T_{MBP} cells were fully activated in vitro before transfer. Although Klf2 deficient T cells are unable to migrate into the white pulp, they can still induce EAE without requiring further activation, as MBP antigen is not present in the spleen. Therefore, the inability of Ccr7 deficient T cells to enter the white pulp does not impact their ability to trigger EAE or migrate to the CNS. This conclusion is further supported by us in vivo migration experiments with Ccr7-KO T cells (Figure 8).

4.1.4. Exit from SLOs by Following S1pr1, a Downstream Molecule of Klf2

Detecting S1pr1 expression in different organs during ex vivo phenotypic analysis meets several technical challenges due to the dynamic changes of S1pr1 on the cell membrane. S1pr1 signaling is primarily driven by an S1p concentration gradient, guiding T cells traffic from low-S1p environments, such as in lymph nodes, toward high-S1p environments like the blood plasma. After entering circulation, abundant S1p in the blood bind to S1pr1 and induce S1pr1 internalization, allowing T cells to resist the concentration gradient and migrate toward tissues with lower S1p levels

(Drouillard et al., 2018). During ex vivo experiments, exposure to serum-containing medium or buffers triggers S1pr1 immediate internalization and the lack of highly specific anti-rat S1pr1 antibodies, making S1pr1 undetectable. To overcome this limitation, we performed in vitro experiments to evaluate S1pr1 expression on mRNA level. Together with functional assays (Transwell Chemotactic Assay), we showed that Klf2 deficiency resulted in a loss of S1pr1 expression and further impaired chemotaxis toward S1p (Figure 10B, C). Combining the evidence of both Klf2-KO T_{MBP} cells and S1pr1-KO T_{MBP} cells showed high accumulation in the ptLNs (Figure 11E), as well as S1pr1 expression is nearly absent in Klf2-KO T_{MBP} cells (Figure 10), we conclude that reduction of S1pr1 due to deletion of klf2 is one of the reasons why these cells are trapped in the ptLNs. To further confirm the role of S1pr1 in T cell migration, we performed overexpression of S1pr1 in Klf2-KO T cells. Due to the not yet solved technological limitation, Klf2 knockout efficiency stays in a low level (KO score around 27). But S1pr1 overexpression was proved that it helped Klf2 deficient T cells restore responsiveness to the S1p (Figure 11C). Ccr7 regulates T cell entry to ptLNs whereas S1pr1 control T cell exit from ptLNs. In contrast, S1pr1 does not play a crucial role on the exit of T cells from spleen, which is supported by the data showing that the number of S1pr1-KO T cells in the spleen is comparable to that in the blood (Figure 11E).

4.1.5. Role of Klf2 during T Cell Migration from the Blood to the CNS

Beyond retention in SLOs, Klf2-KO T cells exhibited impaired infiltration into the CNS, independent of their reduced presence in the bloodstream. This was evident from consistently lower Klf2-KO to control cell ratios in the CSF, meninges, and parenchyma compared to their ratios in the blood (Figure 5C, D). Notably, this defect was not due to a high Ccr7 expression, as Ccr7&Klf2 double-knockout T cells displayed a similarly reduced presence in CNS compartments (Figure 9E). In addition, the reduced S1pr1 expression in Klf2-KO T cells T cells cannot be the reason, since S1pr1 KO alone did not affect T cell migration from the blood into the CNS (Figure 11E). Overall, the impaired CNS infiltration of Klf2-KO T cells is not due to Ccr7 or S1pr1 mediated mechanisms but by another mechanism.

We focused on integrin as an alternative Klf2 mediated inhibition on the migration of T cells from blood to CNS. While their initial post-activation integrin levels appeared normal in vitro, T cells within SLOs, particularly in ptLNs, exhibited a reduced expression of CD49d and CD29, which together form VLA4, while CD11a and CD18, which make up LFA1, were upregulated (Figure 13A, B). VLA4 plays a crucial role in the migration of autoreactive T cells into the CNS during EAE (Kendirli et al., 2023a). VLA4 mediates firm adhesion to VCAM1, which is upregulated on inflamed endothelial cells of the CNS vasculature. The binding of VLA4 to VCAM1 is a key step in facilitating T cell

adhesion to the BBB, allowing T cells to crawl along the endothelial surface in search of suitable sites for transmigration. VLA4 can be activated via chemokine receptor mediated signaling which is transmitted during tethering and rolling of T cells on endothelial cells (Luster et al., 2005). Once activated, integrins undergo conformational changes that enhance their ligand-binding affinity, promoting T cell extravasation either through endothelial junctions (paracellular migration) or directly through endothelial cells (transcellular migration) (Martin-Blondel et al., 2015). Previous studies have demonstrated that knocking out CD49d or CD29 in T_{MBP} cells eliminates VLA4 expression, leading to T cell retention in the spleen and significantly reduced migration into the CNS (Kendirli et al., 2023a). Given these findings, the downregulation of CD49d and CD29 in Klf2-KO T cells likely contributes to their impaired transmigration from the bloodstream into the CNS. However, to date, no other studies have reported a direct link between Klf2 deficiency and reduced Itga4 or Itgb1 expression in T cells. Further research is needed to clarify the molecular mechanisms underlying this connection.

LFA1, another integrin being tested in our study, also mediates T cell adhesion to the endothelium by binding with ICAM, although its binding to ICAM is significantly weaker compared to the VLA4/VCAM interaction (Dominguez et al., 2015, Schläger et al., 2016). Additionally, study showed except mediate T cells/endothelium binding, LFA1 function in facilitating efficient T cell movement within lymph nodes by binding to ICAM expressed on dendritic cells (Katakai et al., 2013).

While VL-4 is essential for T cell extravasation into the CNS, LFA1 is not strictly required for this process (Dominguez et al., 2015, Schläger et al., 2016). However, its role in T cell migration depends on the target organ or tissue. For example, LFA1 is indispensable for T cell infiltration into the retina and bronchial epithelium (Mesri et al., 1994, Porter and Hall, 2009). Since LFA1 expression is upregulated in Klf2-KO T cells, it may instead promote their retention in peripheral tissues, particularly in ptLNs but not likely regulating migration from blood to CNS. Taken together, these findings support the idea that the impaired CNS migration of Klf2-deficient T cells is primarily due to the loss of VLA4. Since LFA1 expression is upregulated in these cells, it may instead promote their retention in peripheral tissues, particularly in ptLNs. Further studies are needed to confirm this hypothesis.

4.1.6. Klf2 in human T cells

When validating our finding of Klf2 transcription factor influencing T cell migration on MS patients, we found that Klf2 showed only a weak influence in T cell migration in human at all (Figure 18). The analysis was conducted using transcriptomic profiling of T cells from MS patients. More specifically,

we extracted the T cells data with overlapping TCRs in both blood and CSF and performed transcriptomic analysis on these TCR-overlapping T cells.

With the human samples being limited to peripheral blood and CSF, our sequencing results were inevitably affected. We speculate that the observed lack of strong correlation between Klf2 and T cell migration into the CNS in MS patients may be attributed to the distinct expression pattern of Klf2 in T cells. Klf2 is highly expressed in naive and memory $CD4^+$ T cells but rapidly downregulated during T cell activation (Jha and Das, 2017, Hart et al., 2012). Due to BBB breakdown and the release of proinflammatory cytokines and chemokines into the bloodstream, $CD4^+$ T cells in MS patients are likely to be in a higher activation state compared to IIH controls (Zhang et al., 1994). This heightened activation suppresses Klf2 expression, potentially covering its role in T cell migration when comparing $CD4^+$ T cells with the same TCR repertoire. To validate this hypothesis, further clinical studies are needed to examine Klf2 expression in human peripheral blood $CD4^+$ T cells.

Although the scRNA-seq did not directly confirm that the Klf2 gene strongly promote $CD4^+$ T cell migration to the CNS in humans MS, its downstream regulatory molecules, Itgb7 (Figure 18) and S1pr1 (Kendirli et al., 2023b), both exhibited a promoting effect on T cell migration. Conversely, Ccr7 and CD69, which their expression is negatively correlate with Klf2 expression, showed an inhibitory effect on T cell migration. Taken together, these findings strongly suggest that Klf2 also facilitates T cell migration in humans.

4.2. Foxo1 Function as the Upstream Transcription of Klf2 and Ccr7

Foxo1 has long been recognized as a critical factor in T cell by maintaining immune balance and supporting the development of central memory T cells (Doan et al., 2024). In MS/ EAE, Foxo1 functions as a critical effector in the PI3K/Akt signaling pathway and is involved in $CD4^+$ T cell differentiation (Kraus et al., 2021). It was shown that inhibiting Foxo1 suppresses Th1 differentiation and expansion while also blocking the conversion of Th17 cells into Th1-like cells during the reactivation of autoreactive $CD4^+$ T cells (Kraus et al., 2021). Additionally, autoreactive T cells treated with Foxo1 inhibitors displayed reduced encephalitogenic potential in adoptive transfer EAE models, highlighting its role in regulating inflammatory T cell responses (Kraus et al., 2021). Similar findings were observed in MS patients, where Foxo1 inhibition led to a significant decrease in Th1 expansion, reinforcing its involvement in disease progression (Kraus et al., 2021). While the role in T cell differentiation and inflammatory responses is well established, its impact on T cell migration during MS/EAE remains largely unknown.

Our findings suggest that Foxo1 deficiency affects T cell distribution and modulates disease severity rather than completely preventing EAE development (Figure 14A). With Foxo1 deficiency, T cells

showed a higher tendency to accumulate in the lymph nodes (Figure 14D). However, this did not affect their ability to infiltrate the CNS. Foxo1 is highly expressed in T cells (Peng, 2008) and is rapidly phosphorylated and inactivated in a PI3K-dependent manner following antigen or cytokine stimulation (Fabre et al., 2005). Upon withdrawal of cytokine signaling, Foxo1 is dephosphorylated and reactivated, contributing to T cell quiescence and homing to lymph nodes (Stahl et al., 2002). In facilitating lymph node entry, Foxo1 directly upregulates Ccr7, CD62L, and Klf2 expression (Kerdiles et al., 2009). Our study confirmed that Foxo1 deficiency in T_{MBP} cells lead Ccr7 and Klf2 expression reduced (Figure 15), providing direct evidence that Foxo1 functions as the upstream transcriptional regulator of these migratory pathways.

The regulation effect of Foxo1 on Ccr7 as well as Klf2 expression can explain the result of Foxo1-KO T_{MBP} cells in vivo migration assay (Figure 14). After Foxo1-KO T_{MBP} cells and NT control T_{MBP} cells being intravenously injected, at the day 3 post-injection, Foxo1-KO T_{MBP} cells preferentially accumulated in the ptLNs, with minimal retention in the spleen (Figure 14). This distribution pattern closely resembled that of Klf2-KO T cells, which were also trapped in the ptLNs and the spleen, with a more pronounced accumulation in ptLNs. As described above, the upregulated Ccr7 and downregulated S1pr1 expression due to Klf2 deficiency both contributed to T cell accumulation in the ptLNs. Although Foxo1-deficient T cells showed significantly lower Klf2 expression, which could in turn lead to the absence of S1pr1 and cause T cells to remain in the ptLNs, their Ccr7 expression remained low (Figure 15B). This likely explains why their accumulation in ptLNs was much less pronounced compared to Klf2-KO T cells.

As for CNS infiltration, Foxo1-KO T cells showed comparable levels to control cells (Figure 14), which is another key difference from Klf2-KO T cells. As above described, Klf2-KO cells not only exhibited severe retention in SLOs, but also failed to enter the CNS (Figure 5D). Therefore, we tested the CD49d (Itga4) expression on the Foxo1-KO T cells. Consistent with the result that CNS infiltration was not affected by Foxo1 deficiency, the CD49d expression showed no changes in Foxo1-KO cells from both spleen and ptLNs (Figure 15C). Klf2 is the downstream transcription factor induced by Foxo1, at the same time Klf2-KO cells showed obviously lower CD49d expression. If Foxo1 only influence CD49d expression through regulate Klf2 expression, we should also see the CD49d downregulation in Foxo1-KO cells. Instead, the fact is that Foxo1-KO cells showed CD49d levels similar to those of control cells. Therefore, both Klf2 and Foxo1 appear to regulate CD49d expression, but in the opposite direction. Unfortunately, until now there are no other studies reported this effect so far. Further research is needed to uncover the underlying molecular mechanisms.

Beyond its regulation of Klf2, Ccr7 and CD49d, Foxo1 is a broad-acting transcription factor involved in critical cellular processes, including cell cycle progression, DNA repair, and apoptosis, and is widely

recognized as a tumor suppressor (Farhan et al., 2017). Additionally, Foxo1 plays a role in oxidative stress responses and aging by mediating reactive oxygen species detoxification and controlling DNA repair pathways (Hedrick et al., 2012).

To further investigate the role of Foxo1-regulated molecules in MS, we performed transcriptomic analysis of T cells from MS patients to examine its influence on T cell migration. The results revealed a negative correlation between Foxo1 and its downstream targets, including Tcf7, sell (CD62L), and Ccr7 with T cell migration in MS patients (Figure 18). Among these, Tcf7 and Ccr7 showed statistically significant associations. As our rat EAE showed Ccr7 upregulation lead T cells trapped autoreactive $CD4^+$ T cells in the peripheral LNs. Additionally, Clinical studies have shown that migrating T cells in MS exhibit reduced Ccr7 mRNA levels (Friess et al., 2017). Tcf7 is known for mediating T cells self-renewal and memory cell formation (Escobar et al., 2020). Furthermore, it has been reported to promote Th2 differentiation while suppressing Th1 differentiation by inhibiting IFN-γ expression (Escobar et al., 2020). But none of the findings about Tcf7 pointed it out for being involved in T cell migration. Also, it remains unclear what role of the Tcf7 gene plays in MS/EAE. Further study needed to uncover its attributes.

4.3. Klf2 as the Important Transcription Factor Regulates T Cell Activation and Migration Phenotype

While Klf2 is primarily known for its role in T cell migration, our findings also indicate that it influences T cell activation, revealing a strong correlation between impaired migration and heightened activation. We propose that Klf2 plays a crucial role in transitioning activated T cells into a migratory state.

4.3.1. Expression of Cell Surface Activation Markers in Klf2-KO T Cells

Under normal conditions, Klf2 deficient T cells can be fully activated in vitro in response to antigen presentation by MBP-loaded APCs, displaying surface activation markers such as CD25, CD134, and TCR at levels comparable to control cells (Figure 4D, F). This indicates that Klf2 is not essential for the initial activation phase following antigen recognition. However, after intravenous transfer, Klf2-KO T cells become restricted in SLOs, particularly in the ptLNs, where they exhibit significantly elevated CD25 expression along with a slight increase in CD134 and TCR levels (Figure 6B, C). Notably, the degree of CD25 upregulation correlates with the extent of T cell accumulation in these compartments, implying a potential link between defective migration and an activated phenotype. However, our study on S1pr1-KO T cells, which also accumulate in the ptLN but do not show activated phenotype there, suggest there is not direct relation between T cell accumulation in the SLOs and their activation.

CD25, also known as the IL-2 receptor alpha chain, is typically expressed at low levels on $CD4^+$ effector T cells and is initially upregulated upon TCR engagement via NF-κB activation (Adamczyk et al., 2023). Later sustaining CD25 high expression relies on IL-2-driven STAT5 signaling. Peak CD25 expression generally occurs around 48 hours post-TCR stimulation, playing a pivotal role in promoting T cell survival and expansion (Adamczyk et al., 2023). Notably, CD25-targeting therapies such as basiliximab and daclizumab, which block IL-2-dependent T cell activation and proliferation, further underscore the critical function of CD25 in maintaining T cell responsiveness (Panackel et al., 2022). Our findings indicate that Klf2-KO T_{MBP} cells, which fail to exit SLOs, remain in a persistently activated state, with excessive IL-2 signaling contributing to their sustained CD25 expression (Figure 6B, C). Additionally, the higher CD25 expression also explain higher proliferation capacity of Klf2-KO T cells compared to control T cells when they were exposed to IL2 in vitro (Figure 4C). Furthermore, the moderate upregulation of CD134 and TCR in Klf2-KO T cells further supports their heightened activation status (Figure 6B, C), as CD134 is known to enhance T cell survival and long-term immune responses (Rogers et al., 2001).

4.3.2. Production of Pro-inflammatory Cytokines in Klf2-KO T cells

Beyond surface marker expression, cytokine profiling revealed that Klf2-KO T cells restricted in SLOs produce significantly higher levels of pro-inflammatory cytokines, including TNF-α, IFN-γ, and IL-17A, under both basal and stimulated conditions (Figure 6D-F). Interestingly, despite this increase in cytokine production, these cells did not exhibit a preferential differentiation toward either the Th1 or Th17 lineage. Instead, the majority of cytokine-producing cells co-expressed IFN-γ and IL-17A, rather than displaying a distinct Th1 or Th17 bias. This pointed out that the absence of Klf2 drives a state of global hyperactivation rather than selectively skewing T cell differentiation toward a particular subset.

The roles of IFN-γ, IL-17A, and TNF-α in the pathogenesis of EAE and MS are complex and, at times, contradictory. IL-17A, predominantly produced by Th17 cells, is a well-established driver of $CD4^+$ T cell infiltration into the brain parenchyma, significantly contributing to disease severity (Harrington et al., 2005). Studies have shown that blocking IL-17A alleviates EAE symptoms, and IL-17A-deficient mice exhibit a milder disease course with delayed onset and lower clinical scores (Langrish et al., 2005). In MS, IL-17A-producing T cells are abundant in active brain lesions, where their presence correlates with disease activity (Fletcher et al., 2010). IFN-γ, on the other hand, exerts paradoxical effects: while exogenous administration of IFN-γ exacerbates MS, mice lacking IFN-γ develop more severe EAE, and blocking IFN-γ worsens disease outcomes (Fletcher et al., 2010). In MS patients, both IFN-γ and IL-17A levels are elevated in the early disease stages, but IFN-γ is particularly associated with relapse phases (O'Connor et al., 2008). The presence of IFN-γ/IL-17A dual-producing T cells in MS brain lesions highlights the plasticity between Th1 and Th17 cells, with Th17 cells potentially shifting toward IFN-γ production as the disease progresses (Fletcher et al., 2010). TNF-α, commonly linked to Th17 cell responses, adds further complexity, as its precise role in regulating $CD4^+$ T cells during EAE remains incompletely understood.

4.3.3 Transition from Activated to Migratory Phenotype

Despite producing elevated levels of CD25, IFN-γ, IL-17A, and TNF-α, Klf2-KO T_{MBP} cells fail to exit SLOs and do not induce EAE, suggesting that their hyperactivated state results from their inability to transition from an activation phenotype to a migratory phenotype. This aligns with findings by Odoardi et al. study, which distinguished between "activation phenotype" and "migratory phenotype" T cells before CNS infiltration (Odoardi et al., 2012). In our EAE model, T_{MBP} cells exhibit an activation phenotype at the peak of in vitro stimulation (day 2 post-activation), characterized by high expression of activation markers and robust antigen-driven proliferation. Upon transfer into rats, migratory phenotype T cells typically reappear in circulation around day 3, enabling their entry into the CNS.

Transcriptomic analysis from Odoardi's study identified Klf2 as the most differentially expressed gene between activation and migratory phenotypes, with high expression in migratory cells along with S1pr1 and Itgb7 (Odoardi et al., 2012). In contrast, activation phenotype cells displayed elevated levels of Il-2ra (CD25), Tnfrsf8, Tnfrc, and Il-17f (Odoardi et al., 2012), all of which were enriched in Klf2-KO T cells. Combing with findings in our study, it is clear that Klf2 is a pivotal transcription factor controlling the shift from activation to migration, and its absence leads to persistent overactivation while preventing T cells from acquiring migratory competence.

4.3.3. Molecules Involved in Klf2 Signaling

Further investigation into Klf2 downstream targets reinforces its pivotal role in regulating the transition between activation and migration. S1pr1, a well-established downstream effector of Klf2, is essential for T cell egress from SLOs (Figure 11E). Loss of S1pr1 mirrors the effects of Klf2 deficiency, as S1pr1-KO T_{MBP} cells also accumulate in ptLNs and fail to migrate into the bloodstream (Figure 11E). To date, no studies have directly implicated S1pr1 in regulating T cell activation during EAE or MS. Only one report suggests that S1p signaling plays a critical role in maintaining the persistence of activated $CD4^+$ T cells at sites of acute inflammation (Jaigirdar et al., 2017). S1pr1 signaling induce mTOR and JAK2/pSTAT3 activation was reported by multiple studies, both of these signaling pathways can enhance Th1/Th17 differentiation and are involved in T cell activation and IL-2 receptor signaling (Priceman et al., 2014, Liu et al., 2010).

Additionally, the endogenous S1pr1 antagonist, CD69, may contribute to this altered activation profile. CD69 is a type II transmembrane receptor that is rapidly upregulated upon T cell activation and serves as an early activation marker. Upon antigen recognition, its expression is induced by IFN-α/β and TNF-α (Martín et al., 2010). CD69 has also been implicated in Th1/Th17 differentiation (Cibrian et al., 2016). While S1pr1 signaling activates JAK2/pSTAT3, CD69 directly binds to S1pr1, leading to its internalization and degradation and further inhibit STAT3 phosphorylate (Shiow et al., 2006). This antagonistic regulation suggests that increased CD69 expression in S1pr1-KO cells could shift signaling dominance toward CD69-associated pathways, potentially explaining the reduced activation observed in these cells despite their retention in SLOs. However, the precise interactions between STAT3 and STAT5 signaling with CD25 expression and T cell activation remain unclear and require further investigation.

Foxo1, an upstream regulator of Klf2, further validate this regulatory network. Foxo1-KO T_{MBP} cells also exhibit reduced CD25 expression in ptLNs, similar as the phenotype observed in S1pr1-KO cells (Figure 16C). This suggests that Foxo1-dependent transcriptional programs influence both activation and migration pathways, positioning Klf2 as a central molecular switch between these two states.

Collectively, these findings establish Klf2 as a key regulator that determines whether T cells remain in an activated state or transition into a migratory phenotype, ultimately dictating their ability to exit SLOs and infiltrate the CNS. The failure of Klf2-KO T_{MBP} cells to undergo this transition results in persistent overactivation and defective migration, preventing EAE induction. In addition, Klf2 regulate migration from blood through BBB to the CNS by regulating VLA4 expression. The interplay between S1pr1, CD69, Foxo1, VLA4 and Klf2 provides a mechanistic framework for understanding how transcriptional and signaling networks coordinate T cell fate in autoimmunity. This emphasizes the essential role of Klf2 in balancing T cell activation and trafficking during neuroinflammation.

REFERENCE

ABOUL-ENEIN, F., BAUER, J., KLEIN, M., SCHUBART, A., FLÜGEL, A., RITTER, T., KAWAKAMI, N., SIEDLER, F., LININGTON, C., WEKERLE, H., LASSMANN, H. & BRADL, M. 2004. Selective and antigen-dependent effects of myelin degeneration on central nervous system inflammation. *J Neuropathol Exp Neurol,* 63**,** 1284-96.

ADAMCZYK, M., BARTOSIŃSKA, J., RACZKIEWICZ, D., KOWAL, M., SURDACKA, A., KRASOWSKA, D., MICHALAK-STOMA, A. & KRASOWSKA, D. 2023. The Expression of Activation Markers CD25 and CD69 Increases during Biologic Treatment of Psoriasis. *J Clin Med,* 12.

AGRAWAL, S. M., SILVA, C., TOURTELLOTTE, W. W. & YONG, V. W. 2011. EMMPRIN: a novel regulator of leukocyte transmigration into the CNS in multiple sclerosis and experimental autoimmune encephalomyelitis. *Journal of Neuroscience,* 31**,** 669-677.

ALLENDE, M. L., DREIER, J. L., MANDALA, S. & PROIA, R. L. 2004. Expression of the Sphingosine 1-Phosphate Receptor, S1P1, on T-cells Controls Thymic Emigration*. *Journal of Biological Chemistry,* 279**,** 15396-15401.

ALOISI, F., RIA, F., COLUMBA-CABEZAS, S., HESS, H., PENNA, G. & ADORINI, L. 1999. Relative efficiency of microglia, astrocytes, dendritic cells and B cells in naive CD4+ T cell priming and Th1/Th2 cell restimulation. *Eur J Immunol,* 29**,** 2705-14.

ANDERSON, K. P., KERN, C. B., CRABLE, S. C. & LINGREL, J. B. 1995. Isolation of a gene encoding a functional zinc finger protein homologous to erythroid Kruppel-like factor: identification of a new multigene family. *Mol Cell Biol,* 15**,** 5957-65.

AO, T., KIKUTA, J. & ISHII, M. 2021. The Effects of Vitamin D on Immune System and Inflammatory Diseases. *Biomolecules,* 11**,** 1624.

ARCHAMBAULT, A. S., SIM, J., GIMENEZ, M. A. & RUSSELL, J. H. 2005. Defining antigen-dependent stages of T cell migration from the blood to the central nervous system parenchyma. *Eur J Immunol,* 35**,** 1076-85.

ASCHERIO, A., MUNGER, K. L. & SIMON, K. C. 2010. Vitamin D and multiple sclerosis. *Lancet Neurol,* 9**,** 599-612.

ASPELUND, A., ANTILA, S., PROULX, S. T., KARLSEN, T. V., KARAMAN, S., DETMAR, M., WIIG, H. & ALITALO, K. 2015. A dural lymphatic vascular system that drains brain interstitial fluid and macromolecules. *J Exp Med,* 212**,** 991-9.

ATTFIELD, K. E., JENSEN, L. T., KAUFMANN, M., FRIESE, M. A. & FUGGER, L. 2022. The immunology of multiple sclerosis. *Nat Rev Immunol,* 22**,** 734-750.

AWASTHI, A., RIOL-BLANCO, L., JÄGER, A., KORN, T., POT, C., GALILEOS, G., BETTELLI, E., KUCHROO, V. K. & OUKKA, M. 2009. Cutting Edge: IL-23 Receptor GFP Reporter Mice Reveal Distinct Populations of IL-17-Producing Cells1. *The Journal of Immunology,* 182**,** 5904-5908.

AZIZI, G., VAN DEN BROEK, B., ISHIKAWA, L. L. W., NAZIRI, H., YAZDANI, R., ZHANG, G.-X., CIRIC, B. & ROSTAMI, A. 2024. IL-7Rα on CD4+ T cells is required for their survival and the pathogenesis of experimental autoimmune encephalomyelitis. *Journal of Neuroinflammation,* 21**,** 253.

BABINSKI, J. 1885. Recherches sur l'anatomie pathologique de la sclerose en plaque et étude comparative des diverses variétés de la scleroses de la moelle. *Arch Physiol (Paris),* 5**,** 186-207.

BAEYENS, A., FANG, V., CHEN, C. & SCHWAB, S. R. 2015. Exit Strategies: S1P Signaling and T Cell Migration. *Trends Immunol,* 36**,** 778-787.

BAI, A., HU, H., YEUNG, M. & CHEN, J. 2007. Kruppel-like factor 2 controls T cell trafficking by activating L-selectin (CD62L) and sphingosine-1-phosphate receptor 1 transcription. *J Immunol,* 178**,** 7632-9.

BANCHEREAU, J. & STEINMAN, R. M. 1998. Dendritic cells and the control of immunity. *Nature,* 392**,** 245-52.

BARGATZE, R. F., JUTILA, M. A. & BUTCHER, E. C. 1995. Distinct roles of L-selectin and integrins α4β7 and LFA-1 in lymphocyte homing to Peyer's patch-HEV in situ: the multistep model confirmed and refined. *Immunity,* 3**,** 99-108.

BARKAUSKAS, D. S., DIXON DORAND, R., MYERS, J. T., EVANS, T. A., BARKAUSKAS, K. J., ASKEW, D., PURGERT, R. & HUANG, A. Y. 2015. Focal transient CNS vessel leak provides a tissue niche for sequential immune cell accumulation during the asymptomatic phase of EAE induction. *Exp Neurol,* 266**,** 74-85.

BARNETT, M. H., PARRATT, J. D., CHO, E. S. & PRINEAS, J. W. 2009. Immunoglobulins and complement in postmortem multiple sclerosis tissue. *Ann Neurol,* 65**,** 32-46.

BARTHOLOMAUS, I., KAWAKAMI, N., ODOARDI, F., SCHLAGER, C., MILJKOVIC, D., ELLWART, J. W., KLINKERT, W. E., FLUGEL-KOCH, C., ISSEKUTZ, T. B., WEKERLE, H. & FLUGEL, A. 2009. Effector T cell interactions with meningeal vascular structures in nascent autoimmune CNS lesions. *Nature,* 462**,** 94-8.

BATOULIS, H., RECKS, M. S., ADDICKS, K. & KUERTEN, S. 2011. Experimental autoimmune encephalomyelitis--achievements and prospective advances. *APMIS,* 119**,** 819-30.

BATTISTINI, L., PICCIO, L., ROSSI, B., BACH, S., GALGANI, S., GASPERINI, C., OTTOBONI, L., CIABINI, D., CARAMIA, M. D., BERNARDI, G., LAUDANNA, C., SCARPINI, E., MCEVER, R. P., BUTCHER, E. C., BORSELLINO, G. & CONSTANTIN, G. 2003. CD8+ T cells from patients with acute multiple sclerosis display selective increase of adhesiveness in brain venules: a critical role for P-selectin glycoprotein ligand-1. *Blood,* 101**,** 4775-82.

BAUER, I. J., FANG, P., LAMMLE, K. F., TYYSTJARVI, S., ALTERAUGE, D., BAUMJOHANN, D., YOON, H., KORN, T., WEKERLE, H. & KAWAKAMI, N. 2023. Visualizing the activation of encephalitogenic T cells in the ileal lamina propria by in vivo two-photon imaging. *Proc Natl Acad Sci U S A,* 120**,** e2302697120.

BEALMEAR, M. & WILSON, R. 1966. Histological comparison of the thymus of germfree (axenic) and conventional CFW mice. *Anat Rec,* 154**,** 261-73.

BELIKAN, P., BUHLER, U., WOLF, C., PRAMANIK, G. K., GOLLAN, R., ZIPP, F. & SIFFRIN, V. 2018. CCR7 on CD4(+) T Cells Plays a Crucial Role in the Induction of Experimental Autoimmune Encephalomyelitis. *J Immunol,* 200**,** 2554-2562.

BENVENISTE, E. N. 1997. Role of macrophages/microglia in multiple sclerosis and experimental allergic encephalomyelitis. *J Mol Med (Berl),* 75**,** 165-73.

BERER, K., MUES, M., KOUTROLOS, M., RASBI, Z. A., BOZIKI, M., JOHNER, C., WEKERLE, H. & KRISHNAMOORTHY, G. 2011. Commensal microbiota and myelin autoantigen cooperate to trigger autoimmune demyelination. *Nature,* 479**,** 538-41.

BERTONI, A., ALABISO, O., GALETTO, A. S. & BALDANZI, G. 2018. Integrins in T Cell Physiology. *Int J Mol Sci,* 19**,** 485.

BETTELLI, E., PAGANY, M., WEINER, H. L., LININGTON, C., SOBEL, R. A. & KUCHROO, V. K. 2003. Myelin oligodendrocyte glycoprotein-specific T cell receptor transgenic mice develop spontaneous autoimmune optic neuritis. *J Exp Med,* 197**,** 1073-81.

BIDDISON, W. E., CRUIKSHANK, W. W., CENTER, D. M., PELFREY, C. M., TAUB, D. D. & TURNER, R. V. 1998. CD8+ myelin peptide-specific T cells can chemoattract CD4+ myelin peptide-specific T cells: importance of IFN-inducible protein 10. *The Journal of Immunology,* 160**,** 444-448.

BIELEKOVA, B., GOODWIN, B., RICHERT, N., CORTESE, I., KONDO, T., AFSHAR, G., GRAN, B., EATON, J., ANTEL, J., FRANK, J. A., MCFARLAND, H. F. & MARTIN, R. 2000. Encephalitogenic potential of the myelin basic protein peptide (amino acids 83-99) in multiple sclerosis: results of a phase II clinical trial with an altered peptide ligand. *Nat Med,* 6**,** 1167-75.

BILL, R., DORING, A., DEUTSCH, U. & ENGELHARDT, B. 2011. PSGL-1 is dispensible for the development of active experimental autoimmune encephalomyelitis in SJL/J mice. *J Neuroimmunol,* 232**,** 207-8.

BOURNEVILLE, D. M. & GUÉRARD, L. 1869. *De la sclérose en plaques disséminées*, Delahaye.

BRANDLE, S. M., OBERMEIER, B., SENEL, M., BRUDER, J., MENTELE, R., KHADEMI, M., OLSSON, T., TUMANI, H., KRISTOFERITSCH, W., LOTTSPEICH, F., WEKERLE, H., HOHLFELD, R. & DORNMAIR, K. 2016. Distinct oligoclonal band antibodies in multiple sclerosis recognize ubiquitous self-proteins. *Proc Natl Acad Sci U S A,* 113**,** 7864-9.

BREART, B., RAMOS-PEREZ, W. D., MENDOZA, A., SALOUS, A. K., GOBERT, M., HUANG, Y., ADAMS, R. H., LAFAILLE, J. J., ESCALANTE-ALCALDE, D., MORRIS, A. J. & SCHWAB, S. R. 2011. Lipid phosphate phosphatase 3 enables efficient thymic egress. *J Exp Med,* 208**,** 1267-78.

BRONTE, V. & PITTET, M. J. 2023. The Spleen in Local and Systemic Regulation of Immunity. *Immunity,* 56**,** 1152.

BUCKLEY, A. F., KUO, C. T. & LEIDEN, J. M. 2001a. Transcription factor LKLF is sufficient to program T cell quiescence via a c-Myc-dependent pathway. *Nat Immunol,* 2**,** 698-704.

BUCKLEY, A. F., KUO, C. T. & LEIDEN, J. M. 2001b. Transcription factor LKLF is sufficient to program T cell quiescence via a c-Myc–dependent pathway. *Nature immunology,* 2**,** 698-704.

CAMPBELL, B., VOGEL, P. J., FISHER, E. & LORENZ, R. 1973. Myelin basic protein administration in multiple sclerosis. *Arch Neurol,* 29**,** 10-5.

CANNELLA, B., CROSS, A. H. & RAINE, C. S. 1993. Anti-adhesion molecule therapy in experimental autoimmune encephalomyelitis. *J Neuroimmunol,* 46**,** 43-55.

CAO, Y., GOODS, B. A., RADDASSI, K., NEPOM, G. T., KWOK, W. W., LOVE, J. C. & HAFLER, D. A. 2015. Functional inflammatory profiles distinguish myelin-reactive T cells from patients with multiple sclerosis. *Sci Transl Med,* 7**,** 287ra74.

CARLSON, C. M., ENDRIZZI, B. T., WU, J., DING, X., WEINREICH, M. A., WALSH, E. R., WANI, M. A., LINGREL, J. B., HOGQUIST, K. A. & JAMESON, S. C. 2006. Kruppel-like factor 2 regulates thymocyte and T-cell migration. *Nature,* 442**,** 299-302.

CHARCOT, J. 1868. Histologie de la sclerose en plaques. *Gazette Hôpitaux,* 41**,** 554.

CHAUVEAU, A., PIRGOVA, G., CHENG, H. W., DE MARTIN, A., ZHOU, F. Y., WIDEMAN, S., RITTSCHER, J., LUDEWIG, B. & ARNON, T. I. 2020. Visualization of T Cell Migration in the Spleen Reveals a Network of Perivascular Pathways that Guide Entry into T Zones. *Immunity,* 52**,** 794-807.e7.

CHEN, W., CUI, Y., LI, C., HE, C., DU, L., LIU, W. & HE, Z. 2024. KLF2 controls proliferation and apoptosis of human spermatogonial stem cells via targeting GJA1. *iScience,* 27**,** 109024.

CHOI, G., PARK, Y.-J., CHO, M., MOON, H., KIM, D., KANG, C.-Y., CHUNG, Y. & KIM, B.-S. 2021. A critical role for Th17 cell-derived TGF-β1 in regulating the stability and pathogenicity of autoimmune Th17 cells. *Experimental & Molecular Medicine,* 53**,** 993-1004.

CHULUUNDORJ, D., HARDING, S. A., ABERNETHY, D. & LA FLAMME, A. C. 2014. Expansion and preferential activation of the CD14(+)CD16(+) monocyte subset during multiple sclerosis. *Immunol Cell Biol,* 92**,** 509-17.

CIBRIAN, D., SAIZ, M. L., DE LA FUENTE, H., SÁNCHEZ-DÍAZ, R., MORENO-GONZALO, O., JORGE, I., FERRARINI, A., VÁZQUEZ, J., PUNZÓN, C., FRESNO, M., VICENTE-MANZANARES, M., DAUDÉN, E., FERNÁNDEZ-SALGUERO, P. M., MARTÍN, P. & SÁNCHEZ-MADRID, F. 2016. CD69 controls the uptake of L-tryptophan through LAT1-CD98 and AhR-dependent secretion of IL-22 in psoriasis. *Nat Immunol,* 17**,** 985-96.

CLARKSON, B. D., WALKER, A., HARRIS, M., RAYASAM, A., SANDOR, M. & FABRY, Z. 2014. Mapping the accumulation of co-infiltrating CNS dendritic cells and encephalitogenic T cells during EAE. *Journal of Neuroimmunology,* 277**,** 39-49.

COMPSTON, A. & COLES, A. 2008. Multiple sclerosis. *Lancet,* 372**,** 1502-17.

CONANT, D., HSIAU, T., ROSSI, N., OKI, J., MAURES, T., WAITE, K., YANG, J., JOSHI, S., KELSO, R., HOLDEN, K., ENZMANN, B. L. & STONER, R. 2022. Inference of CRISPR Edits from Sanger Trace Data. *Crispr j,* 5**,** 123-130.

CONSORTIUM, I. I. G., AGLIARDI, C., ALFREDSSON, L., ALIZADEH, M., ANDERSON, C., ANDREWS, R., SØNDERGAARD, H. B., BAKER, A. & BAND, G. 2013. Analysis of immune-related loci identifies 48 new susceptibility variants for multiple sclerosis. *Nature genetics,* 45**,** 1353-1360.

CRAWFORD, M. P., YAN, S. X., ORTEGA, S. B., MEHTA, R. S., HEWITT, R. E., PRICE, D. A., STASTNY, P., DOUEK, D. C., KOUP, R. A., RACKE, M. K. & KARANDIKAR, N. J. 2004. High prevalence of autoreactive, neuroantigen-specific CD8+ T cells in multiple sclerosis revealed by novel flow cytometric assay. *Blood,* 103**,** 4222-31.

CROSS, A. H., STARK, J. L., LAUBER, J., RAMSBOTTOM, M. J. & LYONS, J. A. 2006. Rituximab reduces B cells and T cells in cerebrospinal fluid of multiple sclerosis patients. *J Neuroimmunol,* 180**,** 63-70.

CROXFORD, A. L., KURSCHUS, F. C. & WAISMAN, A. 2011. Mouse models for multiple sclerosis: Historical facts and future implications. *Biochimica et Biophysica Acta (BBA) - Molecular Basis of Disease,* 1812**,** 177-183.

CYSTER, J. G. & SCHWAB, S. R. 2012. Sphingosine-1-phosphate and lymphocyte egress from lymphoid organs. *Annu Rev Immunol,* 30**,** 69-94.

DANKE, N. A., KOELLE, D. M., YEE, C., BEHERAY, S. & KWOK, W. W. 2004. Autoreactive T cells in healthy individuals. *J Immunol,* 172**,** 5967-72.

DAS, H., KUMAR, A., LIN, Z., PATINO, W. D., HWANG, P. M., FEINBERG, M. W., MAJUMDER, P. K. & JAIN, M. K. 2006. Kruppel-like factor 2 (KLF2) regulates proinflammatory activation of monocytes. *Proceedings of the National Academy of Sciences,* 103**,** 6653-6658.

DAVALOS, D., KYU RYU, J., MERLINI, M., BAETEN, K. M., LE MOAN, N., PETERSEN, M. A., DEERINCK, T. J., SMIRNOFF, D. S., BEDARD, C. & HAKOZAKI, H. 2012. Fibrinogen-induced perivascular microglial clustering is required for the development of axonal damage in neuroinflammation. *Nature communications,* 3**,** 1227.

DE ANDRES, C., RODRIGUEZ-SAINZ, M. C., MUNOZ-FERNANDEZ, M. A., LOPEZ-LAZARENO, N., RODRIGUEZ-MAHOU, M., VICENTE, A., FERNANDEZ-CRUZ, E. & SANCHEZ-RAMON, S. 2004. Short-term sequential analysis of sex hormones and helper T cells type 1 (Th1) and helper T cells type 2 (Th2) cytokines during and after multiple sclerosis relapse. *Eur Cytokine Netw,* 15**,** 197-202.

DEDONI, S., SCHERMA, M., CAMOGLIO, C., SIDDI, C., DAZZI, L., PULIGA, R., FRAU, J., COCCO, E. & FADDA, P. 2023. An overall view of the most common experimental models for multiple sclerosis. *Neurobiology of Disease***,** 106230.

DEL PILAR MARTIN, M., CRAVENS, P. D., WINGER, R., KIESEIER, B. C., CEPOK, S., EAGAR, T. N., ZAMVIL, S. S., WEBER, M. S., FROHMAN, E. M. & KLEINSCHMIDT-DEMASTERS, B. K. 2009. Depletion of B lymphocytes from cerebral perivascular spaces by rituximab. *Archives of neurology,* 66**,** 1016-1020.

DERMITZAKIS, I., THEOTOKIS, P., EVANGELIDIS, P., DELILAMPOU, E., EVANGELIDIS, N., CHATZISAVVIDOU, A., AVRAMIDOU, E. & MANTHOU, M. E. 2023. CNS Border-Associated Macrophages: Ontogeny and Potential Implication in Disease. *Curr Issues Mol Biol,* 45**,** 4285-4300.

DOAN, A. E., MUELLER, K. P., CHEN, A. Y., ROUIN, G. T., CHEN, Y., DANIEL, B., LATTIN, J., MARKOVSKA, M., MOZARSKY, B. & ARIAS-UMANA, J. 2024. FOXO1 is a master regulator of memory programming in CAR T cells. *Nature***,** 1-8.

DOMINGUES, H. S., MUES, M., LASSMANN, H., WEKERLE, H. & KRISHNAMOORTHY, G. 2010. Functional and Pathogenic Differences of Th1 and Th17 Cells in Experimental Autoimmune Encephalomyelitis. *PLOS ONE,* 5**,** e15531.

DOMINGUEZ, G. A., ANDERSON, N. R. & HAMMER, D. A. 2015. The direction of migration of T-lymphocytes under flow depends upon which adhesion receptors are engaged. *Integr Biol (Camb),* 7**,** 345-55.

DROUILLARD, A., NEYRA, A., MATHIEU, A.-L., MARÇAIS, A., WENCKER, M., MARVEL, J., BELOT, A. & WALZER, T. 2018. Human naive and memory T cells display opposite migratory responses to sphingosine-1 phosphate. *The Journal of Immunology,* 200**,** 551-557.

DUAN, H., XING, S., LUO, Y., FENG, L., GRAMAGLIA, I., ZHANG, Y., LU, D., ZENG, Q., FAN, K., FENG, J., YANG, D., QIN, Z., COURAUD, P. O., ROMERO, I. A., WEKSLER, B. & YAN, X. 2013. Targeting endothelial CD146 attenuates neuroinflammation by limiting lymphocyte extravasation to the CNS. *Sci Rep,* 3**,** 1687.

DUGGER, K. J., ZINN, K. R., WEAVER, C., BULLARD, D. C. & BARNUM, S. R. 2009. Effector and suppressor roles for LFA-1 during the development of experimental autoimmune encephalomyelitis. *J Neuroimmunol,* 206**,** 22-7.

DYMENT, D. A., EBERS, G. C. & SADOVNICK, A. D. 2004. Genetics of multiple sclerosis. *Lancet Neurol,* 3**,** 104-10.

EFENDI, H. 2015. Clinically Isolated Syndromes: Clinical Characteristics, Differential Diagnosis, and Management. *Noro Psikiyatr Ars,* 52**,** S1-s11.

EISENBARTH, S. C. 2019. Dendritic cell subsets in T cell programming: location dictates function. *Nat Rev Immunol,* 19**,** 89-103.

ELSAYED, N. S., ASTON, P., BAYANAGARI, V. R. & SHUKLA, S. K. 2022. The gut microbiome molecular mimicry piece in the multiple sclerosis puzzle. *Front Immunol,* 13**,** 972160.

ENDRIZZI, B. T. & JAMESON, S. C. 2003. Differential role for IL‐7 in inducing lung Kruppel‐like factor (Kruppel‐like factor 2) expression by naive versus activated T cells. *International Immunology,* 15**,** 1341-1348.

ENGELHARDT, B. 2010. T cell migration into the central nervous system during health and disease: Different molecular keys allow access to different central nervous system compartments. *Clinical and Experimental Neuroimmunology,* 1**,** 79-93.

ENGELHARDT, B. & RANSOHOFF, R. M. 2012. Capture, crawl, cross: the T cell code to breach the blood-brain barriers. *Trends Immunol,* 33**,** 579-89.

ESCOBAR, G., MANGANI, D. & ANDERSON, A. C. 2020. T cell factor 1: A master regulator of the T cell response in disease. *Sci Immunol,* 5.

FABRE, S., LANG, V., HARRIAGUE, J., JOBART, A., UNTERMAN, T. G., TRAUTMANN, A. & BISMUTH, G. 2005. Stable activation of phosphatidylinositol 3-kinase in the T cell immunological synapse stimulates Akt signaling to FoxO1 nuclear exclusion and cell growth control. *J Immunol,* 174**,** 4161-71.

FARHAN, M., WANG, H., GAUR, U., LITTLE, P. J., XU, J. & ZHENG, W. 2017. FOXO Signaling Pathways as Therapeutic Targets in Cancer. *Int J Biol Sci,* 13**,** 815-827.

FERBER, I. A., BROCKE, S., TAYLOR-EDWARDS, C., RIDGWAY, W., DINISCO, C., STEINMAN, L., DALTON, D. & FATHMAN, C. G. 1996. Mice with a disrupted IFN-gamma gene are susceptible to the induction of experimental autoimmune encephalomyelitis (EAE). *J Immunol,* 156**,** 5-7.

FISNIKU, L. K., BREX, P. A., ALTMANN, D. R., MISZKIEL, K. A., BENTON, C. E., LANYON, R., THOMPSON, A. J. & MILLER, D. H. 2008. Disability and T2 MRI lesions: a 20-year follow-up of patients with relapse onset of multiple sclerosis. *Brain,* 131**,** 808-17.

FLETCHER, J. M., LALOR, S. J., SWEENEY, C. M., TUBRIDY, N. & MILLS, K. H. 2010. T cells in multiple sclerosis and experimental autoimmune encephalomyelitis. *Clin Exp Immunol,* 162**,** 1-11.

FLÜGEL, A., BERKOWICZ, T., RITTER, T., LABEUR, M., JENNE, D. E., LI, Z., ELLWART, J. W., WILLEM, M., LASSMANN, H. & WEKERLE, H. 2001. Migratory activity and functional changes of green fluorescent effector cells before and during experimental autoimmune encephalomyelitis. *Immunity,* 14**,** 547-560.

FRIESS, J., HECKER, M., ROCH, L., KOCZAN, D., FITZNER, B., ANGERER, I. C., SCHRÖDER, I., FLECHTNER, K., THIESEN, H.-J., WINKELMANN, A. & ZETTL, U. K. 2017. Fingolimod alters the transcriptome profile of circulating CD4+ cells in multiple sclerosis. *Scientific Reports,* 7**,** 42087.

FRISCHER, J. M., BRAMOW, S., DAL-BIANCO, A., LUCCHINETTI, C. F., RAUSCHKA, H., SCHMIDBAUER, M., LAURSEN, H., SORENSEN, P. S. & LASSMANN, H. 2009. The relation between inflammation and neurodegeneration in multiple sclerosis brains. *Brain,* 132**,** 1175-1189.

GALATRO, T. F., HOLTMAN, I. R., LERARIO, A. M., VAINCHTEIN, I. D., BROUWER, N., SOLA, P. R., VERAS, M. M., PEREIRA, T. F., LEITE, R. E. P., MÖLLER, T., WES, P. D., SOGAYAR, M. C., LAMAN, J. D., DEN DUNNEN, W., PASQUALUCCI, C. A., OBA-SHINJO, S. M., BODDEKE, E., MARIE, S. K. N. & EGGEN, B. J. L. 2017. Transcriptomic analysis of purified human cortical microglia reveals age-associated changes. *Nat Neurosci,* 20**,** 1162-1171.

GALEA, I., BECHMANN, I. & PERRY, V. H. 2007. What is immune privilege (not)? *Trends in immunology,* 28**,** 12-18.

GARRIS, C. S., BLAHO, V. A., HLA, T. & HAN, M. H. 2014. Sphingosine-1-phosphate receptor 1 signalling in T cells: trafficking and beyond. *Immunology,* 142**,** 347-53.

GASTEIGER, G., ATAIDE, M. & KASTENMÜLLER, W. 2016. Lymph node - an organ for T-cell activation and pathogen defense. *Immunol Rev,* 271**,** 200-20.

GENET, N. 2013. Analysis of immune-related loci identifies 48 new susceptibility variants for multiple sclerosis. *Nat Genet,* 45**,** 1353-1360.

GETAHUN, A. & CAMBIER, J. C. 2019. Non-Antibody-Secreting Functions of B Cells and Their Contribution to Autoimmune Disease. *Annu Rev Cell Dev Biol,* 35**,** 337-356.

GINSBERG, M. H. 2014. Integrin activation. *BMB Rep,* 47**,** 655-9.

GIULIANI, F., GOODYER, C. G., ANTEL, J. P. & YONG, V. W. 2003. Vulnerability of human neurons to T cell-mediated cytotoxicity. *J Immunol,* 171**,** 368-79.

GORDON, E. J., MYERS, K. J., DOUGHERTY, J. P., ROSEN, H. & RON, Y. 1995. Both anti-CD11a (LFA-1) and anti-CD11b (MAC-1) therapy delay the onset and diminish the severity of experimental autoimmune encephalomyelitis. *J Neuroimmunol,* 62**,** 153-60.

GOVERMAN, J., WOODS, A., LARSON, L., WEINER, L. P., HOOD, L. & ZALLER, D. M. 1993. Transgenic mice that express a myelin basic protein-specific T cell receptor develop spontaneous autoimmunity. *Cell,* 72**,** 551-60.

GRAN, B., CHU, N., ZHANG, G. X., YU, S., LI, Y., CHEN, X. H., KAMOUN, M. & ROSTAMI, A. 2004. Early administration of IL-12 suppresses EAE through induction of interferon-gamma. *J Neuroimmunol,* 156**,** 123-31.

GUBBELS BUPP, M. R., EDWARDS, B., GUO, C., WEI, D., CHEN, G., WONG, B., MASTELLER, E. & PENG, S. L. 2009. T cells require Foxo1 to populate the peripheral lymphoid organs. *Eur J Immunol,* 39**,** 2991-9.

HAN, J. M., PATTERSON, S. J. & LEVINGS, M. K. 2012. The Role of the PI3K Signaling Pathway in CD4(+) T Cell Differentiation and Function. *Front Immunol,* 3**,** 245.

HANDEL, A. E., WILLIAMSON, A. J., DISANTO, G., HANDUNNETTHI, L., GIOVANNONI, G. & RAMAGOPALAN, S. V. 2010. An updated meta-analysis of risk of multiple sclerosis following infectious mononucleosis. *PLoS One,* 5**,** e12496.

HARBO, H. F., GOLD, R. & TINTORÉ, M. 2013. Sex and gender issues in multiple sclerosis. *Ther Adv Neurol Disord,* 6**,** 237-48.

HARRINGTON, L. E., HATTON, R. D., MANGAN, P. R., TURNER, H., MURPHY, T. L., MURPHY, K. M. & WEAVER, C. T. 2005. Interleukin 17-producing CD4+ effector T cells develop via a lineage distinct from the T helper type 1 and 2 lineages. *Nat Immunol,* 6**,** 1123-32.

HART, G. T., HOGQUIST, K. A. & JAMESON, S. C. 2012. Kruppel-like factors in lymphocyte biology. *J Immunol,* 188**,** 521-6.

HAUSER, S. L., BAR-OR, A., COMI, G., GIOVANNONI, G., HARTUNG, H. P., HEMMER, B., LUBLIN, F., MONTALBAN, X., RAMMOHAN, K. W., SELMAJ, K., TRABOULSEE, A., WOLINSKY, J. S., ARNOLD, D. L., KLINGELSCHMITT, G., MASTERMAN, D., FONTOURA, P., BELACHEW, S., CHIN, P., MAIRON, N., GARREN, H., KAPPOS, L., OPERA, I. & INVESTIGATORS, O. I. C. 2017. Ocrelizumab versus Interferon Beta-1a in Relapsing Multiple Sclerosis. *N Engl J Med,* 376**,** 221-234.

HAUSER, S. L., WAUBANT, E., ARNOLD, D. L., VOLLMER, T., ANTEL, J., FOX, R. J., BAR-OR, A., PANZARA, M., SARKAR, N., AGARWAL, S., LANGER-GOULD, A., SMITH, C. H. & GROUP, H. T. 2008. B-cell depletion with rituximab in relapsing-remitting multiple sclerosis. *N Engl J Med,* 358**,** 676-88.

HEDRICK, S. M., HESS MICHELINI, R., DOEDENS, A. L., GOLDRATH, A. W. & STONE, E. L. 2012. FOXO transcription factors throughout T cell biology. *Nat Rev Immunol,* 12**,** 649-61.

HEDSTRÖM, A. K., SEGERSSON, D., HILLERT, J., STRIDH, P., KOCKUM, I., OLSSON, T., BELLANDER, T. & ALFREDSSON, L. 2023. Association between exposure to combustion-related air pollution and multiple sclerosis risk. *International Journal of Epidemiology,* 52**,** 703-714.

HEMOND, C. C. & BAKSHI, R. 2018. Magnetic Resonance Imaging in Multiple Sclerosis. *Cold Spring Harb Perspect Med,* 8**,** a028969.

HEPPNER, F. L., GRETER, M., MARINO, D., FALSIG, J., RAIVICH, G., HOVELMEYER, N., WAISMAN, A., RULICKE, T., PRINZ, M., PRILLER, J., BECHER, B. & AGUZZI, A. 2005. Experimental autoimmune encephalomyelitis repressed by microglial paralysis. *Nat Med,* 11**,** 146-52.

HERZ, J., FILIANO, A. J., WILTBANK, A. T., YOGEV, N. & KIPNIS, J. 2017. Myeloid Cells in the Central Nervous System. *Immunity,* 46**,** 943-956.

HEWISON, M. 2011. Chapter two - Vitamin D and Innate and Adaptive Immunity. *In:* LITWACK, G. (ed.) *Vitamins & Hormones.* Academic Press.

HICKEY, W. F. 1991. Migration of Hematogenous Cells Through the Blood-Brain Barrier and the Initiation of CNS Inflammation. *Brain Pathology,* 1**,** 97-105.

HICKEY, W. F. 1999. The pathology of multiple sclerosis: a historical perspective. *J Neuroimmunol,* 98**,** 37-44.

HLA, T., VENKATARAMAN, K. & MICHAUD, J. 2008. The vascular S1P gradient-cellular sources and biological significance. *Biochim Biophys Acta,* 1781**,** 477-82.

HOLDA, J. H., WELCH, A. M. & SWANBORG, R. H. 1980. Autoimmune effector cells: I. Transfer of experimental allergic encephalomyelitis with lymphoid cells cultured with antigen. *European journal of immunology,* 10**,** 657-659.

HOLLENBACH, J. A. & OKSENBERG, J. R. 2015. The immunogenetics of multiple sclerosis: A comprehensive review. *J Autoimmun,* 64**,** 13-25.

HOLMAN, D. W., KLEIN, R. S. & RANSOHOFF, R. M. 2011. The blood-brain barrier, chemokines and multiple sclerosis. *Biochim Biophys Acta,* 1812**,** 220-30.

HOWELL, O. W., REEVES, C. A., NICHOLAS, R., CARASSITI, D., RADOTRA, B., GENTLEMAN, S. M., SERAFINI, B., ALOISI, F., RONCAROLI, F. & MAGLIOZZI, R. 2011. Meningeal inflammation is widespread and linked to cortical pathology in multiple sclerosis. *Brain,* 134**,** 2755-2771.

HUPPERT, J., CLOSHEN, D., CROXFORD, A., WHITE, R., KULIG, P., PIETROWSKI, E., BECHMANN, I., BECHER, B., LUHMANN, H. J., WAISMAN, A. & KUHLMANN, C. R. 2010. Cellular mechanisms of IL-17-induced blood-brain barrier disruption. *Faseb j,* 24**,** 1023-34.

HUTCHINSON, M. 2007. Natalizumab: A new treatment for relapsing remitting multiple sclerosis. *Ther Clin Risk Manag,* 3**,** 259-68.

ISE, W., KOIKE, T., SHIMADA, N., YAMAMOTO, H., TAI, Y., SHIRAI, T., KAWAKAMI, R., KUWABARA, M., KAWAI, C., SHIDA, K., INOUE, T., HOJO, N., ICHIYAMA, K., SAKAGUCHI, S., SHIROGUCHI, K., SUZUKI, K. & KUROSAKI, T. 2025. KLF2 expression in IgG plasma cells at their induction site regulates the migration program. *Journal of Experimental Medicine,* 222.

JAIGIRDAR, S. A., BENSON, R. A., ELMESMARI, A., KUROWSKA-STOLARSKA, M. S., MCINNES, I. B., GARSIDE, P. & MACLEOD, M. K. L. 2017. Sphingosine-1-Phosphate Promotes the Persistence of Activated CD4 T Cells in Inflamed Sites. *Front Immunol,* 8**,** 1627.

JHA, P. & DAS, H. 2017. KLF2 in Regulation of NF-kappaB-Mediated Immune Cell Function and Inflammation. *Int J Mol Sci,* 18**,** 2383.

JOSHI, S. K., SURESH, P. R. & CHAUHAN, V. S. 2001. Flexibility in MHC and TCR recognition: degenerate specificity at the T cell level in the recognition of promiscuous Th epitopes exhibiting no primary sequence homology. *J Immunol,* 166**,** 6693-703.

KABAT, E. A., MOORE, D. H. & LANDOW, H. 1942. AN ELECTROPHORETIC STUDY OF THE PROTEIN COMPONENTS IN CEREBROSPINAL FLUID AND THEIR RELATIONSHIP TO THE SERUM PROTEINS. *J Clin Invest,* 21**,** 571-7.

KAPPOS, L., POLMAN, C. H., FREEDMAN, M. S., EDAN, G., HARTUNG, H. P., MILLER, D. H., MONTALBAN, X., BARKHOF, F., BAUER, L., JAKOBS, P., POHL, C. & SANDBRINK, R. 2006. Treatment with interferon beta-1b delays conversion to clinically definite and McDonald MS in patients with clinically isolated syndromes. *Neurology,* 67**,** 1242-9.

KASKOW, B. J. & BAECHER-ALLAN, C. 2018. Effector T Cells in Multiple Sclerosis. *Cold Spring Harb Perspect Med,* 8**,** a029025.

KATAKAI, T., HABIRO, K. & KINASHI, T. 2013. Dendritic cells regulate high-speed interstitial T cell migration in the lymph node via LFA-1/ICAM-1. *J Immunol,* 191**,** 1188-99.

KATZ SAND, I. 2015. Classification, diagnosis, and differential diagnosis of multiple sclerosis. *Current Opinion in Neurology,* 28**,** 193-205.

KAWAKAMI, N. & FLÜGEL, A. 2010. Knocking at the brain's door: intravital two-photon imaging of autoreactive T cell interactions with CNS structures. *Semin Immunopathol,* 32**,** 275-87.

KAWAKAMI, N., LASSMANN, S., LI, Z., ODOARDI, F., RITTER, T., ZIEMSSEN, T., KLINKERT, W. E., ELLWART, J. W., BRADL, M., KRIVACIC, K., LASSMANN, H., RANSOHOFF, R. M., VOLK, H. D., WEKERLE, H., LININGTON, C. & FLUGEL, A. 2004. The activation status of neuroantigen-specific T cells in the target organ determines the clinical outcome of autoimmune encephalomyelitis. *J Exp Med,* 199**,** 185-97.

KAWAKAMI, N., ODOARDI, F., ZIEMSSEN, T., BRADL, M., RITTER, T., NEUHAUS, O., LASSMANN, H., WEKERLE, H. & FLUGEL, A. 2005. Autoimmune CD4+ T cell memory: lifelong persistence of encephalitogenic T cell clones in healthy immune repertoires. *J Immunol,* 175**,** 69-81.

KAWAKAMI, N. & WEKERLE, H. 2024. Life history of a brain autoreactive T cell: From thymus through intestine to blood-brain barrier and brain lesion. *Neurotherapeutics,* 21**,** e00442.

KENDIRLI, A., DE LA ROSA, C., LÄMMLE, K. F., EGLSEER, K., BAUER, I. J., KAVAKA, V., WINKLMEIER, S., ZHUO, L., WICHMANN, C. & GERDES, L. A. 2023a. A genome-wide in vivo CRISPR screen identifies essential regulators of T cell migration to the CNS in a multiple sclerosis model. *Nature Neuroscience,* 26**,** 1713-1725.

KENDIRLI, A., DE LA ROSA, C., LAMMLE, K. F., EGLSEER, K., BAUER, I. J., KAVAKA, V., WINKLMEIER, S., ZHUO, L., WICHMANN, C., GERDES, L. A., KUMPFEL, T., DORNMAIR, K., BELTRAN, E., KERSCHENSTEINER, M. & KAWAKAMI, N. 2023b. A genome-wide in vivo CRISPR screen identifies essential regulators of T cell migration to the CNS in a multiple sclerosis model. *Nat Neurosci,* 26**,** 1713-1725.

KERDILES, Y. M., BEISNER, D. R., TINOCO, R., DEJEAN, A. S., CASTRILLON, D. H., DEPINHO, R. A. & HEDRICK, S. M. 2009. Foxo1 links homing and survival of naive T cells by regulating L-selectin, CCR7 and interleukin 7 receptor. *Nature immunology,* 10**,** 176-184.

KIMURA, A. & KISHIMOTO, T. 2010. IL-6: regulator of Treg/Th17 balance. *Eur J Immunol,* 40**,** 1830-5.

KING, I. L., DICKENDESHER, T. L. & SEGAL, B. M. 2009. Circulating Ly-6C+ myeloid precursors migrate to the CNS and play a pathogenic role during autoimmune demyelinating disease. *Blood,* 113**,** 3190-7.

KIVISAKK, P., MAHAD, D. J., CALLAHAN, M. K., SIKORA, K., TREBST, C., TUCKY, B., WUJEK, J., RAVID, R., STAUGAITIS, S. M., LASSMANN, H. & RANSOHOFF, R. M. 2004. Expression of CCR7 in multiple sclerosis: implications for CNS immunity. *Ann Neurol,* 55**,** 627-38.

KLINEOVA, S. & LUBLIN, F. D. 2018. Clinical Course of Multiple Sclerosis. *Cold Spring Harb Perspect Med,* 8**,** a028928.

KORITSCHONER, R. & SCHWEINBURG, F. 1925. Induktion von Paralyse und Rückenmarksentzündung durch Immunisierung von Kaninchen mit menschlichem Rückenmarksgewebe. *Z Immunitätsf Exp Therapie,* 42**,** 217-83.

KRAUS, E. E., KAKUK-ATKINS, L., FARINAS, M. F., JEFFERS, M., LOVETT-RACKE, A. E. & YANG, Y. 2021. Regulation of autoreactive CD4 T cells by FoxO1 signaling in CNS autoimmunity. *J Neuroimmunol,* 359**,** 577675.

KUNKL, M., FRASCOLLA, S., AMORMINO, C., VOLPE, E. & TUOSTO, L. 2020. T Helper Cells: The Modulators of Inflammation in Multiple Sclerosis. *Cells,* 9**,** 482.

KUO, C. T., VESELITS, M. L. & LEIDEN, J. M. 1997. LKLF: A transcriptional regulator of single-positive T cell quiescence and survival. *Science,* 277**,** 1986-90.

KUTZELNIGG, A., LUCCHINETTI, C. F., STADELMANN, C., BRUCK, W., RAUSCHKA, H., BERGMANN, M., SCHMIDBAUER, M., PARISI, J. E. & LASSMANN, H. 2005. Cortical demyelination and diffuse white matter injury in multiple sclerosis. *Brain,* 128**,** 2705-12.

KYRATSOUS, N. I., BAUER, I. J., ZHANG, G., PESIC, M., BARTHOLOMAUS, I., MUES, M., FANG, P., WORNER, M., EVERTS, S., ELLWART, J. W., WATT, J. M., POTTER, B. V. L., HOHLFELD, R., WEKERLE, H. & KAWAKAMI, N. 2017. Visualizing context-dependent calcium signaling in encephalitogenic T cells in vivo by two-photon microscopy. *Proc Natl Acad Sci U S A,* 114**,** E6381-E6389.

LAIDLAW, B. J., GRAY, E. E., ZHANG, Y., RAMÍREZ-VALLE, F. & CYSTER, J. G. 2019. Sphingosine-1-phosphate receptor 2 restrains egress of γδ T cells from the skin. *Journal of Experimental Medicine,* 216**,** 1487-1496.

LÄMMLE, K. F. 2023. *Discovery and validation of essential modules of T cell migration into the central nervous system in a genome-wide CRISPR/Cas9 screening in experimental autoimmune encephalomyelitis.* lmu.

LANG, H. L., JACOBSEN, H., IKEMIZU, S., ANDERSSON, C., HARLOS, K., MADSEN, L., HJORTH, P., SONDERGAARD, L., SVEJGAARD, A., WUCHERPFENNIG, K., STUART, D. I., BELL, J. I., JONES, E. Y. & FUGGER, L. 2002. A functional and structural basis for TCR cross-reactivity in multiple sclerosis. *Nat Immunol,* 3**,** 940-3.

LANGRISH, C. L., CHEN, Y., BLUMENSCHEIN, W. M., MATTSON, J., BASHAM, B., SEDGWICK, J. D., MCCLANAHAN, T., KASTELEIN, R. A. & CUA, D. J. 2005. IL-23 drives a pathogenic T cell population that induces autoimmune inflammation. *The Journal of experimental medicine,* 201**,** 233-240.

LASSMANN, H., BRUCK, W. & LUCCHINETTI, C. F. 2007. The immunopathology of multiple sclerosis: an overview. *Brain Pathol,* 17**,** 210-8.

LAZAREVIĆ, M., STANISAVLJEVIĆ, S., NIKOLOVSKI, N., DIMITRIJEVIĆ, M. & MILJKOVIĆ, Đ. 2024. Complete Freund's adjuvant as a confounding factor in multiple sclerosis research. *Frontiers in Immunology,* 15**,** 1353865.

LEE, J. H., LEE, B. H., JEONG, S., JOH, C. S.-Y., NAM, H. J., CHOI, H. S., SSERWADDA, H., OH, J. W., PARK, C.-G. & JIN, S.-P. 2023. Single-cell RNA sequencing identifies distinct transcriptomic signatures between PMA/ionomycin-and αCD3/αCD28-activated primary human T cells. *Genomics & Informatics,* 21.

LEVIN, L. I., MUNGER, K. L., O'REILLY, E. J., FALK, K. I. & ASCHERIO, A. 2010. Primary infection with the Epstein-Barr virus and risk of multiple sclerosis. *Ann Neurol,* 67**,** 824-30.

LEVINE, S., WENK, E. J., DEVLIN, H. B., PIERONI, R. E. & LEVINE, L. 1966. Hyperacute allergic encephalomyelitis: adjuvant effect of pertussis vaccines and extracts. *J Immunol,* 97**,** 363-8.

LI, W., XU, H., XIAO, T., CONG, L., LOVE, M. I., ZHANG, F., IRIZARRY, R. A., LIU, J. S., BROWN, M. & LIU, X. S. 2014. MAGeCK enables robust identification of essential genes from genome-scale CRISPR/Cas9 knockout screens. *Genome Biol,* 15**,** 554.

LIBBEY, J. E., MCCOY, L. L. & FUJINAMI, R. S. 2007. Molecular mimicry in multiple sclerosis. *Int Rev Neurobiol,* 79**,** 127-47.

LIBLAU, R. S., WONG, F. S., MARS, L. T. & SANTAMARIA, P. 2002. Autoreactive CD8 T cells in organ-specific autoimmunity: emerging targets for therapeutic intervention. *Immunity,* 17**,** 1-6.

LINK, H. & HUANG, Y. M. 2006. Oligoclonal bands in multiple sclerosis cerebrospinal fluid: an update on methodology and clinical usefulness. *J Neuroimmunol,* 180**,** 17-28.

LIU, G., YANG, K., BURNS, S., SHRESTHA, S. & CHI, H. 2010. The S1P(1)-mTOR axis directs the reciprocal differentiation of T(H)1 and T(reg) cells. *Nat Immunol,* 11**,** 1047-56.

LIU, T., ZHANG, L., JOO, D. & SUN, S.-C. 2017. NF-κB signaling in inflammation. *Signal Transduction and Targeted Therapy,* 2**,** 17023.

LLOYD, A. F. & MIRON, V. E. 2019. The pro-remyelination properties of microglia in the central nervous system. *Nat Rev Neurol,* 15**,** 447-458.

LOCK, C., HERMANS, G., PEDOTTI, R., BRENDOLAN, A., SCHADT, E., GARREN, H., LANGER-GOULD, A., STROBER, S., CANNELLA, B., ALLARD, J., KLONOWSKI, P., AUSTIN, A., LAD, N., KAMINSKI, N., GALLI, S. J., OKSENBERG, J. R., RAINE, C. S., HELLER, R. & STEINMAN, L. 2002. Gene-microarray

analysis of multiple sclerosis lesions yields new targets validated in autoimmune encephalomyelitis. *Nature Medicine,* 8**,** 500-508.

LOUVEAU, A., HARRIS, T. H. & KIPNIS, J. 2015. Revisiting the Mechanisms of CNS Immune Privilege. *Trends Immunol,* 36**,** 569-577.

LUMSDEN, C. E. 1970. The neuropathology of multiple sclerosis. *Handbook of clinical neurology,* 9**,** 217.

LUSTER, A. D., ALON, R. & VON ANDRIAN, U. H. 2005. Immune cell migration in inflammation: present and future therapeutic targets. *Nature Immunology,* 6**,** 1182-1190.

MACHADO-SANTOS, J., SAJI, E., TRÖSCHER, A. R., PAUNOVIC, M., LIBLAU, R., GABRIELY, G., BIEN, C. G., BAUER, J. & LASSMANN, H. 2018. The compartmentalized inflammatory response in the multiple sclerosis brain is composed of tissue-resident CD8+ T lymphocytes and B cells. *Brain,* 141**,** 2066-2082.

MACKAY, L. K., BRAUN, A., MACLEOD, B. L., COLLINS, N., TEBARTZ, C., BEDOUI, S., CARBONE, F. R. & GEBHARDT, T. 2015. Cutting edge: CD69 interference with sphingosine-1-phosphate receptor function regulates peripheral T cell retention. *J Immunol,* 194**,** 2059-63.

MAGGI, P., MACRI, S. M., GAITAN, M. I., LEIBOVITCH, E., WHOLER, J. E., KNIGHT, H. L., ELLIS, M., WU, T., SILVA, A. C., MASSACESI, L., JACOBSON, S., WESTMORELAND, S. & REICH, D. S. 2014. The formation of inflammatory demyelinated lesions in cerebral white matter. *Ann Neurol,* 76**,** 594-608.

MAGLIOZZI, R., HOWELL, O. W., REEVES, C., RONCAROLI, F., NICHOLAS, R., SERAFINI, B., ALOISI, F. & REYNOLDS, R. 2010. A Gradient of neuronal loss and meningeal inflammation in multiple sclerosis. *Ann Neurol,* 68**,** 477-93.

MARKOVIC-PLESE, S. 2009. Degenerate T-cell receptor recognition, autoreactive cells, and the autoimmune response in multiple sclerosis. *Neuroscientist,* 15**,** 225-31.

MARKOVIC-PLESE, S., HEMMER, B., ZHAO, Y., SIMON, R., PINILLA, C. & MARTIN, R. 2005. High level of cross-reactivity in influenza virus hemagglutinin-specific CD4+ T-cell response: implications for the initiation of autoimmune response in multiple sclerosis. *J Neuroimmunol,* 169**,** 31-8.

MARRODAN, M., ALESSANDRO, L., FAREZ, M. F. & CORREALE, J. 2019. The role of infections in multiple sclerosis. *Mult Scler,* 25**,** 891-901.

MARTIN-BLONDEL, G., PIGNOLET, B., TIETZ, S., YSHII, L., GEBAUER, C., PERINAT, T., VAN WEDDINGEN, I., BLATTI, C., ENGELHARDT, B. & LIBLAU, R. 2015. Migration of encephalitogenic CD8 T cells into the central nervous system is dependent on the α4β1-integrin. *Eur J Immunol,* 45**,** 3302-12.

MARTÍN, P., GÓMEZ, M., LAMANA, A., CRUZ-ADALIA, A., RAMÍREZ-HUESCA, M., URSA, M. A., YÁÑEZ-MO, M. & SÁNCHEZ-MADRID, F. 2010. CD69 association with Jak3/Stat5 proteins regulates Th17 cell differentiation. *Mol Cell Biol,* 30**,** 4877-89.

MASON, D. 1998. A very high level of crossreactivity is an essential feature of the T-cell receptor. *Immunology today,* 19**,** 395-404.

MASOPUST, D. & SCHENKEL, J. M. 2013. The integration of T cell migration, differentiation and function. *Nat Rev Immunol,* 13**,** 309-20.

MATLOUBIAN, M., LO, C. G., CINAMON, G., LESNESKI, M. J., XU, Y., BRINKMANN, V., ALLENDE, M. L., PROIA, R. L. & CYSTER, J. G. 2004. Lymphocyte egress from thymus and peripheral lymphoid organs is dependent on S1P receptor 1. *Nature,* 427**,** 355-360.

MCKENZIE, B. S., KASTELEIN, R. A. & CUA, D. J. 2006. Understanding the IL-23-IL-17 immune pathway. *Trends Immunol,* 27**,** 17-23.

MCRAE, B. L., KENNEDY, M. K., TAN, L. J., DAL CANTO, M. C., PICHA, K. S. & MILLER, S. D. 1992. Induction of active and adoptive relapsing experimental autoimmune encephalomyelitis (EAE) using an encephalitogenic epitope of proteolipid protein. *J Neuroimmunol,* 38**,** 229-40.

MEDANA, I., MARTINIC, M. A., WEKERLE, H. & NEUMANN, H. 2001. Transection of major histocompatibility complex class I-induced neurites by cytotoxic T lymphocytes. *Am J Pathol,* 159**,** 809-15.

MEDANA, I. M., GALLIMORE, A., OXENIUS, A., MARTINIC, M. M., WEKERLE, H. & NEUMANN, H. 2000. MHC class I‐restricted killing of neurons by virus‐specific CD8+ T lymphocytes is effected through the Fas/FasL, but not the perforin pathway. *European journal of immunology,* 30**,** 3623-3633.

MEDAWAR, P. 1948. Immunity to homologous grafted skin. III. The fate of skin homographs transplanted to the brain, to subcutaneous tissue, and to the anterior chamber of the eye. *British journal of experimental pathology,* 29**,** 58.

MESRI, M., LIVERSIDGE, J. & FORRESTER, J. V. 1994. ICAM-1/LFA-1 interactions in T-lymphocyte activation and adhesion to cells of the blood-retina barrier in the rat. *Immunology,* 83**,** 52-7.

MICHEL, L., TOUIL, H., PIKOR, N. B., GOMMERMAN, J. L., PRAT, A. & BAR-OR, A. 2015. B Cells in the Multiple Sclerosis Central Nervous System: Trafficking and Contribution to CNS-Compartmentalized Inflammation. *Front Immunol,* 6**,** 636.

MISHRA, M. K. & YONG, V. W. 2016. Myeloid cells - targets of medication in multiple sclerosis. *Nat Rev Neurol,* 12**,** 539-51.

MIYAUCHI, E., KIM, S. W., SUDA, W., KAWASUMI, M., ONAWA, S., TAGUCHI-ATARASHI, N., MORITA, H., TAYLOR, T. D., HATTORI, M. & OHNO, H. 2020. Gut microorganisms act together to exacerbate inflammation in spinal cords. *Nature,* 585**,** 102-106.

MIZUGUCHI, M., HARA, T., YOSHITA-TAKAHASHI, M., KOHDA, T., TANAKA, Y. & NAKAMURA, M. 2021. Promoter CpG methylation inhibits Kruppel-like factor 2 (KLF2)-Mediated repression of hTERT gene expression in human T-cells. *Biochem Biophys Rep,* 26**,** 100984.

MOSSAKOWSKI, A. A., POHLAN, J., BREMER, D., LINDQUIST, R., MILLWARD, J. M., BOCK, M., POLLOK, K., MOTHES, R., VIOHL, L., RADBRUCH, M., GERHARD, J., BELLMANN-STROBL, J., BEHRENS, J., INFANTE-DUARTE, C., MAHLER, A., BOSCHMANN, M., RINNENTHAL, J. L., FUCHTEMEIER, M., HERZ, J., PACHE, F. C., BARDUA, M., PRILLER, J., HAUSER, A. E., PAUL, F., NIESNER, R. & RADBRUCH, H. 2015. Tracking CNS and systemic sources of oxidative stress during the course of chronic neuroinflammation. *Acta Neuropathol,* 130**,** 799-814.

MUNDT, S., MRDJEN, D., UTZ, S. G., GRETER, M., SCHREINER, B. & BECHER, B. 2019. Conventional DCs sample and present myelin antigens in the healthy CNS and allow parenchymal T cell entry to initiate neuroinflammation. *Sci Immunol,* 4**,** eaau8380.

MUNGER, K. L., LEVIN, L. I., HOLLIS, B. W., HOWARD, N. S. & ASCHERIO, A. 2006. Serum 25-hydroxyvitamin D levels and risk of multiple sclerosis. *JAMA,* 296**,** 2832-8.

MUNGER, K. L., ZHANG, S. M., O'REILLY, E., HERNAN, M. A., OLEK, M. J., WILLETT, W. C. & ASCHERIO, A. 2004. Vitamin D intake and incidence of multiple sclerosis. *Neurology,* 62**,** 60-5.

MURPHY, K. M., OUYANG, W., SZABO, S. J., JACOBSON, N. G., GULER, M. L., GORHAM, J. D., GUBLER, U. & MURPHY, T. L. 1999. T helper differentiation proceeds through Stat1-dependent, Stat4-dependent and Stat4-independent phases. *Curr Top Microbiol Immunol,* 238**,** 13-26.

MURRAY, P. J., ALLEN, J. E., BISWAS, S. K., FISHER, E. A., GILROY, D. W., GOERDT, S., GORDON, S., HAMILTON, J. A., IVASHKIV, L. B., LAWRENCE, T., LOCATI, M., MANTOVANI, A., MARTINEZ, F. O., MEGE, J. L., MOSSER, D. M., NATOLI, G., SAEIJ, J. P., SCHULTZE, J. L., SHIREY, K. A., SICA, A., SUTTLES, J., UDALOVA, I., VAN GINDERACHTER, J. A., VOGEL, S. N. & WYNN, T. A. 2014. Macrophage activation and polarization: nomenclature and experimental guidelines. *Immunity,* 41**,** 14-20.

NAKAJIMA, A., NEGISHI, N., TSURUI, H., KADOWAKI-OHTSUJI, N., MAEDA, K., NANNO, M., YAMAGUCHI, Y., SHIMIZU, N., YAGITA, H., OKUMURA, K. & HABU, S. 2014. Commensal bacteria regulate thymic Aire expression. *PLoS One,* 9**,** e105904.

NALAWADE, S. A., JI, N., KRAIG, E. & FORSTHUBER, T. 2018. Aire is not essential for regulating autoimmune pathology in mice transgenic for human autoimmune-disease associated MHC class II genes HLA-DR2b and HLA-DR4. *The Journal of Immunology,* 200**,** 167.8-167.8.

NALBANT, A. 2019. IL-17, IL-21, and IL-22 Cytokines of T Helper 17 Cells in Cancer. *J Interferon Cytokine Res,* 39**,** 56-60.

NATH, N., PRASAD, R., GIRI, S., SINGH, A. K. & SINGH, I. 2006. T-bet is essential for the progression of experimental autoimmune encephalomyelitis. *Immunology,* 118**,** 384-91.

NELSON, B. H. & WILLERFORD, D. M. 1998. Biology of the interleukin-2 receptor. *Adv Immunol,* 70**,** 1-81.

NEUMANN, H., MEDANA, I. M., BAUER, J. & LASSMANN, H. 2002. Cytotoxic T lymphocytes in autoimmune and degenerative CNS diseases. *Trends Neurosci,* 25**,** 313-9.

NGONO, A. E., PETTRÉ, S., SALOU, M., BAHBOUHI, B., SOULILLOU, J.-P., BROUARD, S. & LAPLAUD, D.-A. 2012. Frequency of circulating autoreactive T cells committed to myelin determinants in relapsing–remitting multiple sclerosis patients. *Clinical immunology,* 144**,** 117-126.

NI, D., TAN, J., ROBERT, R., TAITZ, J., GE, A., POTIER-VILLETTE, C., REYES, J. G. A., SPITERI, A., WISHART, C., MACKAY, C., PICCIO, L., KING, N. J. C. & MACIA, L. 2023. GPR109A expressed on medullary thymic epithelial cells affects thymic Treg development. *Eur J Immunol,* 53**,** e2350521.

NIKIC, I., MERKLER, D., SORBARA, C., BRINKOETTER, M., KREUTZFELDT, M., BAREYRE, F. M., BRUCK, W., BISHOP, D., MISGELD, T. & KERSCHENSTEINER, M. 2011. A reversible form of axon damage in experimental autoimmune encephalomyelitis and multiple sclerosis. *Nat Med,* 17**,** 495-9.

NISHIHARA, H., SOLDATI, S., MOSSU, A., ROSITO, M., RUDOLPH, H., MULLER, W. A., LATORRE, D., SALLUSTO, F., SOSPEDRA, M., MARTIN, R., ISHIKAWA, H., TENENBAUM, T., SCHROTEN, H., GOSSELET, F. & ENGELHARDT, B. 2020. Human CD4+ T cell subsets differ in their abilities to cross endothelial and epithelial brain barriers in vitro. *Fluids and Barriers of the CNS,* 17**,** 3.

NUTTALL, R. K., SILVA, C., HADER, W., BAR‐OR, A., PATEL, K. D., EDWARDS, D. R. & YONG, V. W. 2007. Metalloproteinases are enriched in microglia compared with leukocytes and they regulate cytokine levels in activated microglia. *Glia,* 55**,** 516-526.

O'CONNOR, R. A., PRENDERGAST, C. T., SABATOS, C. A., LAU, C. W., LEECH, M. D., WRAITH, D. C. & ANDERTON, S. M. 2008. Cutting edge: Th1 cells facilitate the entry of Th17 cells to the central nervous system during experimental autoimmune encephalomyelitis. *J Immunol,* 181**,** 3750-4.

OBERMEIER, B., MENTELE, R., MALOTKA, J., KELLERMANN, J., KUMPFEL, T., WEKERLE, H., LOTTSPEICH, F., HOHLFELD, R. & DORNMAIR, K. 2008. Matching of oligoclonal immunoglobulin transcriptomes and proteomes of cerebrospinal fluid in multiple sclerosis. *Nat Med,* 14**,** 688-93.

ODOARDI, F., SIE, C., STREYL, K., ULAGANATHAN, V. K., SCHLAGER, C., LODYGIN, D., HECKELSMILLER, K., NIETFELD, W., ELLWART, J., KLINKERT, W. E., LOTTAZ, C., NOSOV, M., BRINKMANN, V., SPANG, R., LEHRACH, H., VINGRON, M., WEKERLE, H., FLUGEL-KOCH, C. & FLUGEL, A. 2012. T cells become licensed in the lung to enter the central nervous system. *Nature,* 488**,** 675-9.

OISHI, Y. & MANABE, I. 2018. Kruppel-Like Factors in Metabolic Homeostasis and Cardiometabolic Disease. *Front Cardiovasc Med,* 5**,** 69.

OKADA, T. & CYSTER, J. G. 2007. CC chemokine receptor 7 contributes to Gi-dependent T cell motility in the lymph node. *J Immunol,* 178**,** 2973-8.

OKADA, T., NGO, V. N., EKLAND, E. H., FORSTER, R., LIPP, M., LITTMAN, D. R. & CYSTER, J. G. 2002. Chemokine requirements for B cell entry to lymph nodes and Peyer's patches. *J Exp Med,* 196**,** 65-75.

OLSSON, T., BARCELLOS, L. F. & ALFREDSSON, L. 2017. Interactions between genetic, lifestyle and environmental risk factors for multiple sclerosis. *Nat Rev Neurol,* 13**,** 25-36.

PANACKEL, C., MATHEW, J. F., FAWAS, N. M. & JACOB, M. 2022. Immunosuppressive Drugs in Liver Transplant: An Insight. *J Clin Exp Hepatol,* 12**,** 1557-1571.

PANITCH, H. 1980. Adoptive transfer of EAE with activated spleen cells: comparison of in vitro activation by concavalin A and myelin basic protein. *Cell Immunol,* 56**,** 163-171.

PARONI, M., MALTESE, V., DE SIMONE, M., RANZANI, V., LARGHI, P., FENOGLIO, C., PIETROBONI, A. M., MILENA, A., CROSTI, M. C. & MAGLIE, S. 2017. Recognition of viral and self-antigens by TH1 and TH1/TH17 central memory cells in patients with multiple sclerosis reveals distinct

roles in immune surveillance and relapses. *Journal of Allergy and Clinical Immunology,* 140**,** 797-808.

PENDER, M. P. & GREER, J. M. 2007. Immunology of multiple sclerosis. *Curr Allergy Asthma Rep,* 7**,** 285-92.

PENG, S. L. 2008. Foxo in the immune system. *Oncogene,* 27**,** 2337-44.

PENNA, G. & ADORINI, L. 2000. 1α, 25-dihydroxyvitamin D3 inhibits differentiation, maturation, activation, and survival of dendritic cells leading to impaired alloreactive T cell activation. *The Journal of Immunology,* 164**,** 2405-2411.

PERRY, J. S. A., LIO, C. J., KAU, A. L., NUTSCH, K., YANG, Z., GORDON, J. I., MURPHY, K. M. & HSIEH, C. S. 2014. Distinct contributions of Aire and antigen-presenting-cell subsets to the generation of self-tolerance in the thymus. *Immunity,* 41**,** 414-426.

PESCE, B., RIBEIRO, C. H., LARRONDO, M., RAMOS, V., SOTO, L., CATALÁN, D. & AGUILLÓN, J. C. 2022. TNF-α Affects Signature Cytokines of Th1 and Th17 T Cell Subsets through Differential Actions on TNFR1 and TNFR2. *Int J Mol Sci,* 23.

PESIC, M., BARTHOLOMAUS, I., KYRATSOUS, N. I., HEISSMEYER, V., WEKERLE, H. & KAWAKAMI, N. 2013. 2-photon imaging of phagocyte-mediated T cell activation in the CNS. *J Clin Invest,* 123**,** 1192-201.

PETERS, B. A. & HINRICHS, D. J. 1982. Passive transfer of experimental allergic encephalomyelitis in the Lewis rat with activated spleen cells: differential activation with mitogens. *Cell Immunol,* 69**,** 175-85.

PHAM, T. H., OKADA, T., MATLOUBIAN, M., LO, C. G. & CYSTER, J. G. 2008. S1P1 receptor signaling overrides retention mediated by G alpha i-coupled receptors to promote T cell egress. *Immunity,* 28**,** 122-33.

POLITIS, M., GIANNETTI, P., SU, P., TURKHEIMER, F., KEIHANINEJAD, S., WU, K., WALDMAN, A., MALIK, O., MATTHEWS, P. M., REYNOLDS, R., NICHOLAS, R. & PICCINI, P. 2012. Increased PK11195 PET binding in the cortex of patients with MS correlates with disability. *Neurology,* 79**,** 523-30.

POLLAK, N. M., HOFFMAN, M., GOLDBERG, I. J. & DROSATOS, K. 2018. Kruppel-like factors: Crippling and un-crippling metabolic pathways. *JACC Basic Transl Sci,* 3**,** 132-156.

PORTER, J. C. & HALL, A. 2009. Epithelial ICAM-1 and ICAM-2 regulate the egression of human T cells across the bronchial epithelium. *Faseb j,* 23**,** 492-502.

PRESTON, G. C., FEIJOO-CARNERO, C., SCHURCH, N., COWLING, V. H. & CANTRELL, D. A. 2013. The impact of KLF2 modulation on the transcriptional program and function of CD8 T cells. *PLoS One,* 8**,** e77537.

PRICEMAN, S. J., SHEN, S., WANG, L., DENG, J., YUE, C., KUJAWSKI, M. & YU, H. 2014. S1PR1 is crucial for accumulation of regulatory T cells in tumors via STAT3. *Cell Rep,* 6**,** 992-999.

PRINZ, M., JUNG, S. & PRILLER, J. 2019. Microglia Biology: One Century of Evolving Concepts. *Cell,* 179**,** 292-311.

RABACAL, W., PABBISETTY, S. K., HOEK, K. L., CENDRON, D., GUO, Y., MASEDA, D. & SEBZDA, E. 2016. Transcription factor KLF2 regulates homeostatic NK cell proliferation and survival. *Proc Natl Acad Sci U S A,* 113**,** 5370-5.

RANGACHARI, M. & KUCHROO, V. K. 2013. Using EAE to better understand principles of immune function and autoimmune pathology. *J Autoimmun,* 45**,** 31-9.

REDMOND, W. L., RUBY, C. E. & WEINBERG, A. D. 2009. The role of OX40-mediated co-stimulation in T-cell activation and survival. *Crit Rev Immunol,* 29**,** 187-201.

RIVERS, T. M., SPRUNT, D. H. & BERRY, G. P. 1933. Observations on Attempts to Produce Acute Disseminated Encephalomyelitis in Monkeys. *J Exp Med,* 58**,** 39-53.

ROBINSON, A. P., HARP, C. T., NORONHA, A. & MILLER, S. D. 2014. The experimental autoimmune encephalomyelitis (EAE) model of MS: utility for understanding disease pathophysiology and treatment. *Handb Clin Neurol,* 122**,** 173-89.

ROBINSON, W. H. & STEINMAN, L. 2022. Epstein-Barr virus and multiple sclerosis. *Science,* 375**,** 264-265.

ROCCA, M. A., PREZIOSA, P., BARKHOF, F., BROWNLEE, W., CALABRESE, M., DE STEFANO, N., GRANZIERA, C., ROPELE, S., TOOSY, A. T., VIDAL-JORDANA, À., DI FILIPPO, M. & FILIPPI, M. 2024. Current and future role of MRI in the diagnosis and prognosis of multiple sclerosis. *The Lancet Regional Health - Europe,* 44**,** 100978.

ROGERS, P. R., SONG, J., GRAMAGLIA, I., KILLEEN, N. & CROFT, M. 2001. OX40 promotes Bcl-xL and Bcl-2 expression and is essential for long-term survival of CD4 T cells. *Immunity,* 15**,** 445-55.

ROMAGNANI, S., MAGGI, E., LIOTTA, F., COSMI, L. & ANNUNZIATO, F. 2009. Properties and origin of human Th17 cells. *Mol Immunol,* 47**,** 3-7.

ROSEN, Y., DAICH, J., SOLIMAN, I., BRATHWAITE, E. & SHOENFELD, Y. 2016. Vitamin D and autoimmunity. *Scand J Rheumatol,* 45**,** 439-447.

SAKAGUCHI, S., WING, K. & MIYARA, M. 2007. Regulatory T cells - a brief history and perspective. *Eur J Immunol,* 37 Suppl 1**,** S116-23.

SALEEM, S., ANWAR, A., FAYYAZ, M., ANWER, F. & ANWAR, F. 2019. An Overview of Therapeutic Options in Relapsing-remitting Multiple Sclerosis. *Cureus,* 11**,** e5246.

SALEMI, G., CALLARI, G., GAMMINO, M., BATTAGLIERI, F., CAMMARATA, E., CUCCIA, G., D'AMELIO, M., LUPO, I., RAGONESE, P. & SAVETTIERI, G. 2004. The relapse rate of multiple sclerosis changes during pregnancy: a cohort study. *Acta Neurol Scand,* 110**,** 23-6.

SALOU, M., NICOL, B., GARCIA, A. & LAPLAUD, D. A. 2015. Involvement of CD8(+) T Cells in Multiple Sclerosis. *Front Immunol,* 6**,** 604.

SANCHEZ-RAMON, S., NAVARRO, A. J., ARISTIMUNO, C., RODRIGUEZ-MAHOU, M., BELLON, J. M., FERNANDEZ-CRUZ, E. & DE ANDRES, C. 2005. Pregnancy-induced expansion of regulatory T-lymphocytes may mediate protection to multiple sclerosis activity. *Immunol Lett,* 96**,** 195-201.

SASAKI, K., BEAN, A., SHAH, S., SCHUTTEN, E., HUSEBY, P. G., PETERS, B., SHEN, Z. T., VANGURI, V., LIGGITT, D. & HUSEBY, E. S. 2014. Relapsing-remitting central nervous system autoimmunity mediated by GFAP-specific CD8 T cells. *J Immunol,* 192**,** 3029-42.

SASAKI, T., TOME, S. & TAKEI, Y. 2020. Intraventricular IL-17A administration activates microglia and alters their localization in the mouse embryo cerebral cortex. *Molecular Brain,* 13**,** 93.

SATO, S., KAWANO, T., IKE, E., TAKAHASHI, K., SAKURAI, J., MIYASAKA, T., MIYAUCHI, Y., ISHIZAWA, F., TAKAYANAGI, M. & TAKAHASHI, T. 2023. IL-1β Derived Th17 Immune Responses Are a Critical Factor for Neutrophilic-Eosinophilic Airway Inflammation on Psychological Stress-Induced Immune Tolerance Breakdown in Mice. *Int Arch Allergy Immunol,* 184**,** 797-807.

SAWCER, S., FRANKLIN, R. J. & BAN, M. 2014. Multiple sclerosis genetics. *Lancet Neurol,* 13**,** 700-9.

SCALFARI, A., NEUHAUS, A., DEGENHARDT, A., RICE, G. P., MURARO, P. A., DAUMER, M. & EBERS, G. C. 2010. The natural history of multiple sclerosis: a geographically based study 10: relapses and long-term disability. *Brain,* 133**,** 1914-29.

SCHAFFLICK, D., XU, C. A., HARTLEHNERT, M., COLE, M., SCHULTE-MECKLENBECK, A., LAUTWEIN, T., WOLBERT, J., HEMING, M., MEUTH, S. G., KUHLMANN, T., GROSS, C. C., WIENDL, H., YOSEF, N. & MEYER ZU HORSTE, G. 2020. Integrated single cell analysis of blood and cerebrospinal fluid leukocytes in multiple sclerosis. *Nat Commun,* 11**,** 247.

SCHLÄGER, C., KÖRNER, H., KRUEGER, M., VIDOLI, S., HABERL, M., MIELKE, D., BRYLLA, E., ISSEKUTZ, T., CABAÑAS, C., NELSON, P. J., ZIEMSSEN, T., ROHDE, V., BECHMANN, I., LODYGIN, D., ODOARDI, F. & FLÜGEL, A. 2016. Effector T-cell trafficking between the leptomeninges and the cerebrospinal fluid. *Nature,* 530**,** 349-53.

SCHUERWEGH, A. J., STEVENS, W. J., BRIDTS, C. H. & DE CLERCK, L. S. 2001. Evaluation of monensin and brefeldin A for flow cytometric determination of interleukin-1 beta, interleukin-6, and tumor necrosis factor-alpha in monocytes. *Cytometry,* 46**,** 172-6.

SCIMONE, M. L., FELBINGER, T. W., MAZO, I. B., STEIN, J. V., VON ANDRIAN, U. H. & WENINGER, W. 2004. CXCL12 mediates CCR7-independent homing of central memory cells, but not naive T cells, in peripheral lymph nodes. *J Exp Med,* 199**,** 1113-20.

SENBANERJEE, S., LIN, Z., ATKINS, G. B., GREIF, D. M., RAO, R. M., KUMAR, A., FEINBERG, M. W., CHEN, Z., SIMON, D. I., LUSCINSKAS, F. W., MICHEL, T. M., GIMBRONE, M. A., JR., GARCÍA-CARDEÑA,

G. & JAIN, M. K. 2004. KLF2 Is a novel transcriptional regulator of endothelial proinflammatory activation. *J Exp Med,* 199**,** 1305-15.

SERAFINI, B., ROSICARELLI, B., MAGLIOZZI, R., STIGLIANO, E. & ALOISI, F. 2004. Detection of ectopic B-cell follicles with germinal centers in the meninges of patients with secondary progressive multiple sclerosis. *Brain Pathol,* 14**,** 164-74.

SHARMA, N., BENECHET, A. P., LEFRANÇOIS, L. & KHANNA, K. M. 2015. CD8 T Cells Enter the Splenic T Cell Zones Independently of CCR7, but the Subsequent Expansion and Trafficking Patterns of Effector T Cells after Infection Are Dysregulated in the Absence of CCR7 Migratory Cues. *J Immunol,* 195**,** 5227-36.

SHATROVA, A. N., MITYUSHOVA, E. V., VASSILIEVA, I. O., AKSENOV, N. D., ZENIN, V. V., NIKOLSKY, N. N. & MARAKHOVA, II 2016. Time-Dependent Regulation of IL-2R α-Chain (CD25) Expression by TCR Signal Strength and IL-2-Induced STAT5 Signaling in Activated Human Blood T Lymphocytes. *PLoS One,* 11**,** e0167215.

SHEPPARD, K. A., ROSE, D. W., HAQUE, Z. K., KUROKAWA, R., MCINERNEY, E., WESTIN, S., THANOS, D., ROSENFELD, M. G., GLASS, C. K. & COLLINS, T. 1999. Transcriptional activation by NF-kappaB requires multiple coactivators. *Mol Cell Biol,* 19**,** 6367-78.

SHI, H. & SHAO, B. 2023. LFA-1 Activation in T-Cell Migration and Immunological Synapse Formation. *Cells,* 12.

SHIOW, L. R., ROSEN, D. B., BRDICKOVÁ, N., XU, Y., AN, J., LANIER, L. L., CYSTER, J. G. & MATLOUBIAN, M. 2006. CD69 acts downstream of interferon-alpha/beta to inhibit S1P1 and lymphocyte egress from lymphoid organs. *Nature,* 440**,** 540-4.

SHIRAI, Y. 1921. On the transplantation of the rat sarcoma in adult heterogenous animals. *Jap Med World,* 1**,** 14-15.

SONG, C. Z., KELLER, K., MURATA, K., ASANO, H. & STAMATOYANNOPOULOS, G. 2002. Functional interaction between coactivators CBP/p300, PCAF, and transcription factor FKLF2. *J Biol Chem,* 277**,** 7029-36.

SOSPEDRA, M. & MARTIN, R. 2005. Immunology of multiple sclerosis. *Annu Rev Immunol,* 23**,** 683-747.

STAHL, M., DIJKERS, P. F., KOPS, G. J., LENS, S. M., COFFER, P. J., BURGERING, B. M. & MEDEMA, R. H. 2002. The forkhead transcription factor FoxO regulates transcription of p27Kip1 and Bim in response to IL-2. *J Immunol,* 168**,** 5024-31.

STRACHAN-WHALEY, M., RIVEST, S. & YONG, V. W. 2014. Interactions between microglia and T cells in multiple sclerosis pathobiology. *Journal of Interferon & Cytokine Research,* 34**,** 615-622.

STRITESKY, G. L., YEH, N. & KAPLAN, M. H. 2008. IL-23 promotes maintenance but not commitment to the Th17 lineage. *J Immunol,* 181**,** 5948-55.

STROMNES, I. M. & GOVERMAN, J. M. 2006. Active induction of experimental allergic encephalomyelitis. *Nat Protoc,* 1**,** 1810-9.

STUBBS, L., SUN, Y. & CAETANO-ANOLLES, D. 2011. Function and Evolution of C2H2 Zinc Finger Arrays. *Subcell Biochem,* 52**,** 75-94.

STUVE, O., MARRA, C. M., BAR-OR, A., NIINO, M., CRAVENS, P. D., CEPOK, S., FROHMAN, E. M., PHILLIPS, J. T., ARENDT, G., JEROME, K. R., COOK, L., GRAND'MAISON, F., HEMMER, B., MONSON, N. L. & RACKE, M. K. 2006. Altered CD4+/CD8+ T-cell ratios in cerebrospinal fluid of natalizumab-treated patients with multiple sclerosis. *Arch Neurol,* 63**,** 1383-7.

SUN, D., WHITAKER, J. N., HUANG, Z., LIU, D., COLECLOUGH, C., WEKERLE, H. & RAINE, C. S. 2001. Myelin antigen-specific CD8+ T cells are encephalitogenic and produce severe disease in C57BL/6 mice. *J Immunol,* 166**,** 7579-87.

TAKADA, K., WANG, X., HART, G. T., ODUMADE, O. A., WEINREICH, M. A., HOGQUIST, K. A. & JAMESON, S. C. 2011. Kruppel-like factor 2 is required for trafficking but not quiescence in postactivated T cells. *The Journal of Immunology,* 186**,** 775-783.

TAKENAKA, A., MINEGAWA, H., KANEKA, K., MORI, R. & ITOYAMA, Y. 1986. Adoptive transfer of EAE with lectin activated spleen cells, part 2. Studies on T-cell subsets and interleukin 2 production. *J Neurol Sci,* 72**,** 337-345.

TAKEUCHI, H., JIN, S., WANG, J., ZHANG, G., KAWANOKUCHI, J., KUNO, R., SONOBE, Y., MIZUNO, T. & SUZUMURA, A. 2006. Tumor necrosis factor-alpha induces neurotoxicity via glutamate release from hemichannels of activated microglia in an autocrine manner. *J Biol Chem,* 281**,** 21362-21368.

TEJERA-ALHAMBRA, M., FERNÁNDEZ-PAREDES, L., DE ANDRÉS, C. & SÁNCHEZ-RAMÓN, S. 2016. Multiple Sclerosis: Where do we go from here. *EMJ Neurol,* 4**,** 84-95.

THOMANN, A. S., MCQUADE, C. A., PINJUŠIĆ, K., KOLZ, A., SCHMITZ, R., KITAMURA, D., WEKERLE, H. & PETERS, A. 2023. AB cell–driven EAE mouse model reveals the impact of B cell–derived cytokines on CNS autoimmunity. *Proceedings of the National Academy of Sciences,* 120**,** e2300733120.

THOMPSON, A. J., BANWELL, B. L., BARKHOF, F., CARROLL, W. M., COETZEE, T., COMI, G., CORREALE, J., FAZEKAS, F., FILIPPI, M., FREEDMAN, M. S., FUJIHARA, K., GALETTA, S. L., HARTUNG, H. P., KAPPOS, L., LUBLIN, F. D., MARRIE, R. A., MILLER, A. E., MILLER, D. H., MONTALBAN, X., MOWRY, E. M., SORENSEN, P. S., TINTORE, M., TRABOULSEE, A. L., TROJANO, M., UITDEHAAG, B. M. J., VUKUSIC, S., WAUBANT, E., WEINSHENKER, B. G., REINGOLD, S. C. & COHEN, J. A. 2018a. Diagnosis of multiple sclerosis: 2017 revisions of the McDonald criteria. *Lancet Neurol,* 17**,** 162-173.

THOMPSON, A. J., BARANZINI, S. E., GEURTS, J., HEMMER, B. & CICCARELLI, O. 2018b. Multiple sclerosis. *Lancet,* 391**,** 1622-1636.

TIAN, J., CHEN, J., SUN, Q., HUANG, T., XU, H., WANG, J. & MA, Z. 2024. Effects of the S1P/S1PR1 Signaling Pathway on High Glucose-Induced NRK-52E Epithelial-Mesenchymal Transition Via Regulation of ROS/NLRP3. *Inflammation*.

TILNEY, N. L. 1971. Patterns of lymphatic drainage in the adult laboratory rat. *J Anat,* 109**,** 369-83.

TOMPKINS, S. M., PADILLA, J., DAL CANTO, M. C., TING, J. P.-Y., VAN KAER, L. & MILLER, S. D. 2002. De novo central nervous system processing of myelin antigen is required for the initiation of experimental autoimmune encephalomyelitis. *The Journal of Immunology,* 168**,** 4173-4183.

TSUNODA, I., KUANG, L. Q., THEIL, D. J. & FUJINAMI, R. S. 2000. Antibody association with a novel model for primary progressive multiple sclerosis: induction of relapsing-remitting and progressive forms of EAE in H2s mouse strains. *Brain Pathol,* 10**,** 402-18.

TUOHY, V. K., LU, Z., SOBEL, R. A., LAURSEN, R. A. & LEES, M. B. 1989. Identification of an encephalitogenic determinant of myelin proteolipid protein for SJL mice. *J Immunol,* 142**,** 1523-7.

TURNER, J. & CROSSLEY, M. 1999. Mammalian Krüppel-like transcription factors: more than just a pretty finger. *Trends in biochemical sciences,* 24**,** 236-240.

TURPAEV, K. T. 2020. Transcription Factor KLF2 and Its Role in the Regulation of Inflammatory Processes. *Biochemistry (Mosc),* 85**,** 54-67.

UEDA, P., RAFATNIA, F., BAARNHIELM, M., FROBOM, R., KORZUNOWICZ, G., LONNERBRO, R., HEDSTROM, A. K., EYLES, D., OLSSON, T. & ALFREDSSON, L. 2014. Neonatal vitamin D status and risk of multiple sclerosis. *Ann Neurol,* 76**,** 338-46.

ULVESTAD, E., WILLIAMS, K., VEDELER, C., ANTEL, J., NYLAND, H., MØRK, S. & MATRE, R. 1994. Reactive microglia in multiple sclerosis lesions have an increased expression of receptors for the Fc part of IgG. *Journal of the neurological sciences,* 121**,** 125-131.

VAJKOCZY, P., LASCHINGER, M. & ENGELHARDT, B. 2001. Alpha4-integrin-VCAM-1 binding mediates G protein-independent capture of encephalitogenic T cell blasts to CNS white matter microvessels. *J Clin Invest,* 108**,** 557-65.

VALLITTU, A.-M., SARASTE, M. & AIRAS, L. 2007. CCR7 expression on peripheral blood lymphocytes is up-regulated following treatment of multiple sclerosis with interferon-beta. *Neurological research,* 29**,** 763-766.

VAN DER MEI, I. A., PONSONBY, A. L., DWYER, T., BLIZZARD, L., SIMMONS, R., TAYLOR, B. V., BUTZKUEVEN, H. & KILPATRICK, T. 2003. Past exposure to sun, skin phenotype, and risk of multiple sclerosis: case-control study. *BMJ,* 327**,** 316.

VAN HORSSEN, J., WITTE, M. E., SCHREIBELT, G. & DE VRIES, H. E. 2011. Radical changes in multiple sclerosis pathogenesis. *Biochim Biophys Acta,* 1812**,** 141-50.

VENTURI, G. M., TU, L., KADONO, T., KHAN, A. I., FUJIMOTO, Y., OSHEL, P., BOCK, C. B., MILLER, A. S., ALBRECHT, R. M., KUBES, P., STEEBER, D. A. & TEDDER, T. F. 2003. Leukocyte migration is regulated by L-selectin endoproteolytic release. *Immunity,* 19**,** 713-24.

VOSKUHL, R. R., MARTIN, R., BERGMAN, C., DALAL, M., RUDDLE, N. H. & MCFARLAND, H. F. 1993. T Helper 1 (TH1) Functional Phenotype of Human Myelin Basic Protein-Specific T Lymphocytes. *Autoimmunity,* 15**,** 137-143.

WALDNER, H., WHITTERS, M. J., SOBEL, R. A., COLLINS, M. & KUCHROO, V. K. 2000. Fulminant spontaneous autoimmunity of the central nervous system in mice transgenic for the myelin proteolipid protein-specific T cell receptor. *Proc Natl Acad Sci U S A,* 97**,** 3412-7.

WALLIN, M. T., CULPEPPER, W. J., CAMPBELL, J. D., NELSON, L. M., LANGER-GOULD, A., MARRIE, R. A., CUTTER, G. R., KAYE, W. E., WAGNER, L., TREMLETT, H., BUKA, S. L., DILOKTHORNSAKUL, P., TOPOL, B., CHEN, L. H., LAROCCA, N. G. & WORKGROUP, U. S. M. S. P. 2019. The prevalence of MS in the United States: A population-based estimate using health claims data. *Neurology,* 92**,** e1029-e1040.

WANG, C., ZHANG, C.-J., MARTIN, B. N., BULEK, K., KANG, Z., ZHAO, J., BIAN, G., CARMAN, J. A., GAO, J., DONGRE, A., XUE, H., MILLER, S. D., QIAN, Y., HAMBARDZUMYAN, D., HAMILTON, T., RANSOHOFF, R. M. & LI, X. 2017. IL-17 induced NOTCH1 activation in oligodendrocyte progenitor cells enhances proliferation and inflammatory gene expression. *Nature Communications,* 8**,** 15508.

WANG, Y., KAI, H., CHANG, F., SHIBATA, K., TAHARA-HANAOKA, S., HONDA, S., SHIBUYA, A. & SHIBUYA, K. 2007. A critical role of LFA-1 in the development of Th17 cells and induction of experimental autoimmune encephalomyelytis. *Biochem Biophys Res Commun,* 353**,** 857-62.

WASCHBISCH, A., SCHRODER, S., SCHRAUDNER, D., SAMMET, L., WEKSLER, B., MELMS, A., PFEIFENBRING, S., STADELMANN, C., SCHWAB, S. & LINKER, R. A. 2016. Pivotal Role for CD16+ Monocytes in Immune Surveillance of the Central Nervous System. *J Immunol,* 196**,** 1558-67.

WEINREICH, M. A., TAKADA, K., SKON, C., REINER, S. L., JAMESON, S. C. & HOGQUIST, K. A. 2009a. KLF2 deficiency in T cells results in unrestrained cytokine production and bystander chemokine receptor upregulation. *Immunity,* 31**,** 122.

WEINREICH, M. A., TAKADA, K., SKON, C., REINER, S. L., JAMESON, S. C. & HOGQUIST, K. A. 2009b. KLF2 Transcription-Factor Deficiency in T Cells Results in Unrestrained Cytokine Production and Upregulation of Bystander Chemokine Receptors. *Immunity,* 31**,** 122-130.

WEKERLE, H., LININGTON, C., LASSMANN, H. & MEYERMANN, R. 1986. Cellular immune reactivity within the CNS. *Trends in Neurosciences,* 9**,** 271-277.

WELLS, J. M., GAGGAR, A. & BLALOCK, J. E. 2015. MMP generated matrikines. *Matrix Biology,* 44-46**,** 122-129.

WESTALL, F. C. 2006. Molecular mimicry revisited: gut bacteria and multiple sclerosis. *J Clin Microbiol,* 44**,** 2099-104.

WHITAKER, J. N. 1998. Effects of pregnancy and delivery on disease activity in multiple sclerosis. Mass Medical Soc.

WILSON, R., BEALMEAR, M. & SOBONYA, R. 1965. Growth and Regression of the Germfree (Axenic) Thymus. *Proc Soc Exp Biol Med,* 118**,** 97-9.

WINGERCHUK, D. M. 2011. Environmental factors in multiple sclerosis: Epstein-Barr virus, vitamin D, and cigarette smoking. *Mt Sinai J Med,* 78**,** 221-30.

WITTNER, J. & SCHUH, W. 2021. Kruppel-like Factor 2 (KLF2) in Immune Cell Migration. *Vaccines (Basel),* 9**,** 1171.

WOOD, H. 2015. Uncovering the secrets of the 'brain drain'—the CNS lymphatic system is finally revealed. *Nature Reviews Neurology,* 11**,** 367-367.

WORBS, T., MEMPEL, T. R., BÖLTER, J., VON ANDRIAN, U. H. & FÖRSTER, R. 2007. CCR7 ligands stimulate the intranodal motility of T lymphocytes in vivo. *J Exp Med,* 204**,** 489-95.

WU, J. & LINGREL, J. B. 2004. KLF2 inhibits Jurkat T leukemia cell growth via upregulation of cyclin-dependent kinase inhibitor p21WAF1/CIP1. *Oncogene,* 23**,** 8088-96.

WU, J., OLSSON, T., HILLERT, J., ALFREDSSON, L. & HEDSTROM, A. K. 2023. Influence of oral tobacco versus smoking on multiple sclerosis disease activity and progression. *J Neurol Neurosurg Psychiatry,* 94**,** 589-596.

XU, H., MANIVANNAN, A., LIVERSIDGE, J., SHARP, P. F., FORRESTER, J. V. & CRANE, I. J. 2003. Requirements for passage of T lymphocytes across non-inflamed retinal microvessels. *J Neuroimmunol,* 142**,** 47-57.

YANG, C.-C., HSIAO, L.-D., SU, M.-H. & YANG, C.-M. 2020. Sphingosine 1-Phosphate Induces Cyclooxygenase-2/Prostaglandin E2 Expression via PKCα-dependent Mitogen-Activated Protein Kinases and NF-κB Cascade in Human Cardiac Fibroblasts. *Frontiers in Pharmacology,* 11.

YONG, V. W., POWER, C., FORSYTH, P. & EDWARDS, D. R. 2001. Metalloproteinases in biology and pathology of the nervous system. *Nat Rev Neurosci,* 2**,** 502-11.

YOU, T., BI, Y., LI, J., ZHANG, M., CHEN, X., ZHANG, K. & LI, J. 2017. IL-17 induces reactive astrocytes and up-regulation of vascular endothelial growth factor (VEGF) through JAK/STAT signaling. *Scientific Reports,* 7**,** 41779.

YU, W., JIANG, N., EBERT, P. J., KIDD, B. A., MÜLLER, S., LUND, P. J., JUANG, J., ADACHI, K., TSE, T. & BIRNBAUM, M. E. 2015. Clonal deletion prunes but does not eliminate self-specific αβ CD8+ T lymphocytes. *Immunity,* 42**,** 929-941.

YURKOVETSKIY, L. A., PICKARD, J. M. & CHERVONSKY, A. V. 2015. Microbiota and autoimmunity: exploring new avenues. *Cell Host Microbe,* 17**,** 548-52.

ZECCA, C., ROTH, S., FINDLING, O., PERRIARD, G., BACHMANN, V., PLESS, M. L., BAUMANN, A., KAMM, C. P., LALIVE, P. H. & CZAPLINSKI, A. 2018. Real-life long-term effectiveness of fingolimod in Swiss patients with relapsing-remitting multiple sclerosis. *Eur J Neurol,* 25**,** 762-767.

ZHANG, J., MARKOVIC-PLESE, S., LACET, B., RAUS, J., WEINER, H. L. & HAFLER, D. A. 1994. Increased frequency of interleukin 2-responsive T cells specific for myelin basic protein and proteolipid protein in peripheral blood and cerebrospinal fluid of patients with multiple sclerosis. *J Exp Med,* 179**,** 973-84.

ZHANG, S., SHEN, J., LI, D. & CHENG, Y. 2021. Strategies in the delivery of Cas9 ribonucleoprotein for CRISPR/Cas9 genome editing. *Theranostics,* 11**,** 614-648.

CONTRIBUTIONS

- PD. Dr. Naoto Kawakami and Dr. Katrin Franziska Lämmle in collaboration with group of Prof. Kerschensteiner including Dr. Arek Kendirli and Clara de la Rosa del Val performed the genome-wide CRISPR/Cas9 screening research.
- Clara de la Rosa del Val performed the bioinformatics analyses in this study and created the resulting graphical representation.
- The in vivo two-photon imaging experiment was supported and performed Dr. Kawakami.

ACKNOWLEDGEMENT

I would like to express my deepest gratitude to everyone who contributed to this thesis and supported me throughout my PhD journey, both academically and personally.

My deepest gratitude goes to my supervisor PD Dr. Naoto Kawakami. Without the opportunity he gave me, I would not have been able to pursue my PhD in Germany. I sincerely appreciate his guidance, his patience in answering my questions, and his generosity in offering help whenever I needed. He showed me that research can be a source of pure joy and taught me to be well-knit in work and relaxed in life. I am also deeply grateful for the time and effort he dedicated to helping me with my thesis writing. Beyond work, I truly enjoyed our conversations, whether about science or completely random topics. There is so much more to thank him for, and I would like to express my heartfelt appreciation once again.

Sincere thanks goes to all the members of our lab group. Bella and Katrin, their warm welcome, introductions to all colleagues when I first joined the institute helps me a lot in integrating into the institute. I truly appreciate the time and effort they put into sharing protocols, teaching me new experiments, and always being there when I needed guidance and support. I would like to thank Katie, our conversations brightened countless hours of desk work, thank you for that. Special thanks also to Tobias, Sam, Cheng, Leonie and all the other wonderful colleagues at the institute. With all of you, my PhD journey was not just about research but also a truly memorable and enriching experience.

At the same time, I would like to thank the China Scholarship Council (CSC) for the scholarship. With the support of the scholarship, I can concentrate on my PhD research without the pressure of life, and complete my PhD research in Munich.

Thanks to Robin especially for supporting me during my thesis writing time. And thanks to myself for overcoming all the difficulties and pressures to reach this point.

感谢爸爸妈妈对我追求人生理想道路上一如既往毫无保留的支持和理解，愿他们身体健康。

Affidavit

Zhuo, La

Surname, first name

I hereby declare, that the submitted thesis entitled:

Krüppel-Like Factor 2: A Key Transcription Factor Mediates CD4+ T Cells Migration in Experimental Autoimmune Encephalomyelitis

is my own work. I have only used the sources indicated and have not made unauthorised use of services of a third party. Where the work of others has been quoted or reproduced, the source is always given.

I further declare that the dissertation presented here has not been submitted in the same or similar form to any other institution for the purpose of obtaining an academic degree.

Tübingen, 01.Feb.2026

Place, Date

La Zhuo

Signature doctoral candidate

LMU LUDWIG-MAXIMILIANS-UNIVERSITÄT MÜNCHEN

Dekanat Medizinische Fakultät
Promotionsbüro

Confirmation of congruency between printed and electronic version of the doctoral thesis

Zhuo, La

name, first name

I hereby declare that the electronic version of the submitted thesis, entitled:

Krüppel-Like Factor 2: A Key Transcription Factor Mediates CD4+ T Cells Migration in Experimental Autoimmune Encephalomyelitis

is congruent with the printed version both in content and format.

Tübingen, 01.Feb.2026

Place, Date

La Zhuo

Signature doctoral candidate

LIST OF PUBLICATIONS

1. Kendirli, A., de la Rosa, C., Lämmle, K. F., Eglseer, K., Bauer, I. J., Kavaka, V., Winklmeier, S**., Zhuo, L.**, Wichmann, C., Gerdes, L. A., Kümpfel, T., Dornmair, K., Beltrán, E., Kerschensteiner, M., & Kawakami, N. (2023). A genome-wide in vivo CRISPR screen identifies essential regulators of T cell migration to the CNS in a multiple sclerosis model. Nature neuroscience, 26(10), 1713–1725. https://doi.org/10.1038/s41593-023-01432-2
2. Liu, L., Ma, D., **Zhuo, L**., Pang, X., You, J., & Feng, J. (2021). Progress and Promise of Nur77-based Therapeutics for Central Nervous System Disorders. Current neuropharmacology, 19(4), 486–497. https://doi.org/10.2174/1570159X18666200606231723
3. Pang, X., Hao, Y., Ma, L., **Zhuo, L**., Liu, L., & Feng, J. (2021). Subacute combined degeneration of the spinal cord concurrent with acute pulmonary embolism: a case report. The Journal of international medical research, 49(5), 3000605211016815. https://doi.org/10.1177/03000605211016815
4. Pang, X., Ma, L., **Zhuo, L**., Liu, L., & Feng, J. (2021). The first report of human primary pyogenic ventriculitis caused by Streptococcus suis: a case report. Annals of palliative medicine, 10(7), 8448–8453. https://doi.org/10.21037/apm-21-45